General Disclaimer

One or more of the Following Statements may affect this Document

- This document has been reproduced from the best copy furnished by the organizational source. It is being released in the interest of making available as much information as possible.

- This document may contain data, which exceeds the sheet parameters. It was furnished in this condition by the organizational source and is the best copy available.

- This document may contain tone-on-tone or color graphs, charts and/or pictures, which have been reproduced in black and white.

- This document is paginated as submitted by the original source.

- Portions of this document are not fully legible due to the historical nature of some of the material. However, it is the best reproduction available from the original submission.

CR-135300

LIGHTWEIGHT, LOW COMPRESSION AIRCRAFT DIESEL ENGINE

T.L. Gaynor

M.S. Bottrell

C.D. Eagle

Prepared by:

The University of Michigan
Aerospace Engineering Department
Aircraft Research Labs

July 1977

ERRATA

Report No. CR-135300

LIGHTWEIGHT, LOW COMPRESSION AIRCRAFT DIESEL ENGINE

by

T. L. Gaynor
M. S. Bottrell
C. D. Eagle

July 1977

Page 41: The caption for Figure 15 (c) should read:

AD-131 Piston (10:1 CR)

and the caption for Figure 15(d) should read:

AD-118 Piston (10:1 CR) Showing Fuel Impingement.

Page 44: Figure 18(a): Change ' Modified GTSOP-520 Cylinder ' to ' Modified GTSIO-520 Cylinder' .

Page 36: Figure 36: Change ' standard GRSIO-520 Cylinder' to ' standard GTSIO-520 Cylinder' .

CR-135300

LIGHTWEIGHT, LOW COMPRESSION AIRCRAFT DIESEL ENGINE

T.L. Gaynor

M.S. Bottrell

C.D. Eagle

Prepared by:

The University of Michigan
Aerospace Engineering Department
Aircraft Research Labs

July 1977

1. Report No.	2. Government Accession No.	3. Recipient's Catalog No.
CR-135300		

4. Title and Subtitle	5. Report Date
LIGHTWEIGHT, LOW COMPRESSION AIRCRAFT DIESEL ENGINE	July 1977
	6. Performing Organization Code

7. Author(s)	8. Performing Organization Report No.
T.L. Gaynor, M.S. Bottrell, C.D. Eagle C.F. Bachle (Section 3.3.10)	
	10. Work Unit No.

9. Performing Organization Name and Address	11. Contract or Grant No.
The University of Michigan Department of Aerospace Engineering Ann Arbor, Michigan 48109	NAS3-20051
	13. Type of Report and Period Covered
12. Sponsoring Agency Name and Address	Contractor Report
NASA-Lewis Research Center 21000 Brookpark Road Cleveland, OH 44135	14. Sponsoring Agency Code

15. Supplementary Notes

Project Director, R.A. Kroeger
The University of Michigan
Ann Arbor, Michigan 48109

Assistant Project Director, C.D. Eagle
The University of Michigan
Ann Arbor, Michigan 48109

16. Abstract

A study was performed on the feasibility of converting a spark ignition aircraft engine to the diesel cycle. This report: 1) presents procedures necessary to convert a single cylinder GTSIO-520 spark ignition engine to the diesel cycle; 2) describes a single cylinder diesel engine test program; 3) presents a study into the modification of the GTSIO-520 engine to employ the Hot Port cooling concept; 4) shows potential gains in aircraft performance with the incorporation of the diesel engine and Hot Port concept.

The conversion presented here includes a modified camshaft, crankshaft, spark plug holes and pistons machined for compression ratios of 10:1, 11:1, and 12:1. An induction air system to simulate turbocharging is described in addition to the necessary instrumentation to conduct single cylinder engine testing.

The diesel engine test program is outlined including an injection nozzle survey and injection, swirl and fuel impingement tests. Circumstance that hampered the recording of reliable data are also discussed.

A study of the Hot Port cooling concept applied to the aircraft diesel is presented with outlines of two model studies used to formulate the preliminary layouts.

A digital computer graphics simulation of a twin engine aircraft incorporating the diesel engine and Hot Port concept is presented showing some potential gains in aircraft performance. Sample results of the computer program used in the simulation are included.

17. Key Words (Suggested by Author(s))	18. Distribution Statement
Aircraft Diesel Hot Port Low Compression Ratio Experimental engine testing	

19. Security Classif. (of this report)	20. Security Classif. (of this page)	21. No. of Pages	22. Price*
UNCLASSIFIED	UNCLASSIFIED	95	

* For sale by the National Technical Information Service, Springfield, Virginia 22161

TABLE OF CONTENTS

TABLE OF CONTENTS (cont.)

LIST OF ILLUSTRATIONS

LIST OF ILLUSTRATIONS (cont.)

LIST OF TABLES

I. INTRODUCTION AND SUMMARY

1.1 SUMMARY

The objective of this graduate research program was four fold:

1. Modification of a single cylinder test engine to incorporate a cylinder from an existing spark-ignition engine converted to diesel operation and preparation of a test cell to provide induction air heating and simulated turbocharging.
2. Testing of the modified single cylinder engine to provide data on the characteristics of a low-compression turbocharged diesel engine.
3. Design of a cylinder employing the "Hot Port" concept.
4. Analyze the potential performance of the low compression ratio diesel with respect to general aviation aircraft applications.

To minimize cost and conversion time, an ATAC-IH-LABECO engine used in previous diesel research was retained and modified utilizing standard GTSIO-520 engine parts donated by Teledyne Continental Motors. A new crankshaft was installed along with a standard GTSIO-520 camshaft modified to fit the single cylinder diesel test engine. Spark plug holes were closed by installing a cylinder pressure transducer in one hole and the clamping mechanism for the injection nozzle in the other. Flat top pistons were machined to provide compression ratios of 10:1, 11:1, and 12:1 and clearance volume cavities to suit the injection spray. The ATAC-IH-LABECO engine test cell was instrumented and modified to simulate turbocharging with an induction air system which included intake air heater, air bypass, surge tank and back pressure regulator. Instrumentation included a Hartridge and a Bosch Smoke Meter, dynamometer speed regulator, exhaust pressure manometer, fuel injector needle lift transducer, fuel flowmeter, and a magnetic pick-up for RPM determination. Cylinder cooling air and oil temperature control were supplied.

Experimental engine testing was performed using compression ratios of 10:1 and 11:1. An injection nozzle spray survey was undertaken followed by after injection, air swirl and fuel impingement tests. Intake air temperature and pressure as well as manifold pressure were examined for effect on the ignition point and ignition lag. Until late in the diesel test program, test equipment and procedures hampered the recording of reliable data. Further testing is therefore recommended and needed to confirm or reject previous test observations.

The Hot Port cooling concept was applied early in the program to the design of the GTSIO-520 spark ignition cylinders. Bench testing a model of the cylinder dome showed that the center attachment point of the valve guide/support must be within 1.27 cm (.50 in.) of the center of the dome in order to maintain valve seat/valve guide alignment. A second model of the cylinder head indicated that it has several structural advantages including a valve rocker position such that the fulcrum force reaction is taken in an independent structure to the cylinder dome making an exceptional valve mechanism by stiffening and low thermal expansion effect. A preliminary Hot Port cylinder layout was submitted to Automotive Pattern of Detroit who determined that existing pattern equipment for the GTSIO-520 could not be successfully modified to incorporate the Hot Port cooling design. Work on the Hot Port cooling concept was then discontinued at The University of Michigan with further design studies being proposed.

The analytical engine characterization could not be performed due to the incomplete results of the experimental diesel engine testing. However, a digital graphics computer simulation was performed on a "typical" aircraft showing possible gains in performance by utilizing the aircraft diesel and the Hot Port cylinder.

1.2 INTRODUCTION

The University of Michigan is extensively involved in research and education programs related to general aviation aircraft and general aviation power plants. The greatest emphasis is placed on technical problems associated with the third level aircarrier fleet due to the increasing significance of these aircraft to the U.S. business transportation system. Solution of these technical problems would mean increased safety, fuel economy and performance while decreasing maintenance costs and emissions.

To resolve these technical problems a University/Industrial program was defined by NASA that would provide design information necessary for improved aircraft piston engines. The basis of the single cylinder diesel engine research program was to demonstrate the feasibility of converting an off-the-shelf spark ignition aircraft engine to the diesel cycle. This was to be accomplished without major engine component redesign in order to minimize cost and weight penalties. In addition, the research effort was defined to investigate the Hot Port cylinder cooling concept and subsequent increase in aircraft performance.

NASA contract NAS 3-20051 to research the feasibility of a lightweight, low compression aircraft diesel engine was awarded to The University of Michigan by Lewis Research Center in April 1976. All work under this contract was directed by the University Project Director under the technical direction of a NASA Project Manager. This project is being continued as a Grant (NSG 3161), and will concentrate on combustion analysis and general engine performance of the present low compression ratio diesel engine. This subsequent work is conducted under the guidance of Professor Bolt of The University of Michigan.

All principal measurements and calculations were made using the English system. Conversion to the S.I. system was made for reporting purposes.

The purpose of this final contractor's report is to present the findings of the lightweight, low compression aircraft diesel engine research program performed under the contract.

II. TASK I - TEST INSTALLATION

2.1 OBJECTIVE

The objective of this task was to modify a single cylinder test engine, to incorporate a cylinder from an existing spark ignition engine converted to diesel operation and prepare a test cell to provide induction air heating and simulated turbocharging.

2.2 TECHNICAL DISCUSSION

2.2.1 Standard Test Cell Equipment

In accordance with the proposal submitted by The University of Michigan in December, 1975, concerning "A Graduate Research Program Entitled, 'An Aircraft Piston Engine with Improved Fuel Consumption, Cooling Drag, and Exhaust Emission'", the ATAC-IH-LABECO engine and associated equipment, which was used for basic diesel research in the past, was retained and used on this project. The main advantage in doing so was the ability to keep initial hardware cost to a minimum. All test equipment was modified and ready for testing by December 15, 1976. Further substantial improvements took place following an initial testing phase and were completpd by May 24, 1977. These improvements are given on page 7. A complete list of equipment identification is given in Appendix A. The following is a list of equipment used for the ATAC-IH-LABECO engine which was retained and used on this project:

1. An electric dynamometer capable of delivering 100 hp in the motoring mode and absorbing 150 hp in the absorbing mode, shown in Fig. 8.
2. Beam scale capable of reading to 67.4 N (300 lbs), shown in Fig. 1.
3. Digital counter to determine crankshaft RPM to the nearest 1 RPM with second by second update capability, shown in Fig. 1.
4. Induction airflow metering system with a continuous capacity of 327.4 kg/hr (722 lbs/hr). Airflow is determined by a bank of rounded approach critical flow orifices with diameters of 8.2 mm (1/8 in.), 5.5 mm (7/32 in.), 2.3 mm (3/32 in.), and 4.7 mm (3/16 in.) as illustrated in Fig. 2 and shown in Fig. 3.
5. A CFR (Cooperative Fuel Research) fuel weighing station to determine fuel flow rate by measuring the time in which a given mass of fuel is consumed, illustrated in Fig. 4 and shown in Fig. 5.
6. A 20 kw electric air heater capable of heating induction air to 371°C (700°F) to simulate the intake temperature characteristics of turbocharging, shown in Fig. 6.

7. Brown indicating potentiometer consisting of two ranges; a low temperature range from -17.7 to 315°C (0°F to 600°F) with .55°C (1°F) increments, and a high temperature range from -17.7°C to 982.2°C (0°F to 1800°F) with 2.7°C (5°F) increments, shown in Fig. 7.

8. Exhaust surge tank of 148 ℓ (5.23 ft^3) capacity (exhaust tank volume to displacement volume of 105.4:1) plenum to reduce the effect of pressure pulsations from the engine, shown in Fig. 8. Exhaust gas entering this tank is cooled by a water spray illustrated in Fig. 2. The water spray is capable of cooling the exhaust gas to 65.5°C (150°F) at high engine power settings. The exhaust surge tank outlet is restricted by a valve to give exhaust gas back pressures to simulate turbo-charged conditions.

2.2.2 Initial Test Cell Modifications
(September 9, 1976 to December 15, 1976, see Fig. 9)

Replacing the liquid cooled ATAC cylinder with an air cooled aircraft cylinder and adding a cooling air fan and ducting was the only major change required in the test equipment. Appropriate instrumentation was added so that the measurements required by the work statement could be taken.

A more detailed description of the initial test cell modification including instrumentation is given in the following:

1. A 10 hp cooling air fan and associated ducting capable of producing 38.1 cm (15 in.) H_2O pressure drop across the cylinder was installed in the equipment room above the test cell. A 20.3 cm (8 in.) fan outlet valve was installed which is controlled from the main instrument panel to provide a range in pressure from 1.27 cm (0.5 in.) to 38.1 cm (15 in.) of H_2O. The cylinder cooling air was confined to the cylinder fins by standard cylinder baffles as in the flight aircraft (see Fig. 8).

2. An intake surge tank was installed with a volume of 33.9 ℓ (1.2 ft^3) (see Fig. 5), which served as a plenum for the pressurized induction air to reduce the pressure pulsations from the intake valve. After initial engine testing, this surge tank was determined to be too small. It was removed and replaced with a 192.4 (6.8 ft^3) intake tank (volume to displacement volume of 136.5:1). The installation of the larger tank is discussed on page 8 and schematically shown in Fig. 2.

3. A heater bypass was provided for the induction air to blend the hot and the cold air streams to give fast time response to the temperature control (schematically shown in Fig. 2 and photograph, Fig. 6). Pressure of combustion air ahead of the cylinder is controlled by a gate valve. This bypass system (shown in Fig. 6), used in conjunction with the thermostat installed on the heater, was capable of providing constant induction air temperature within ± .55°C (± 1°F).

4. Thermocouples were installed at the following locations and displayed on the Brown potentiometer at the main instrument panel:

   a) Induction air system
      Before intake air heater
      In intake surge tank
      At intake port

   b) Exhaust system
      At exhaust port
      In exhaust surge tank

   c) Oil system
      In oil sump
      In oil gallery

   d) Fuel system
      After fuel filter

   e) Cooling air system
      Before cylinder head
      Before cylinder barrel
      After cylinder head
      After cylinder barrel

   A thermocouple was installed to determine cylinder head metal temperature using the location which is a standard location on all GTSIO-520 cylinders for such measurements (see Fig. 10). The cooling air thermocouples used an exposed wire type. All other thermocouples, listed above, were the immersion type. The exhaust system used Chromel-Alumel thermocouples while all the other systems used Copper-Constantan.

5. Induction and exhaust pressures were indicated on a 254 cm (100 in.) Hg U-tube manometer. Differential pressure measurements of both crankcase blowby, and cooling air across the cylinder were measured by 91.4 cm (36 in.) H_2O U-tubes (see Fig. 11). Combustion chamber pressure was measured by a water cooled Kistler quartz pressure transducer installed in one of the two spark plug holes of the GTSIO-520 cylinder head (see Figs. 10 and 12a). The output was displayed on a dual beam oscilloscope. Calibration of this complete pressure transducer system was made using a balanced diaphragm pressure indicator.

6. A magnetic pick-up was installed in close proximity to a steel plate mounted on the crankshaft. Holes at three degree increments were placed along the plate perimeter allowing crankshaft timing determination (see Fig. 12c). The output was displayed on the dual beam oscilloscope along with the cylinder pressure trace, see Fig. 28.

7. In order to determine the fuel injection characteristics, a needle lift transducer was installed on the fuel injection nozzle. Three nozzles were modified to accept this device which are shown in Table I. The output of the needle lift detector was displayed on the dual beam oscilloscope.

8. Exhaust smoke was measured with a Bosch smoke meter. The smoke meter sampling probe was inserted 15.2 cm (6 in.) into the exhaust pipe.

9. To provide engine operation with various diesel fuel cetane ratings, a separate tank with an 18.9 liter (5 gal) capacity was installed immediately upstream of the CFR weighing system. The plumbing permitted switching from type C-B diesel fuel oil (47.5 cetane value) in the main storage tank to either the 54 cetane fuel or 71 cetane fuel in the 18.9 liter (5 gal) tank with the engine running. This system is schematically shown in Fig. 4.

2.2.3 Subsequent Test Cell Modifications (April 20, 1977 to May 24, 1977, see Fig. 9)

All initial data was taken using the above instrumentation and equipment. After approximately 70 hrs. of engine firing time, combustion data indicated that further improvements in the test cell setup were necessary to provide reliable data. Also in order to improve testing operations, changes were made to more closely hold operating values on the desired point. Equipment was therefore added to increase both the running stability of the engine, and the accuracy of some key measurements. A list of these test cell changes are as follows:

1. An oil cooler and a 1 kw heater were installed to provide a constant oil temperature. The oil heater greatly reduced the time required to reach stabilized oil temperature (approximately 20 min. after the start of firing at moderate loads compared to approximately 50 min. without the heater). The oil cooler and controller held oil temperature constant once the desired oil temperature was reached.

2. A larger pressure regulator in the induction airflow measuring system was installed. This provided pressure regulation of the total induction air supply to the engine. The original system employed a smaller regulator with a bypass. This change improved the pressure regulation of the critical flow orifices. Along with the larger pressure regulator a pressure gauge was changed to improve the accuracy of the induction mass airflow measurement. The pressure gauge which measured induction air pressure before the sonic orifices [previously had an accuracy of .6894 N/cm^2 (1 $lb/in.^2$)] was replaced by a gauge with an accuracy of .0689 N/cm^2 (.1 $lb/in.^2$).

3. The smaller induction air surge tank was replaced by a large surge tank [192.41 liters (6.8 ft^3)] along with a smaller insulated 180° turning chamber [4.69 liters (.166 ft^3)] which was needed to adapt the surge tank to the intake port. The large intake tank has the ratio of intake tank volume to displacement volume of 136.5:1 (see Fig. 8).

4. A hydraulic actuator was installed on the injection pump manual timing mechanism which enabled full timing adjustment of 24 crankshaft degrees while viewing the oscilloscope displaying cylinder pressure.

5. The Bosch batch type smoke meter was replaced with a continuous reading Hartridge smoke density meter.

6. A fuel flow meter was installed providing instantaneous readings replacing the CFR weighing station.

7. A proportional speed control system capable of holding the RPM constant to within $\pm$ 5 RPM at 2600 RPM was added to the dynamometer control. The ability to hold the engine at a particular RPM during a test run reduced the amount of time required for a given test and reduced the time needed to obtain a test point.

8. The dynamometer beam oil damping was increased in order to reduce pointer wander, thereby reducing a possible reading error from $\pm$ 5% to zero.

2.2.4 Test Engine Modifications
(July 19, 1976 to October 29, 1976, see Fig. 9)

The ATAC-IH-LABECO test engine was last used on a combustion research program for ATAC. The engine construction is such that the liquid cooled cylinder could be replaced by the GTSIO-520 aircooled cylinder. The following briefly describes the changes that were made to convert the engine.

Teledyne Continental Motors, Aircraft Products Division, Mobile, Alabama, made available a supply of standard GTSIO-520 engine parts at no cost to the program which are listed in Appendix B. Therefore, the conversion of the LABECO engine was designed and built around the Continental engine components.

Maintaining the stroke of the GTSIO-520 engine required a crankshaft of shorter stroke, 10.1 cm (4.0 in.). A new crankshaft having a 10.1 cm (4.0 in.) stroke and counterweights designed around the proposed piston rod components was supplied by Teledyne. Other than the stroke and counterweights, the original LABECO crankshaft design was unchanged. The new crankshaft was installed using standard LABECO bearings and assembly procedures.

The GTSIO-520 diesel conversion planned to use the standard spark ignition camshaft and valve train, e.g. tappets, pushrods, etc. The conversion was done by cutting a one cylinder cam section from the drive end of a six cylinder camshaft (Part No. 635033), adapting to this part of the shaft the rear bearing from the LABECO camshaft, machining the front bearing, and adding an injection pump drive.

The LABECO cylinder block was replaced with a steel deck plate designed to accept the GTSIO-520 engine cylinder assembly. LABECO crankcase tappet bores were fitted with sleeves to place the hydraulic valve actuating tappets in position for the GTSIO-520 engine camshaft. The deck plate required shortened pushrods and housings in conjunction with the modified tappet bores. Pushrods and pushrod housings are standard GTSIO-520 engine parts which have been shortened from 34.67 to 30.38 cm (13.65 to 11.96 in.) and 28.63 to 25.6 cm (11.27 to 10.08 in.) respectively. Pushrod housing seals, springs and other hardware remain standard GTSIO-520 engine parts.

Two standard GTSIO-520 engine cylinder assemblies were modified to accept a Stanodyne-Hartford Division (Roosa-Master) fuel injection nozzle. One of the spark plug holes was used to adapt a pressure transducer to monitor cylinder pressure. The other was used to adapt the clamping mechanism for holding the injection nozzle, as shown in Figs. 10 and 14.

Normally the engine is run as a horizontal opposed piston engine; since the engine was run with the cylinder in a vertical position, proper oil drainage from the rocker housings through the pushrod housings to the crankcase was impaired. To provide better oil drainage of the valve rocket chamber, external tube connections were made as shown in Figs. 10 and 14.

The injection pump, an American Bosch single cylinder model APE-IB-100P-6336A, was installed, shown in Fig. 5. The plunger used was 10 mm (.3937 in.) in diameter which was of sufficient size to service the engine.

The existing LABECO connecting rod was used. However, in order to use a standard GTSIO-520 piston, the standard GTSIO-520 piston pin and pin bearing were also used. The piston pin is 1.52 cm (0.6 in.) smaller in diameter than the pin-hole of the LABECO connecting rod. A steel bushing was used to reduce the connecting rod piston pin hole from a 4.378 cm (1.724 in.) diameter to the 2.854 cm (1.124 in.) diameter required by the standard GTSIO-520 piston pin. Appropriate oil holes were also provided for pin and bearing surface lubrication.

Pistons were received in semi-finished condition except for the combustion cavity and are standard GTSIO-520 engine pistons (Part No. 632491) including piston skirt profile, drop and piston running clearances. However the distance from the top ring to the top of casting of the piston is 1.90 cm (.75 in.) greater, see Fig. 15a. With this extra material on top, various compression ratios and combustion chamber shapes were machined without prohibitive decreasing of the thickness of the piston crown. Figure 16 shows the four piston configurations which were fabricated. All but the 12:1 compression ratio piston were tested. The chamber volume and squish ratio for the various pistons are given in Table II. A dimensional check using the 10:1 CR "Mexican Hat" piston was made to determine piston to cylinder head clearances. This was accomplished by barring the engine over with modeling clay affixed to the top of the piston. Measured clearances were found to be 1.17 mm to 2.28 mm (.07 to .09 in.) compared to the desired clearance of 1.27 mm to 1.52 mm (.05 to .07 in.). A further discussion of piston combustion chamber design is given in the discussion of Task II.

Nine different injection nozzles were procured from Roosa-Master. Each nozzle varied in either included spray angle or total orifice area. Three of these nozzles have been adapted to accept the injection needle lift transducer which was described under "test-cell modification". Table I lists these nozzles and their drilling constants. It was assumed that all these nozzles had a valve opening pressure of 1930 to 2068 N/cm^2 (2800 to 3000 $lbs/in.^2$). Figure 12b shows a typical fuel injection nozzle which was tested. Figure 18a shows the Bosch nozzle as compared to the Stanodyne nozzle which was used. Injection nozzle placement restriction is indicated on a model shown in Fig. 18b. The projected path of the unperturbed fuel spray with respect to spray angle and combustion chamber shapes are given in Figs. 17 and 18c.

III. TASK II - TESTING OF THE EXPERIMENTAL ENGINE

3.1 OBJECTIVE

The objective of this task was to test the modified single cylinder engine to provide data on the characteristics of a low compression ratio, turbocharged diesel engine. The goal for the development of the diesel engine is to maintain the same weight as the gasoline engine. This precludes any increase in structure which may result with dieselization. Therefore, to achieve this goal the cylinder pressure limit of 758.4 N/cm^2 (1100 psi) for the gasoline engine was maintained. Table III is a list of engine performance goals that will be attempted to be met by the low compression ratio diesel. The following is a summary of the testing performed.

3.2 INITIAL TEST ENGINE FIRING AS A DIESEL

Prior to receiving the special pistons which were used for the diesel engine testing, the engine was assembled using a standard GTSIO-520 spark ignition engine piston. The compression ratio of this "flat top" piston was 7.5:1. The major reasons for assembling the engine with the standard gasoline engine piston was to check out the engine and test cell systems with the engine in a motoring mode.

In the process of checking out the induction air heater, the engine was initially fired (October 26, 1976) using a nozzle with a 150° included angle, at an induction air temperature of 112.7°C (235°F). Subsequent firings using the 7.5:1 gasoline piston were limited to 2,000 RPM, no load condition. These constraints were followed because instrumentation was incomplete at that time. Specifically, the cylinder pressure transducer was not yet installed. After 3.6 hours of total running time (1.5 hours of firing time) the engine was disassembled for visual inspection. All components were in excellent condition, see Fig. 15b. The engine was reassembled using the newly machined 10:1 compression ratio Mexican Hat configuration piston (P/N AD-118) for a piston to cylinder dome clearance dimensional check and subsequent firings.

3.3 OBSERVED TEST RESULTS

3.3.1 Effect of Various Fuel Injection Nozzles on Engine Performance

A series of tests were run to determine the nozzle spray pattern which would best fit the combustion space. For these tests, six different injection nozzles were used, all having the same orifice distribution and total orifice area (see Table I). The included spray angles varied from 110° to 160° in 10° increments. A nozzle line of 2.13 mm ID x 6.3 mm OD x 838 mm long (.084 x .250 x 33.0 in.) and the 10:1 compression ratio Mexican Hat piston (AD-118) (see Fig. 15c), were used for this series of tests. Test conditions were set to 45.5 ± 1.3 IHP and induction air pressure to 139.7 cm ± 4.06 cm (55.0 ± 1.6 in.) Hg absolute. Table IV gives pertinent operating conditions for this test and all the other tests conducted in Task II. The variation from the intended induction air pressure was caused by the use of an under-sized pressure regulator. This was later corrected by installing a larger capacity airflow pressure regulator. Engine speed was held at 2600 RPM for this and all other tests discussed in this report unless otherwise specified. This value was used since it is a suitable cruising RPM for the GTSIO-520 engine. Due to the unavailability of nozzle needle lift instrumentation and accurate smoke readings at this time, indicated specific fuel consumption (ISFC) was used as criterion of nozzle performance. Figure 19a roughly shows that a 135° included spray angle would give best ISFC with a projected minimum of .183 kg/IHP-hr (.405 lbs/IHP-hr). With this as a basis, three nozzles with 135° included spray angles, but varying orifice sizes and distributions (Table I), were obtained.

3.3.2 Evaluation of After-Injection

After the initial series of injection nozzle spray pattern tests, it was suspected that after-injection was affecting the results. This would explain the higher than expected values for ISFC which were observed during the spray pattern tests. To rough test the theory that secondaries were causing the poor fuel consumption (in the absence of a needle lift instrument), a larger diameter fuel line (2.36 mm ID x 6.35 mm OD x 838 mm long) (.093 x .250 x 33.0 in.) was installed and tested. This change from 2.13 mm ID to 2.36 mm ID produced no significant change in the engine overall performance. It was later found when the nozzle needle transducer was installed (February 10, 1977) that there were no after-injections.

3.3.3 Effect of Induction Air Temperature and Pressure on the Point of Ignition

The effect of varying induction air temperature and pressure on relative ignition is shown in Fig. 20. The needle lift instrumentation was not available at the time of these tests. The injection timing was kept constant, and the variation in the point of ignition was observed on the oscilloscope. The variation of the point of ignition relative to the unknown point of injection is what is meant by relative ignition delay. These tests were run at no load with a 140° included spray angle nozzle (P/N AD-122). Three different combinations of induction air pressure and temperature were tested.

At an induction pressure of 886.4 mm (34.9 in.) Hg absolute, when the induction temperature was increased from 135°C (275°F) to 193.3°C (380°F), the observed ignition point was reduced from 18° ATC (after top center) to 4° ATC. At an atmospheric induction air pressure, when the temperature was increased from 165.5°C (330°F) to 212.7°C (415°F), the observed point of ignition was reduced from 26° ATC to 18° ATC, as shown in Fig. 20. Examination of Fig. 20 shows a reasonable comparison when comparing ignition points for similar tests. The point of ignition corresponding to the constant value of 886.4 mm (34.9 in.) Hg absolute pressure line at 204.4°C (400°F) is 3.5° ATC. When comparing this to the point of ignition corresponding to 886.4 mm (34.9 in.) Hg absolute along the 204.4°C (400°F) constant temperature line, a value of 5.5° ATC is found; a difference of only 2.0°. Considering that the point of ignition is determined in this test by measurements from the oscilloscope trace, it is felt this difference is reasonable. However, if the point of ignition corresponding to atmospheric pressure is examined, a larger discrepancy is observed. In this case the point of ignition corresponding to the constant atmospheric pressure line at 204.4°C (400°F) is 19° ATC. When comparing this value to the point of ignition corresponding to atmospheric pressure along the 204.4°C (400°F) constant temperature line, a value of 7° ATC is found, a difference of 12°. This difference cannot presently be explained. It is believed that the tests corresponding to the constant atmospheric pressure line are in error, and the values of ignition lag are too large. A further discussion of the effect of intake air temperature on engine performance is given on pages 17 and 18.

3.3.4 Effect of Induced Swirl on Engine Performance

A. Engine Testing with Instrument Imperfection

Tests were made to determine the effect of swirl on engine performance. A swirl plate as shown in Fig. 21a was used between the intake elbow and cylinder flange of the intake port. The plate, which has a normal radial distance of .635 cm (0.25 in.) from the chord to the arc, was tested over 360° of rotation in 45° increments. No definite relation was observed between swirl plate position and engine ISFC.

B. Engine Testing

This phase of engine testing took place with modifications to the test cell as outlined in Task I under "subsequent test cell modifications." The following engine operating conditions were held constant throughout this phase of testing unless otherwise specified:

1)	Intake manifold pressure	177.8 cm (70 in.) Hg absolute
2)	Exhaust manifold pressure	127 cm (50 in.) Hg absolute
3)	RPM	2600
4)	Cooling air pressure drop	35.5 cm (14 in.) H_2O
5)	Intake air temperature	121.1°C (250°F)

It was concluded that the airflow restriction of the swirl plate used during the initial engine testing was too small. A new swirl plate was therefore installed (see Fig. 22) which could be positioned during engine operation. To obtain swirl effect from the intake baffle it was considered that the induction airflow should be reduced about 2 to 3%. Accordingly, the normal radial distance from the chord to the arc of the baffle was increased from 1.58 cm (.625 in.) to 2.85 cm (1.125 in.) in steps. The precision of the air measuring system was also greatly improved at this time by the installation of a precision Heise gauge to measure the metering orifices differential pressure. With this modification a 6.6% decrease in volumetric efficiency was measured, and the effect was constant regardless of the position of the restriction.

Using this larger baffle, a preliminary test of the effect of swirl on torque, cylinder firing pressure, and smoke was made. Nozzle AD-129 was used for this test. In all of these observations, the effect of varying swirl plate position was still undetectable. It is concluded that either the swirl baffle was ineffective or some other factor was preventing the swirl from having an effect. A bench test of the GTSIO-520 cylinder with steady flow air supply to the intake port was planned and preliminary measurements were made after the termination of this contract. In this test, air swirl in the cylinder is explored using an air vane swirl device supplied by C. Bachle, see Fig. 23. The results of this are given in Fig. 24.

3.3.5 Friction Horsepower Determination

A. Engine Testing with Instrument Imperfection

Motoring friction horsepower was measured at various engine speeds and at two absolute induction air pressures. The two values of induction pressure were 759 mm (28.9 in.) Hg and 104.1 cm (41.0 in.) Hg absolute. The engine speed was varied from 1460 to 3030 RPM. No temperature controller was installed in the oil system at this time; therefore the oil temperature varied from 46.1°C (115°F) to 75.0°C (167°F). The results are given in Fig. 19b as well as the GTSIO-520 engine friction horsepower divided by six. From the atmospheric curve, friction horsepower for this engine at 2600 RPM is [27.83 N/cm^2 (40.44 psia) FMEP]. This value was used in the calculation of IHP during the initial proof testing.

B. Engine Testing

With the electric oil heater and cooling heat exchanger installed, it was possible to maintain oil temperature to ± 1.8°C (± 1°F). Additional tests at constant induction air pressure of 1778 mm (70 in.) Hg absolute and 2600 RPM gave 11.0 Hp [26.63 N/cm^2 (38.66 psia) FMEP] at 76.6°C (170°F) oil temperature, and 12.4 Hp [30.0 N/cm^2 (38.66 psia) FMEP] at 62.7°C (145°F). Since testing described as "Engine Testing" took place with the oil temperature close to 76.6°C (170°F), the friction Hp value for IHP calculations under "Engine Testing" was 11.0 Hp. It should be noted that subsequent to this friction determination, an approximately .674 N (3 lbs) error in the beam scale was found. The error associated with this faulty reading would be about 15%; therefore this value for friction Hp should not be regarded as final.

3.3.6 Effect of Intake Manifold Pressure on Ignition Lag

After installing the needle lift instrumentation using nozzle AD-126, a test was made to determine the effect of intake manifold pressure on ignition lag. These tests were run without the swirl plate, at light loads (27.7 to 29.1 indicated corrected Hp), 2600 RPM, and an intake manifold temperature held to 118-124°C (245-256°F). Results show a 9° reduction in ignition lag for a 558 mm (22.0 in.) Hg increase of manifold pressure.

3.3.7 Effect of Fuel Impingement

Ignition lag variations with respect to engine load were observed. At approximately 68 N/cm^2 (87.6 psia) IMEP, ignition lag was 30°, with injection being completed 11° before ignition occurs. At 124 N/cm^2 (188 psia) IMEP, the ignition lag was 15° and ignition occurred 15° before the end of injection. This unexpected effect plus the fuel impingement marks on the combustion chamber walls shown in Fig. 15c indicated that fuel impingement might be affecting engine performance. That is, due to poor spray evaporation, a high percentage of fuel was impacting the chamber walls and therefore not meeting oxygen until late in the expansion cycle. This would explain high indicated fuel consumption and poor air utilization.

To test this theory a new piston (AD-130) with a compression and squish ratio of 11:1 and 0.8 respectively, was machined and installed. This piston had a larger bowl diameter than the previous 10:1 piston (AD-118), but the bowl depth was shallower and did not have the Mexican Hat shape (see Fig. 16).

Figure 25 gives the test results showing some key performance parameters, including ignition lag, using AD-130, the 11:1 compression ratio piston. A summary of the testing with the 11:1 compression ratio piston shows that using constant fuel injection timing of 22° BTC, 758.4 N/cm^2 (1100 psi) cylinder pressure limitation was reached at 86.1 N/cm^2 (125 IMEP) at about 54% of full power. Testing did not proceed beyond this 758.4 N/cm^2 (1100 psi) value nor was the timing varied. Although Fig. 25 shows ignition lag to be almost constant, the effect of a larger bowl diameter piston on ignition lag is inconclusive due to unresolved errors in the data.

3.3.8 Effect of Lowering Compression Ratio

A test was made to determine the effect of reducing the compression ratio of the 11:1 piston (AD-130) to a 10:1 piston (designated AD-131) while maintaining nearly the same combustion chamber shape (see Fig. 15d). This was done by increasing the bowl depth of the 11:1 piston (AD-130) by 1.9 mm (.075 in.). Figure 26 shows the performance of this 10:1 compression ratio piston (AD-131) in which, unlike the test of the 11:1 piston (AD-130) where induction air pressure was held constant at

149.5 cm (58.86 in.) Hg absolute, air-fuel ratio was held constant. In testing the 10:1 compression ratio large bowl diameter piston (AD-131), no significant change in overall engine performance was observed in comparison with the 10:1 compression ratio Mexican Hat piston (AD-118), i.e. the indicated fuel consumption continued high.

3.3.9 Effect of Cetane Value on Engine Performance

With the 11:1 CR piston (AD-130), a test was made to determine the effect of a fuel with improved ignition qualities. A direct comparison was made using type C-B diesel fuel oil having a cetane rating of 47.5 and a refernece fuel with a cetane rating of 71. As expected, Fig. 27 shows a reduction in fuel consumption, cylinder pressure and ignition lag with the engine operating at the same basic power level and air-fuel ratio using the 71 cetane rating fuel. A significant reduction in the rate of pressure rise, and a significant reduction in combustion noise was oberved, as also indicated by the indicator cards given in Fig. 28. From this it might be inferred that unsuitable nozzle discharge resulting in poor air utilization is causing the high fuel consumption.

3.3.10 Effect of Intake Air Temperature (An appraisal of Fig. 29 by C.F. Bachle)

By June 9, 1977, all instrumentation and cell equipment had been improved to the point where believable data could be obtained. Conversely most data obtained prior to this date should be regarded as unreliable or incomplete.

Figure 29 gives the effect of intake air temperature on performance obtained on June 9 and 11, 1977, and the following are observations from this data.

1. The indicated specific fuel consumption is about what experience considerations indicate should be expected when the A/F is about 55 [.16 kg/IHP-Hr (.35 lbs/IHP-Hr)] but at 25 A/F, the fuel consumption is about 40% greater [.236 kg/IHP-Hr (.52 lbs/IHP-Hr)].

2. Raising the intake temperature from 93 to 204°C (200 to 400°F), lowered the peak combustion pressure from 672 to 585 N/cm^2 (975 to 850 $lbs/in.^2$) - this is surprising and may indicate instrumentation error.

3. Smoke, exhaust temperature and fuel consumption indicates that the deterioration in performance begins at A/F of 55 and degrades at a faster rate at 35 and again at a faster rate at about 27.

4. The increase in intake temperature did not alter the ISFC.

Conclusions from Fig. 29

1. The fuel is not reaching a major portion of the air.

2. Higher intake air temperature did not alter the performance which means that ignition lag is not the culprit.

3. The following steps in the trouble shooting process should include:

   a. Increased fuel nozzle pressure

   b. Different nozzle hole drilling

   c. Different shape of cavity in combustion chamber formed by the piston contour

   d. Higher air swirl

   e. Increase rate of fuel delivery from pump

Discussion of Fig. 29

It can be visualized that the fuel does not reach the air in a variety of different ways, one of which is illustrated in the following sketch.

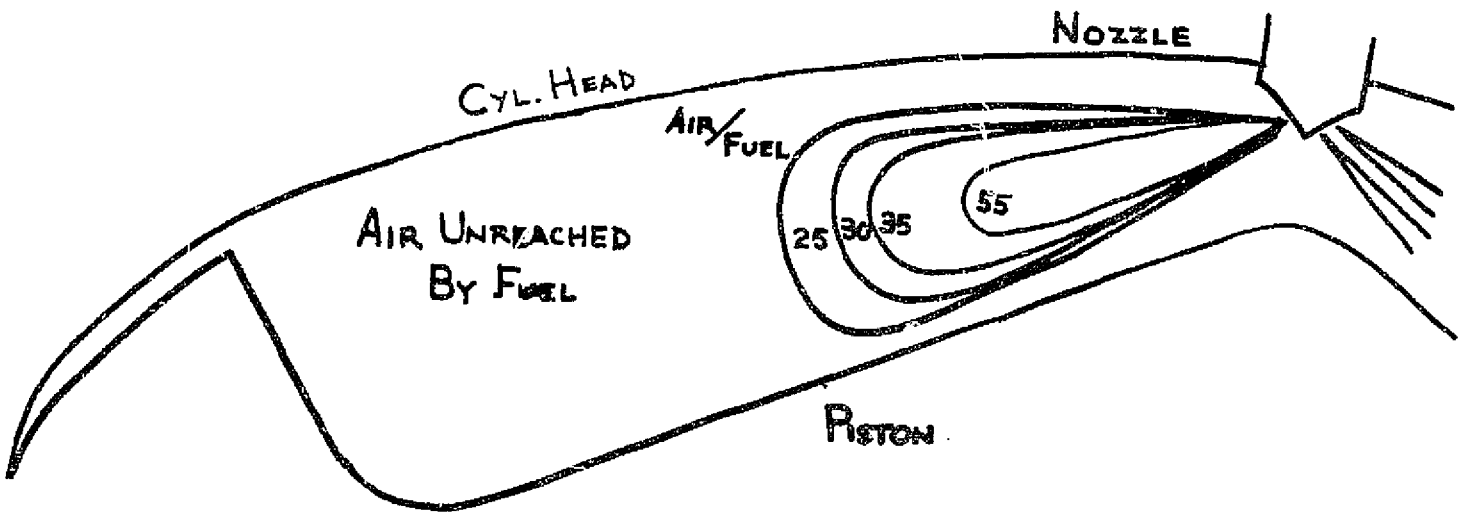

Lack of fuel penetration would explain the zero effect of air swirl observed. That is, if the fuel is not reaching the outer spaces of the combustion cavity, swirl does not have a chance to improve mixing.

To summarize then, the evidence so far leads to the idea that the high fuel consumption is explanable on poor air utilization and that normal cut and try development should quickly give results that will explain the high fuel consumption. (A further disquieting development is that after the tests of June 11, possible errors in the fuel flow system were uncovered making repeat of the test of Fig. 29 all the more important.)

3.4 ENGINE INSPECTION

After 43.6 hours of accumulated firing time, the engine was disassembled for inspection. The 10:1 compression ratio, Mexican Hat configuration piston (AD-118) accumulated 40.7 hours at speeds up to 3,000 RPM, peak cylinder pressures up to 895.7 N/cm^2 (1300 psi) and loads up to 43 indicated horsepower. Visual inspection of the piston indicated small scuffing (almost nominal) of the top land on the thrust side. Figure 30 shows this scuffing as well as the thrust and anti-thrust side of the

piston. The piston pin showed no abnormalities (Fig. 21b). The piston rings, which are standard GTSIO-520 parts, showed no unusual visual signs of wear. Therefore, the engine was reassembled, unchanged, with the exception of the piston top land diameter which was reduced by .127 cm (.005 in.) diameter. Figure 15a shows the top of the piston (combustion chamber). The fuel impingement marks on the chamber wall can be noted. These marks are discussed in Section 3.3.7 on page 16.

3.5 CONCLUDING REMARKS

Analysis of the data plots generated from the testing of the experimental single cylinder engine is inconclusive due to conflicting and nonrepeatable experimental data. The suspects are instrumentation, test cell equipment and experimental procedure. Corrective action on the first two suspects did improve the data. However, the number of data points taken after the correction measures were implemented are too few to postulate that the data are either: (a) reliable; or (b) representative of the performance characteristics of a low compression ratio turbocharged diesel engine. The test cell should be scrutinized and modified where it is necessary to improve the accuracy of the data and more data should be taken before characterizing the engine.

4. TASK III - DESIGN OF HOT PORT SINGLE-CYLINDER

4.1 OBJECTIVE

Design an experimental cylinder and cylinder head assembly incorporating the "Hot Port" concept suitable for testing the modified ATAC-IH-LABECO engine.

4.2 DEFINITION, DESCRIPTION, AND BACKGROUND OF THE "HOT PORT"

The "Hot Port" concept is a means for reducing the cooling airflow requirement by thermally isolating the exhaust port and therefore the exhaust gases from the cylinder head, and disposing of a greater portion of the waste heat directly through the exhaust system. Shown in Fig. 34 is a model of the "Hot Port". In this model thermal isolation is achieved by incorporating the exhaust port as an integral part of the aluminum finned ferrous metal dome, allowing higher metal temperatures than the conventional aluminum head. The exhaust valve stem is insulated by an air gap at the point of penetration into the exhaust port passageway. Heat that passes through the air gap and the heat that is conducted up the valve stem is taken out of the stem by a cooled copper shunt.

The problem was how best to transfer the results of work done for AVDS 1360 (military tank engine) Hot Port cylinder to the special conditions of the 520 aircraft cylinder, see Fig. 31. The AVDS 1360 was made of welded heavy section steel components since low weight was not a principal problem. In addition, the AVDS 1360 was an experiment and not intended as a final design. The GTSIO-520 cylinder, in contrast, is intended for flight and to be executed in such a way as to preserve as much of the standard GTSIO-520 structure as practical. With these considerations in mind, the study herein reported uses a cast dome screwed on in the standard way to a standard nitrided steel cylinder barrel. In addition, the valve rocker and pushrod are from the standard engine.

4.3 MODEL STUDY

4.3.1 Rubber Cylinder Dome Model Study

A simulation of the iron dome of the GTSIO-520 cylinder was made in order to determine deflection magnitudes in an exaggerated way (see Fig. 32). In the Hot Port cylinder principle, great emphasis is placed on the structure supporting the exhaust valve guide by the cylinder dome in such a way as to preserve the alignment of the exhaust valve with the exhaust valve seat in the head as the dome distorts. As the dome bulges from combustion pressure or from temperature distortion, the resulting change in dome

contour would be predictable except for the hole cut-outs for the intake and exhaust ports. These together cause a great increase in strain and therefore distortion where the two holes come closest together at the center of the dome. Figure 33 is a line drawing describing dome distortion as was estimated and as was confirmed by test.

The rubber model of the cylinder head dome was made to determine where the valve guide support attachment points to the dome could best be made to maintain valve seat/valve guide alignment under distorted conditions. The rubber model when distorted, indicates the trends due to thermal and/or pressure forces. A variety of attachment points were tested by using two 35.56 cm (14 in.) pointers; one representing the valve seat in the head and the other representing the valve guide attached to the cylinder dome in several ways. Air pressure was used to give a distortion to the dome with a standardized pressure of 1.4 N/cm^2 (2 psi) base and 3.4 N/cm^2 (5 psi) under strained conditions. Thus a differential pressure of 2.0 N/cm^2 (3 psi) was used to evaluate the various valve guide structure attachment points.

It was found that the poorest attachment points would show a distortion misalignment on the end of the two 35.56 cm (14 in.) pointers of about 1.27 cm (.50 in.), whereas, the best was about 0.7 mm (.03 in.). The main idea evolving from the tests was that one attachment point must be at the center of the dome or within 1.27 cm (.50 in.) of the center. The other two attachment points may be in the region of the outer diameter of the dome with considerable freedom but the third point must be near the dome center.

4.3.2 Model of Hot Port Cylinder Head

Since there are diverse three-dimensional space-use considerations in designing a Hot Port cylinder on the GTSIO-520 basic design, a wood and plastic model was made to assist in formulating ideas for a final design. Figure 34 is a sketch representation of one type of design and Figs. 35 and 36 are photographs of the model. This is not a final or accurate portrait of a design but can be used effectively in making a final design. Of note, in this model, is how the valve guide structure rests on the "between valve" stiffening rib. Of further note is how the valve rocker fulcum force reaction is taken in an independent structure to the cylinder dome making for exceptional stiffening and low thermal expansion.

4.4 PRELIMINARY DESIGN STUDIES

Prior to the NASA/U of M contract, Mr. Bachle worked with Mr. R. Walker of Automotive Pattern Company (makers of the production GTSIO-520 cylinder head pattern equipment) and Mr. C. Peterson of Eck Foundries, Incorporated (foundry presently producing the GTSIO-520 cylinder head). Consultations with Messrs. Walker and Peterson indicated the possibility of producing (for test purposes)

an interim Hot Port design using modified sand cores made from production pattern equipment. This concept has been termed "screw-on ferrous metal dome."

Work under Task III, initiated in November 1976, resulted in a preliminary concept layout from which studies could be made to determine the course of action to be followed. This initial drawing was a basis from which recommendations could be made to enhance the design. Prints of the layout were submitted to Automotive Pattern Company of Detroit with a request for quote. This initial design was discarded because the mounting of the valve guide would have resulted in large movement of the center-line due to pressure and temperature distortion. This design was also difficult to apply since it meant that none of the GTSIO-520 production pattern equipment could be used. At this time it was concluded that an entirely new cylinder head pattern would be required to produce a Hot Port cylinder. With this as a basis, work at The University of Michigan on Task III ended.

4.5 SELECTED MATERIAL AND FABRICATION

An evaluation of recent metallurgical improvements was made by discussion with Thomas Weidig (Metallurgist) and A.H. Engstrom (aluminum casting expert). The result of this discussion was that the dome could be made of ductile iron (sometimes called nodular iron) and that the valve guide support structure could be made easily of 1010 investment casting and possibly of ductile iron. No metallurgical problems were foreseen for the remaining parts.

5. TASK IV - ANALYTICAL ENGINE CHARACTERIZATION

5.1 OBJECTIVE

The objective of the task was to conduct analyses characterizing the potential performance of the low-compression ratio diesel with respect to general aircraft applications.

5.2 TECHNICAL DISCUSSION

Due to the inconclusive results obtained in Task II, it was not feasible to proceed with these analyses per se. Instead, a parametric study was conducted to define the performance tradeoffs for a representative aircraft utilizing the low-compression ratio diesel powerplant and the Hot-Port cylinder concept. This effort was part of the specified Task IV requirements with the exception that derived engine data would have been used instead of the parameterized input.

The parametric study was performed using the General Aviation Synthesis Program (GASP) described in Reference 1. This is an advanced, interactive digital computer program for aircraft preliminary design and performance prediction. Aircraft geometry and powerplant input parameters were provided to GASP to develop a baseline case similar to a Cessna 421B turn-engine aircraft equipped with TCM GTSIO-520F spark-ignition engines. The powerplant was sized to the proper horsepower for the GASP survey by fixing the gear ratio and maximum crankshaft speed and iterating on the required take-off distance and take-off simulation parameters.

The baseline aircraft geometry and dimensions are illustrated in Fig. 37. A general weight breakdown for the baseline aircraft is tabulated in Table V. The GASP computer results for the aerodynamic performance and cruise performance of the baseline aircraft are shown in Figs. 38 and 39, respectively.

For this performance survey the airframe geometry, powerplant horsepower and fuel payload were fixed. Since a Hot-Port, low-compression ratio diesel directly affects the baseline fuel consumption, gross weight and engine cooling drag, these variables were selected as GASP parametric inputs.

To assess the performance of a production spark-ignition engine operating as a low-compression ratio diesel, the fuel consumption of the baseline case was decreased by 10% and 20%. These two values of fuel consumption represent typical low-compression ratio diesel engine characteristics. The aircraft gross weight was also changed from the baseline case by - 2%, + 2% and + 4%. These changes represent powerplant modifications necessary for operating a production engine as a diesel. The equipment which might be added or removed in a typical diesel conversion is listed in Table VI. The actual weight change will depend upon the aircraft operating environment, equipment certification requirements and safety

provisions. The + 4% increase also indicates trade-offs available between range performance and payload.

The use of Hot Port cylinders in an aircraft diesel engine will affect the cooling characteristics. The cooling airflow requirements of a representative spark-ignition engine and the estimated characteristics of the Hot Port diesel are shown in Fig. 40. The reduced mass flow required by the Hot Port diesel will decrease the powerplant cooling drag penalty. In this survey the engine cooling drag coefficient was changed from the baseline value by - 33% and - 67%. These changes were derived from a Hot Port diesel cooling drag analysis similar to the method in Ref. 2.

The results of the parametric study for 16 cases are presented in Table VII. A graph illustrating the performance of the baseline case and the trade-offs available from the low-compression diesel is shown in Fig. 41. The computer results for a typical case are contained in Appendix C.

From this data the range sensitivities may be determined with respect to each of the parameters. The sensitivity to gross weight is - 40.7 km (-22 NM) per percent increase in gross weight, the sensitivity to fuel consumption is 5.15 km (+27.8 NM) per percent decrease in fuel consumption and the range sensitivity to cooling drag coefficient is 5.7 km (+3.1 NM) per ten thousandth decrease in cooling drag coefficient. Although these numbers vary somewhat from case to case, they give a good first approximation to the sensitivity of the aircraft performance to the parameters selected.

6. CONCLUDING REMARKS

Work on the aircraft diesel engine involved modifying a test cell previously used in the testing of an ATAC-IH-LABECO diesel engine so that an air-cooled GTSIO-520 single cylinder test engine could be installed. Modification of the ATAC-IH-LABECO engine took place such that a GTSIO-520 single cylinder could be adapted to it. Testing of this experimental engine as well as a preliminary design study of the Hot Port cylinder and an analytical study of the experimental test engine was performed. The following is a breakdown of the status at the end of the contract.

Task I All necessary equipment and instrumentation required for engine testing concentrating on combustion analysis has been installed. All but the CFR weighing system, and the fuel line pressure transducer appear to be in good working order. At this time, the integrity of the CFR system is in question until an extensive calibration check has taken place. It is believed that the difficulty experienced with the fuel line pressure transducer is due to a circuitry problem. Further work in this area is also warranted.

Task II Combustion difficulties were encountered early in the diesel engine test program and engine testing was then concentrated on solving these combustion problems. Unreliable results were obtained during this period due to inadequate test equipment. It is now felt that this condition has been improved and that further engine testing, concentrating on combustion analysis, using appropriate test procedures can be attempted.

Task III The initial studies of the Hot Port cylinder conducted at The University of Michigan were of the kind which resulted in extensive cylinder pattern changes without compensating advantages. An entirely new cylinder head pattern would have been required and further work was stopped.

Task IV The computer graphics simulation indicated that with the diesel engine, the potential increase in aircraft performance was attractive. Employing the Hot Port and low-compression diesel concepts the projected aircraft powerplant is characterized by an increase in gross weight with a decrease in cooling drag and fuel consumption. The range performance sensitivities of these parameters were found to be - 40.7 km (-27.8 NM) per percent increase in gross weight, + 51.5 km (+27.8 NM) per percent decrease in fuel consumption and + 5.7 km (+3.1 NM) per ten thousandth decrease in cooling drag coefficient.

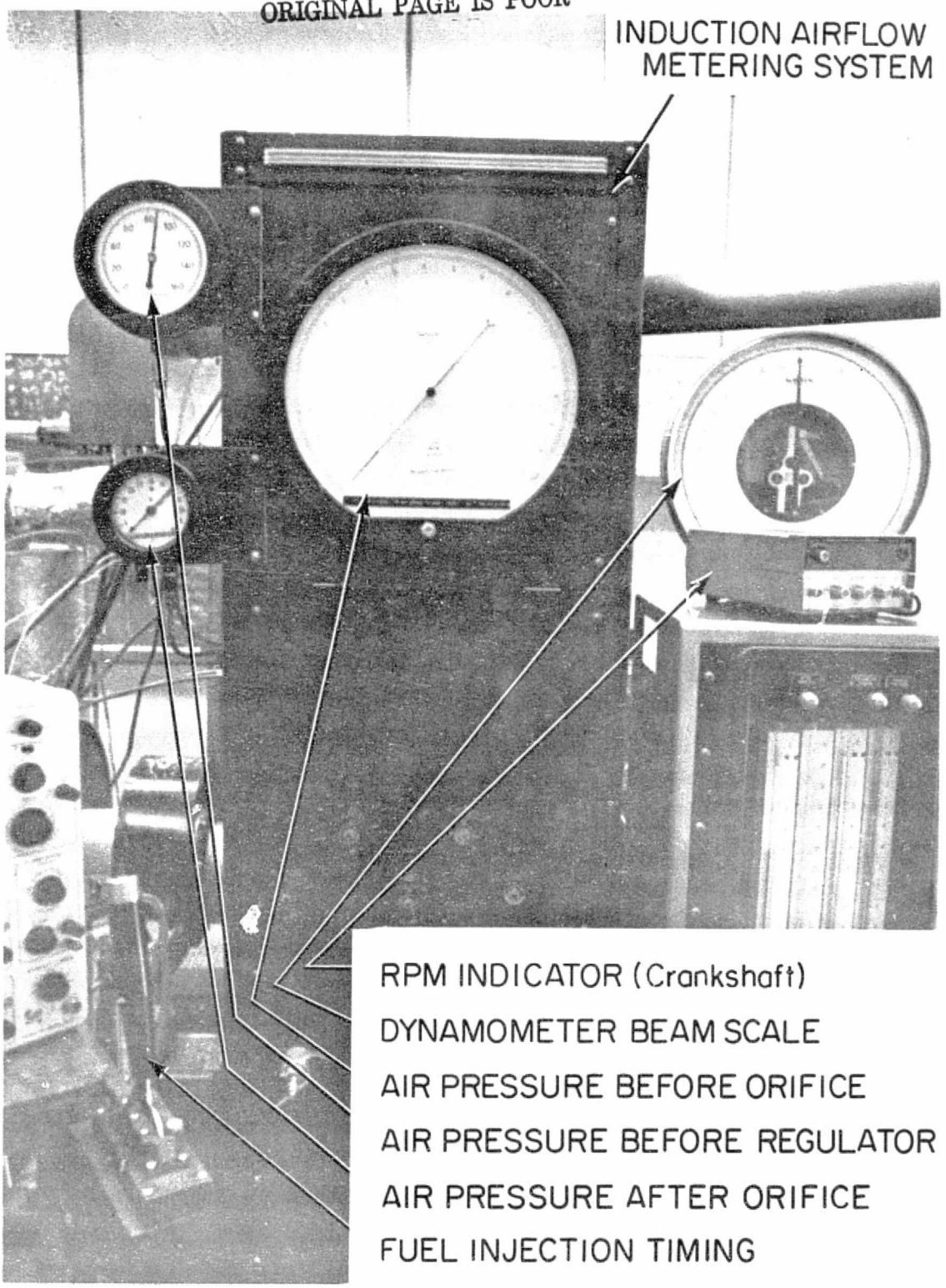

Figure 1. View of Induction Airflow Metering System

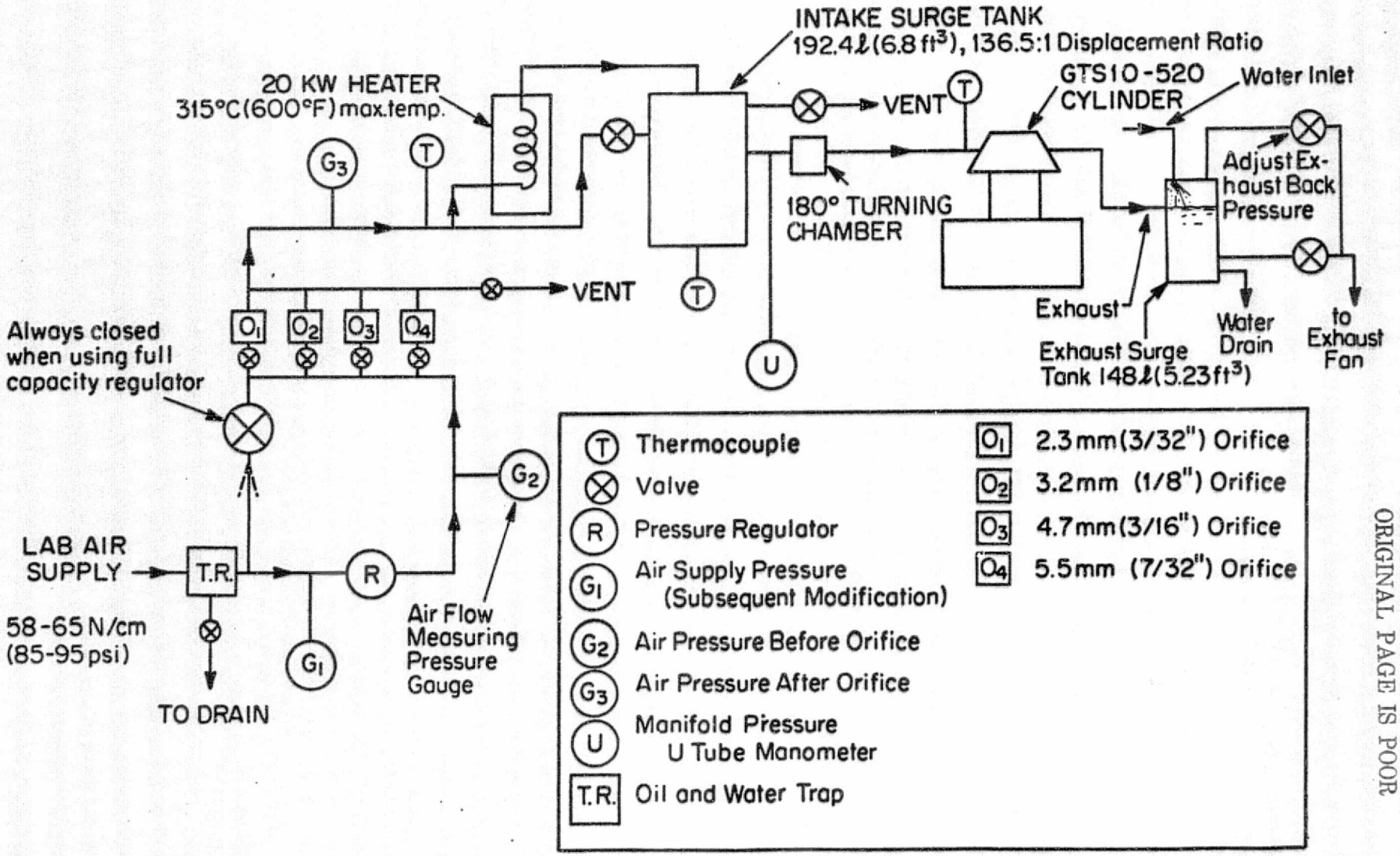

Figure 2. Schematic of Induction Air and Exhaust System

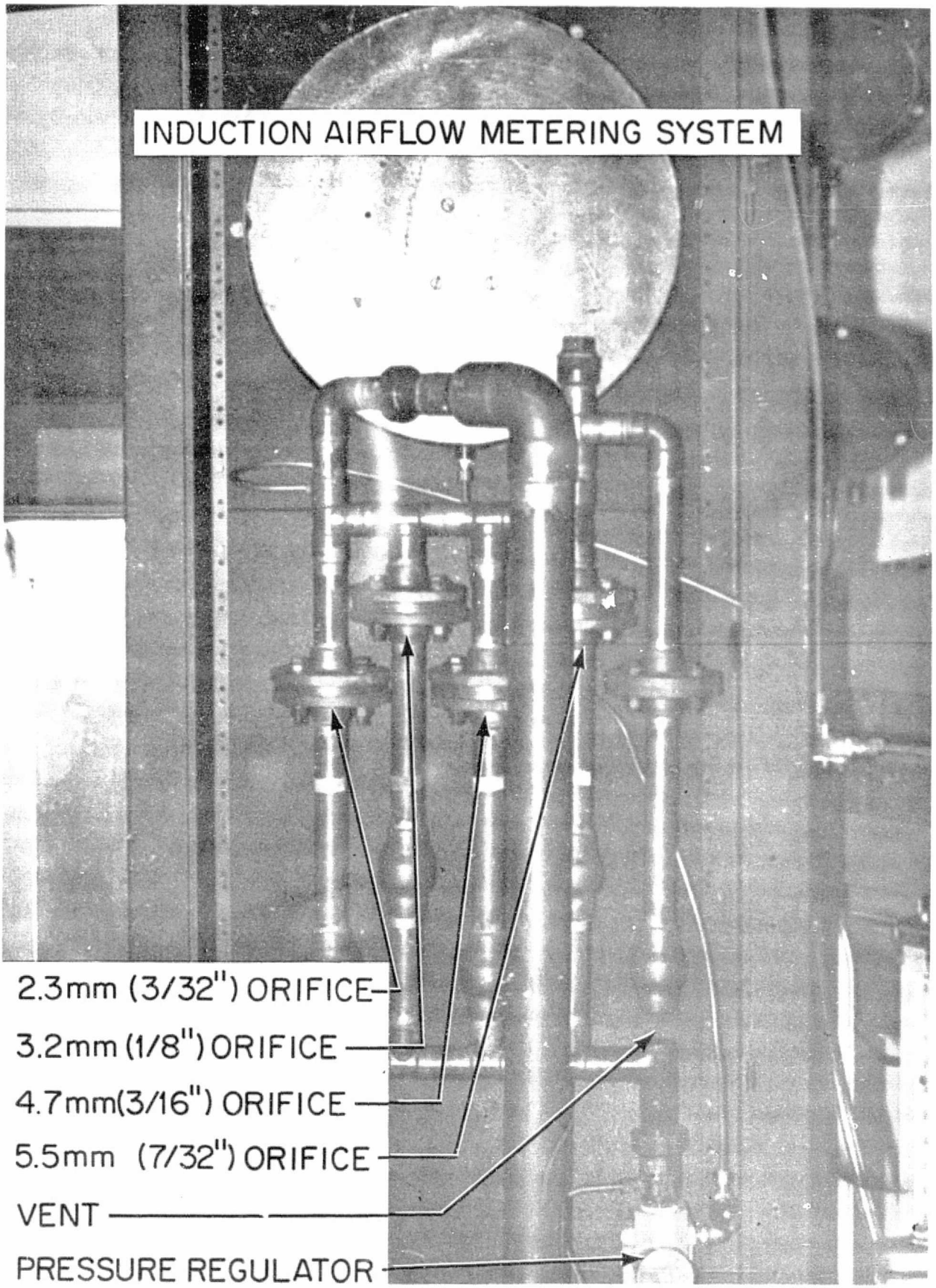

Figure 3. Critical Flow Orifices Shown in the Back of the Induction Airflow Metering System

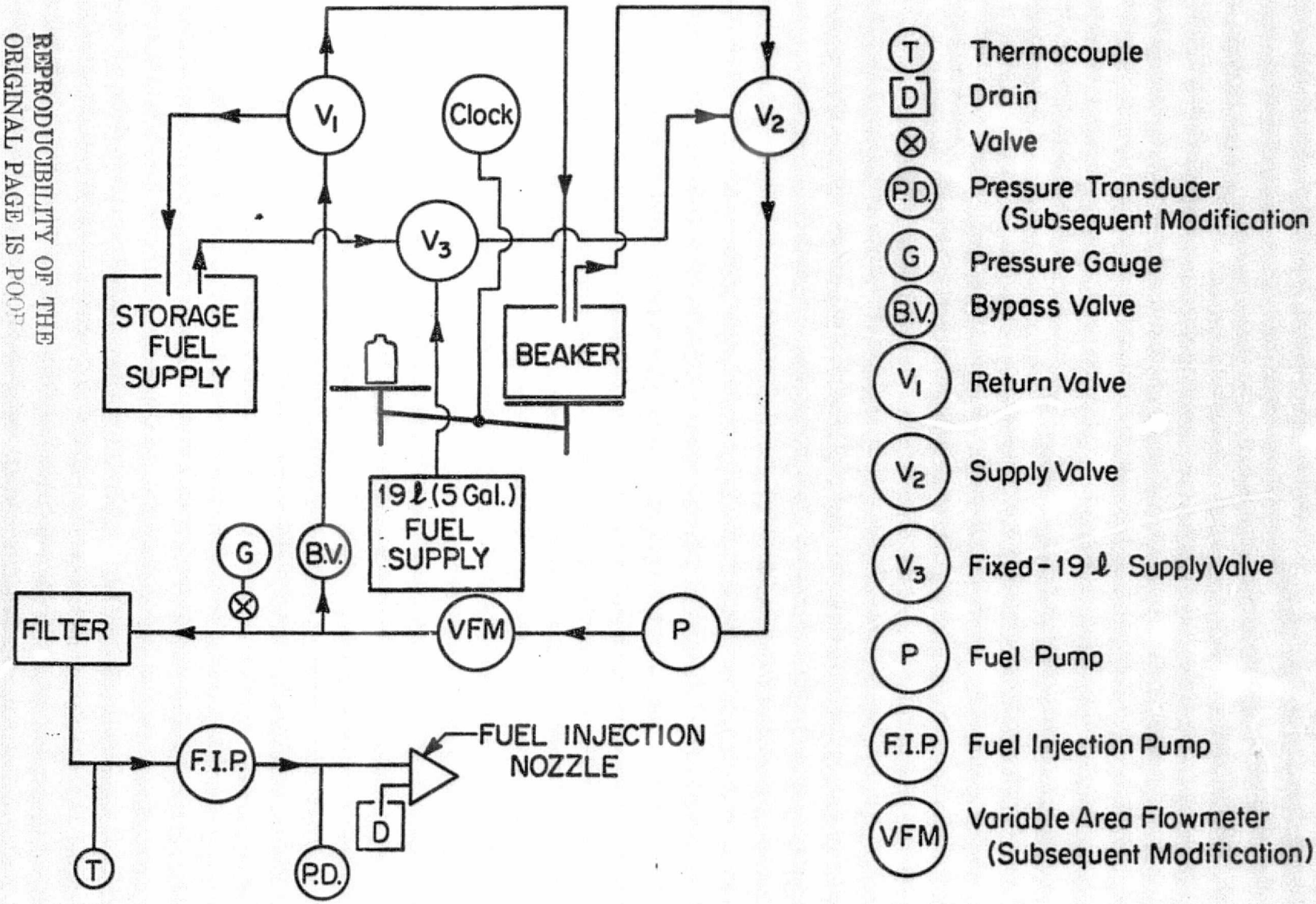

Figure 4. Schematic of Fuel System

Figure 5. View of Test Installation from Fuel Weighing Station

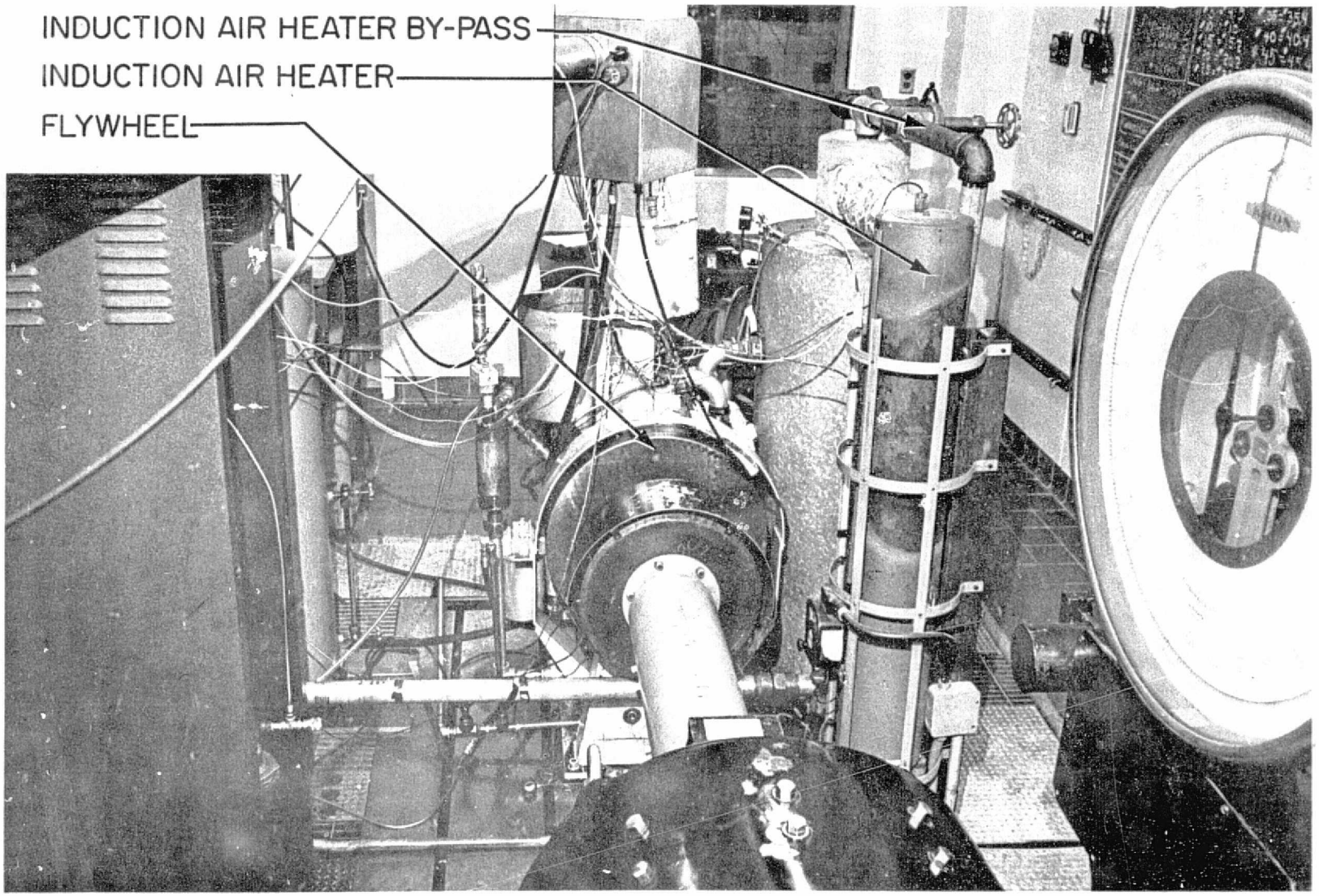

Figure 6. View of Test Engine from the Dynamometer

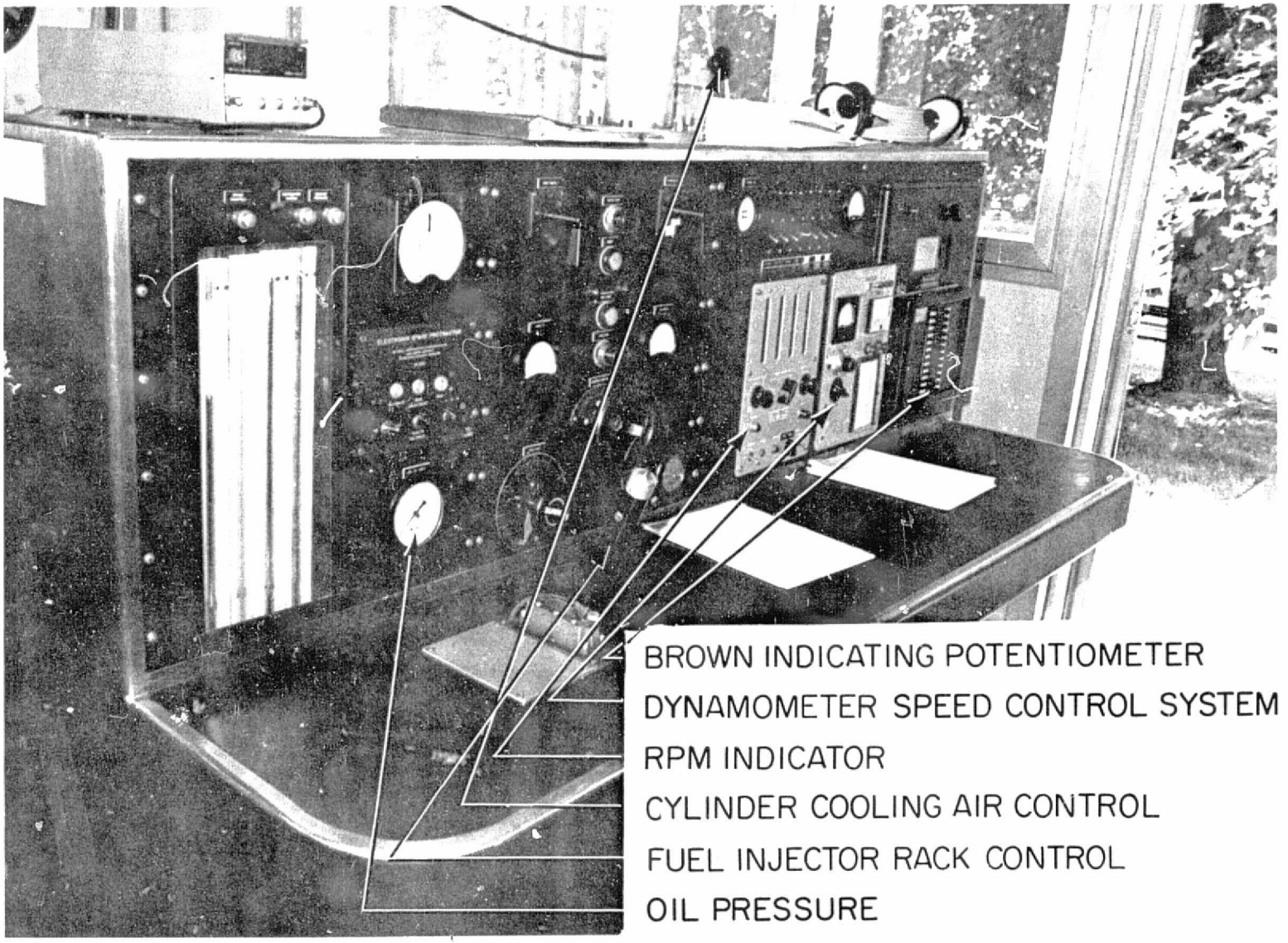

Figure 7. View of Control Console

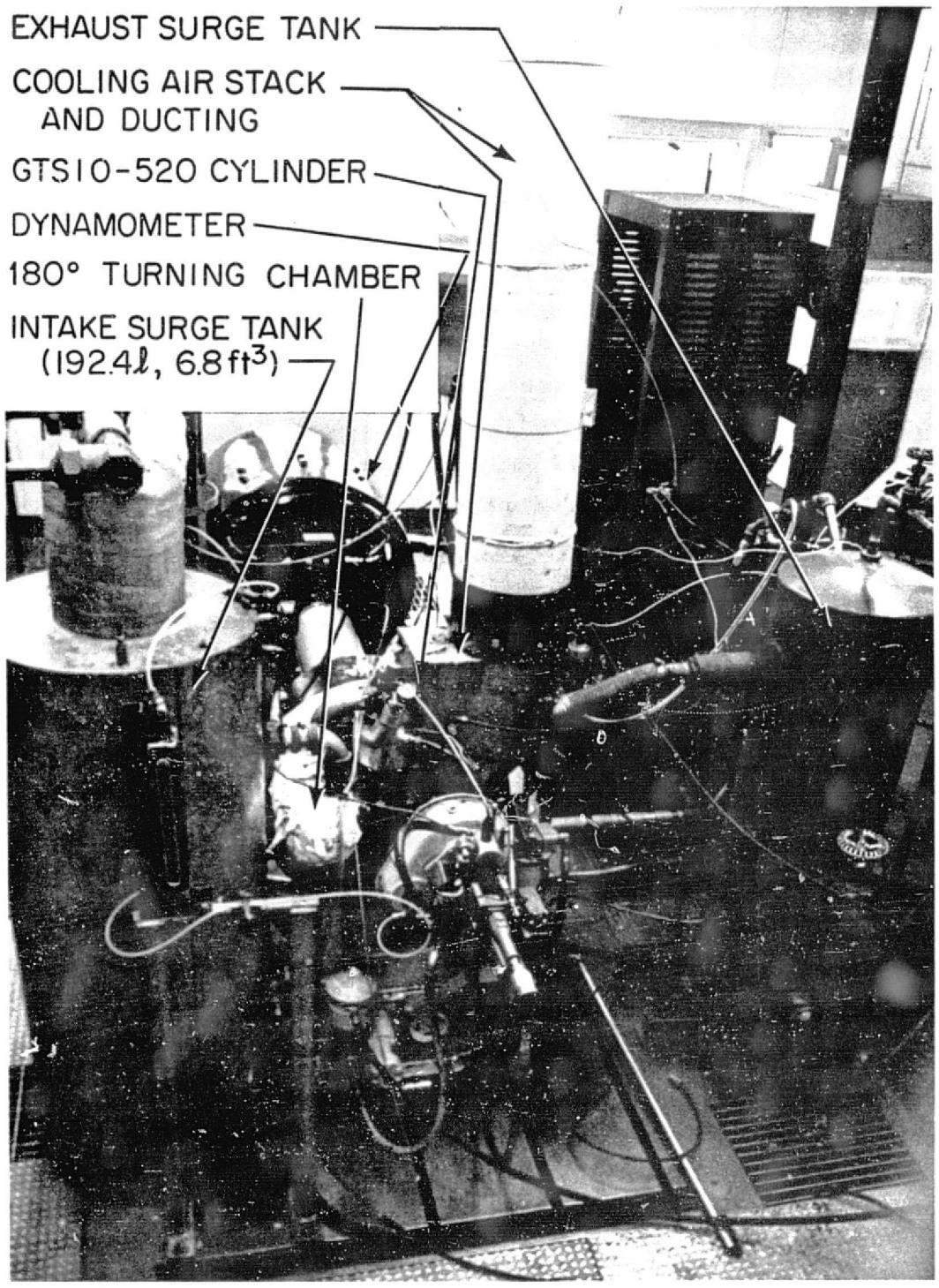

Figure 8. View overlooking Engine Test Installation

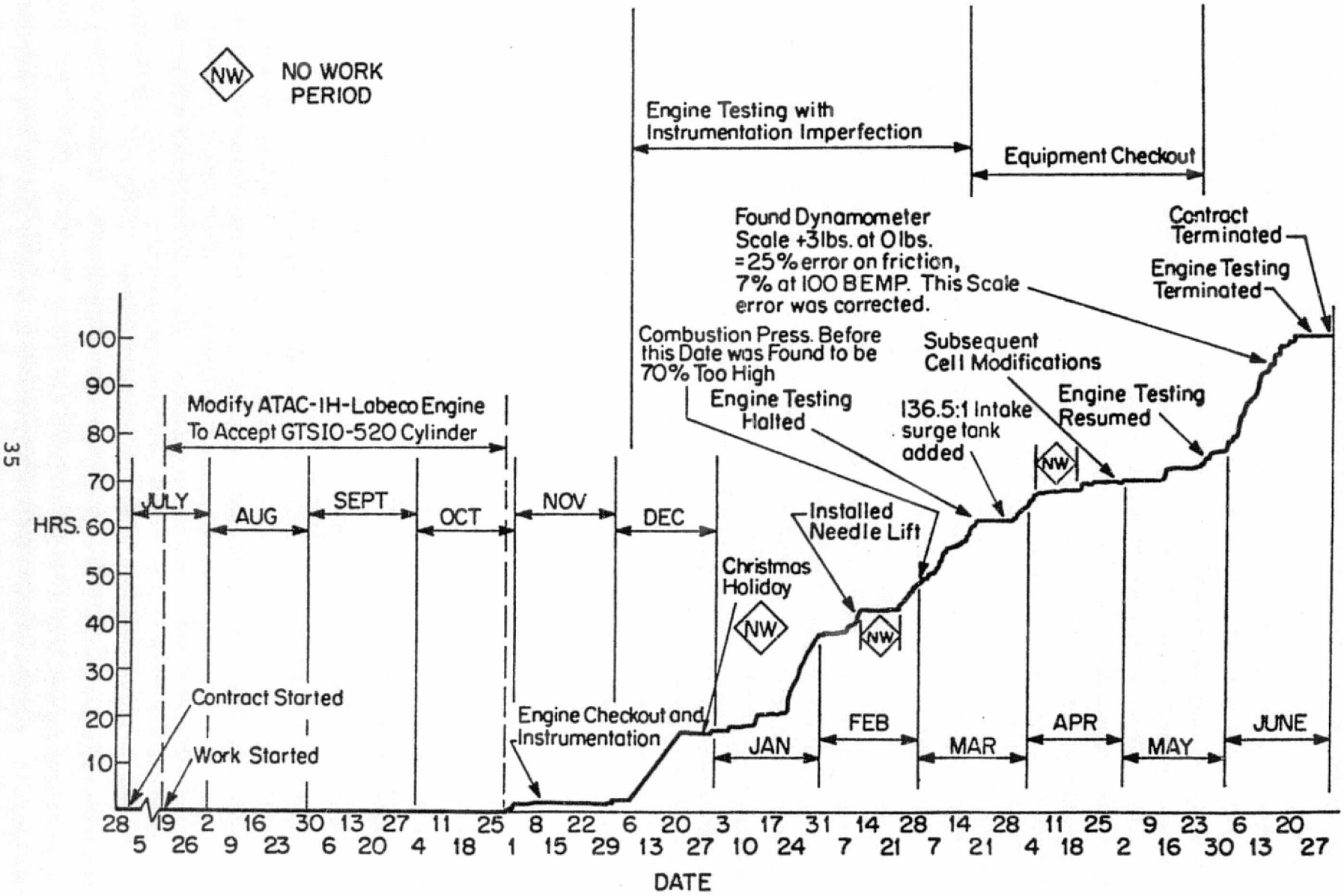

Fig. 9. Engine Firing Time vs DATE: July 1, 1976 to June 30, 1977; Total Firing Time = 100.25 HRS.

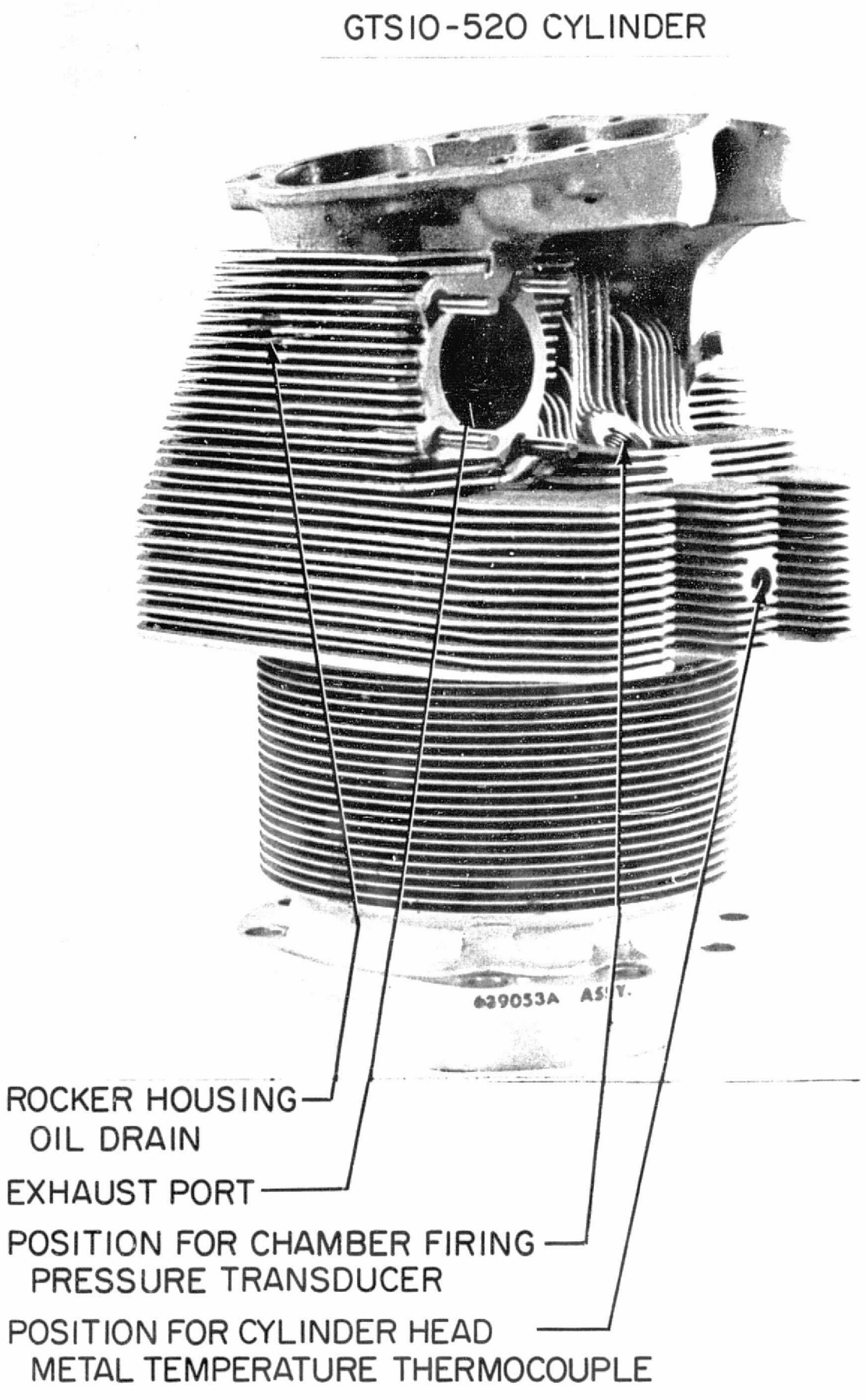

Figure 10 Exhaust Port Side of Modified GTSIO-520 Cylinder Before Assembly

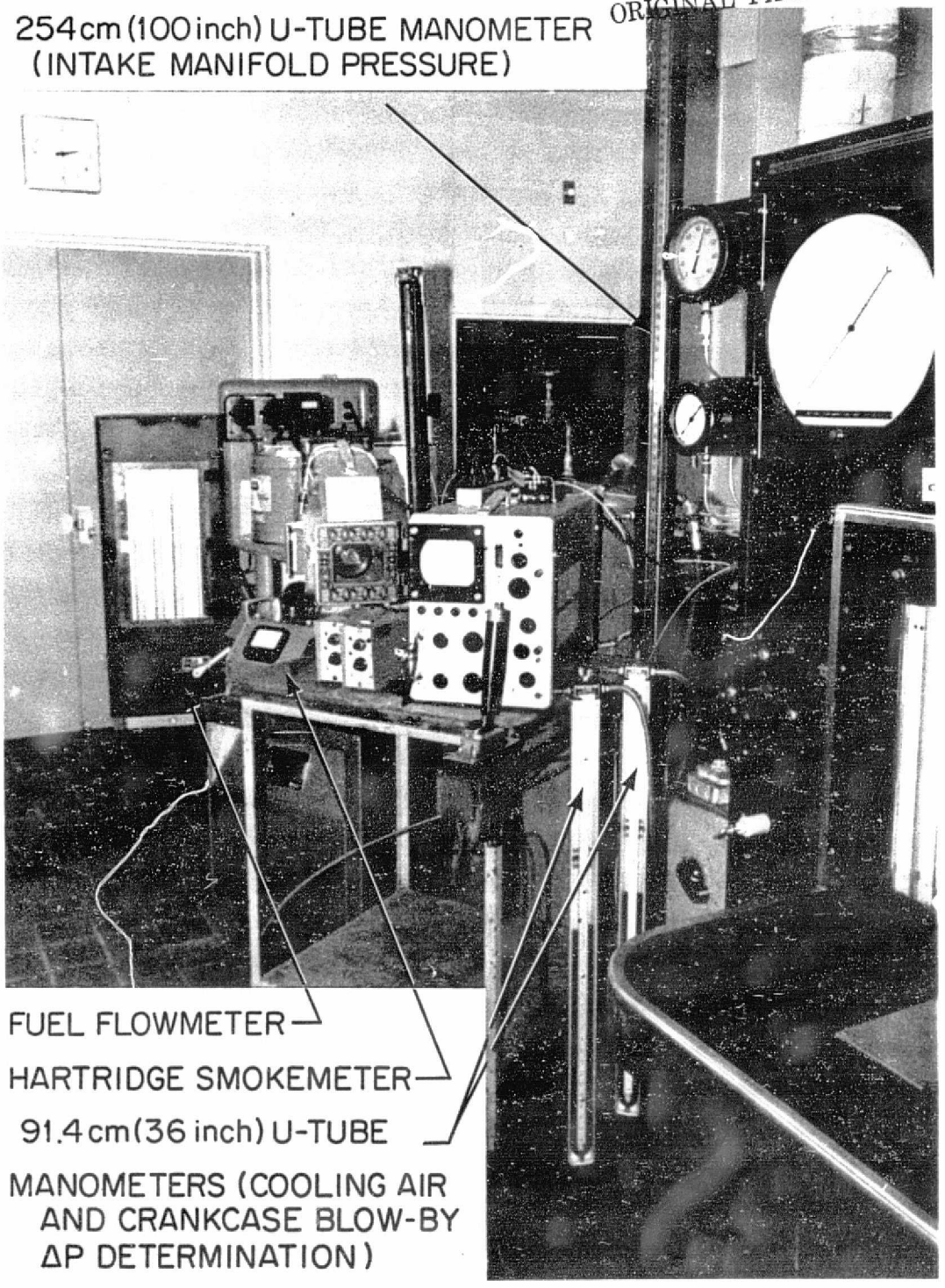

Figure 11. View from Dynamometer as of June 9, 1977

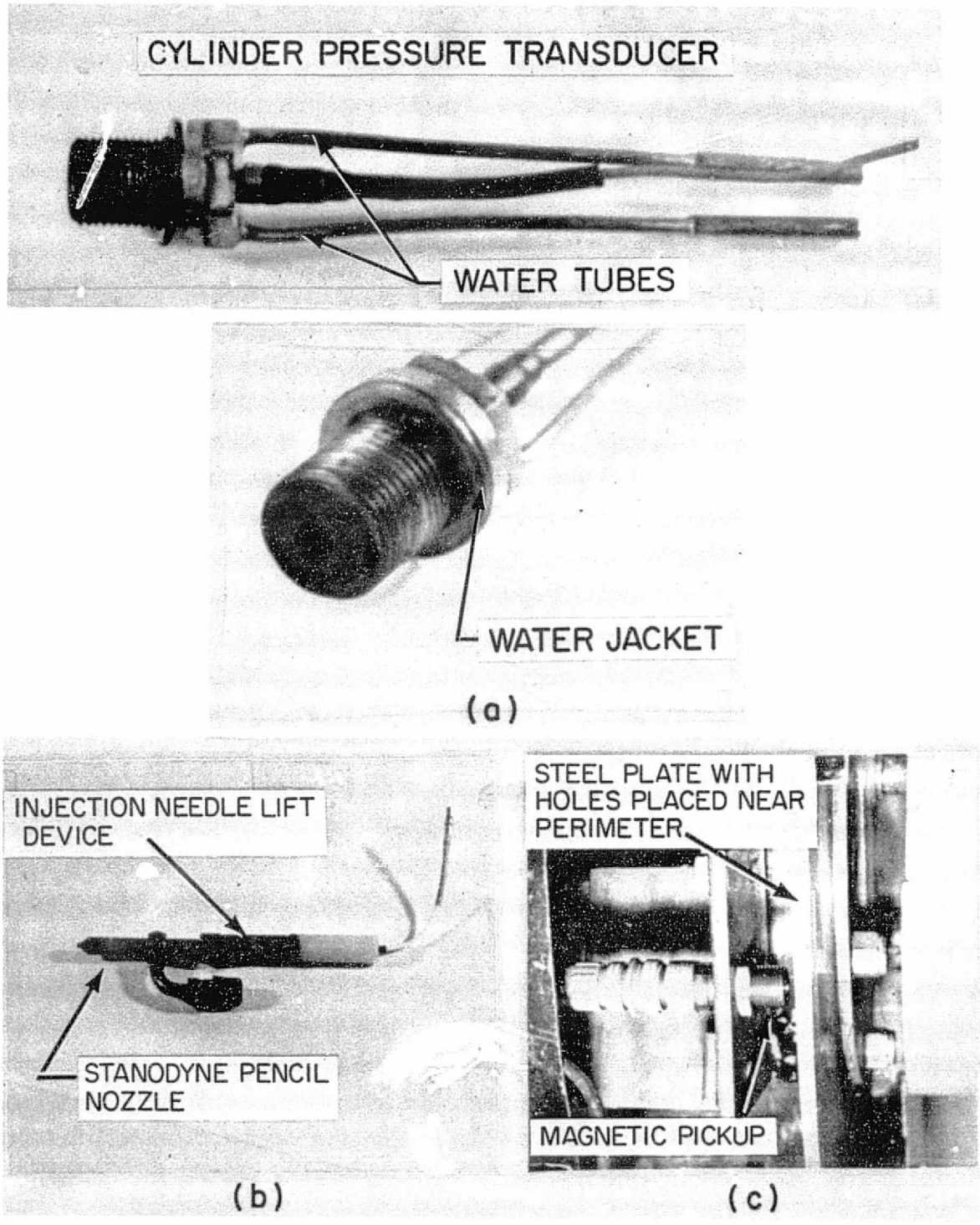

Figure 12. a) Cylinder Pressure Transducer
b) Injection Nozzle with attatched Needle Lift Device
c. Magnetic Pick-up used to determine Crankshaft Rotation

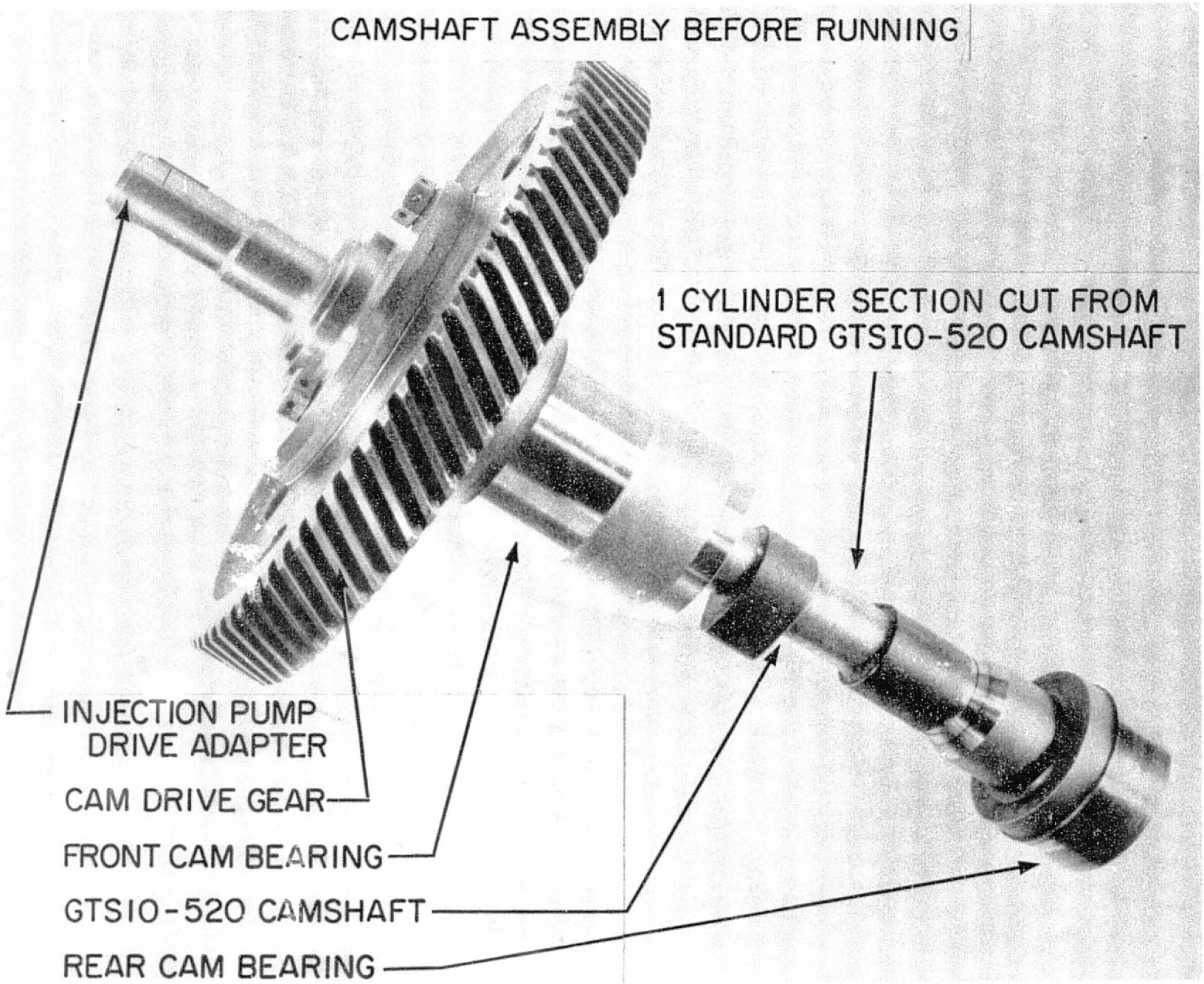

Figure 13. Camshaft Assembly showing GTSIO-520 Camshaft Modified

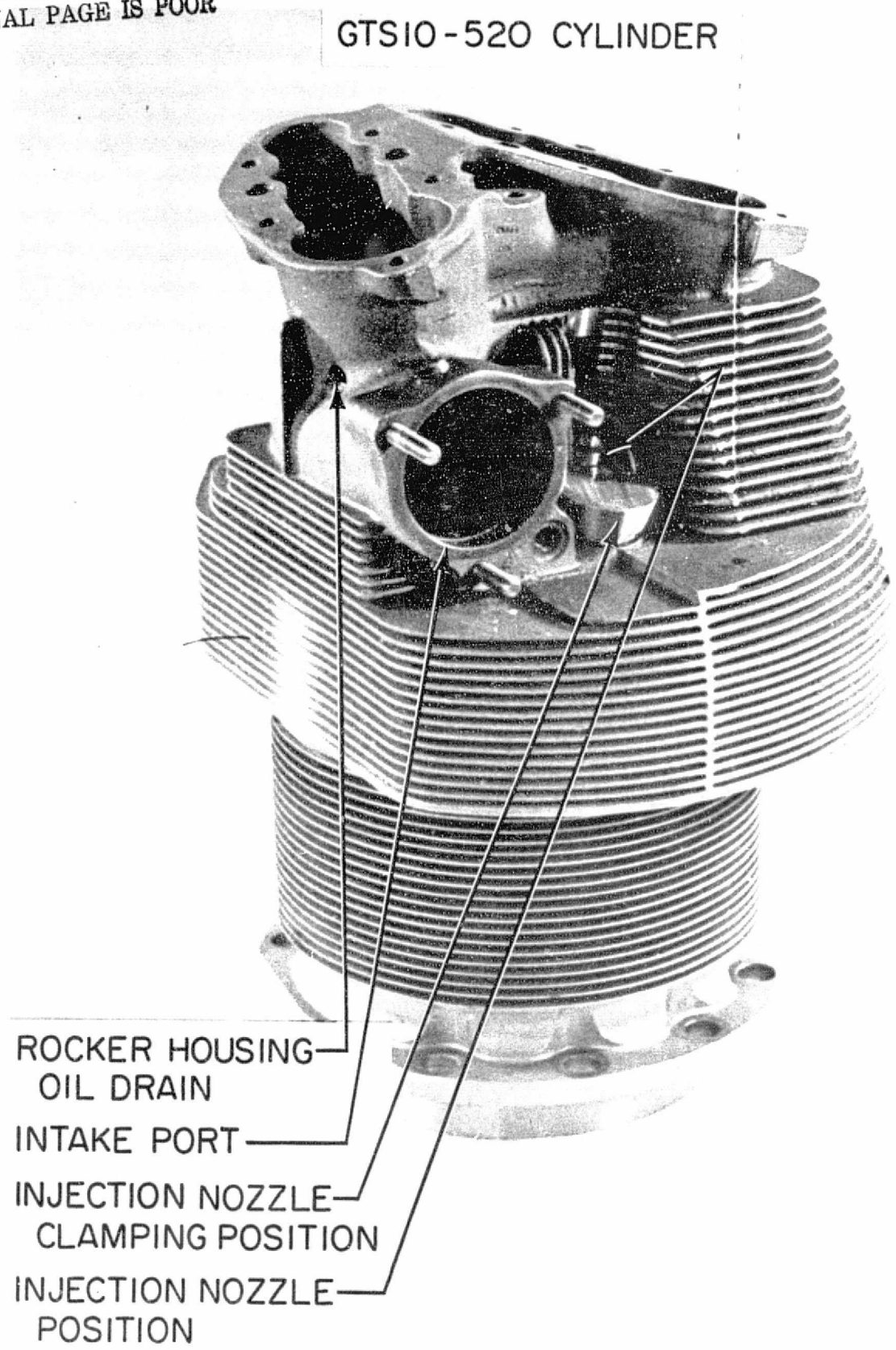

Figure 14. Intake Port Side of Modified GTSIO-520 Cylinder Before Assembly

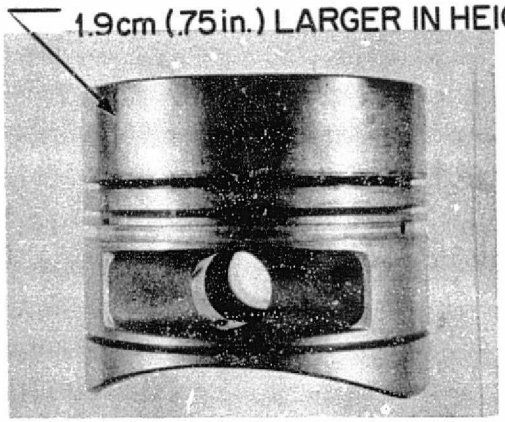

DIESEL PISTON IN SEMI-FINISHED CONDITION

(a)

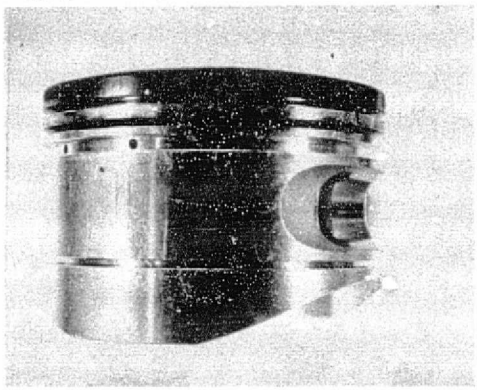

STANDARD GTSIO-520 PISTON (7.5:1 C.R.) AFTER 1.5 HRS. OF FIRING TIME

(b)

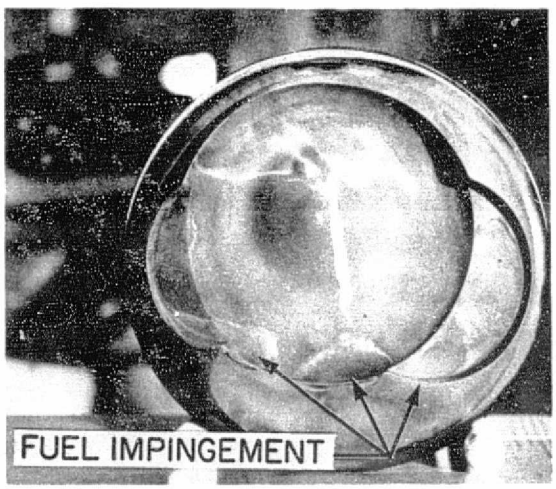

AD-118 PISTON (10:1 C.R.)

(d)

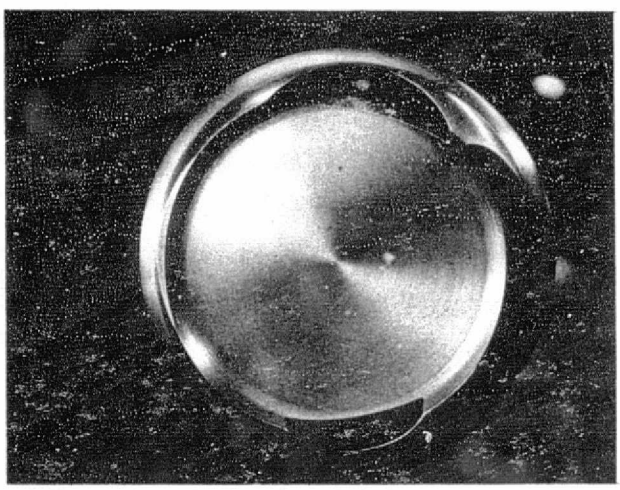

AD-131 PISTON (10:1 C.R.)

(c)

Figure 15. Pistons Used in Engine Testing
a) Diesel Piston Without Combustion Cavity
b) Standard GTSIO-520 Piston (P/N 632491)
c) AD-118 Piston (10:1 CR) Showing Fuel Impingement
d) AD-131 Piston (10:1 CR)

PISTON CROWN CONFIGURATIONS WITH VARIOUS COMPRESSION RATIOS

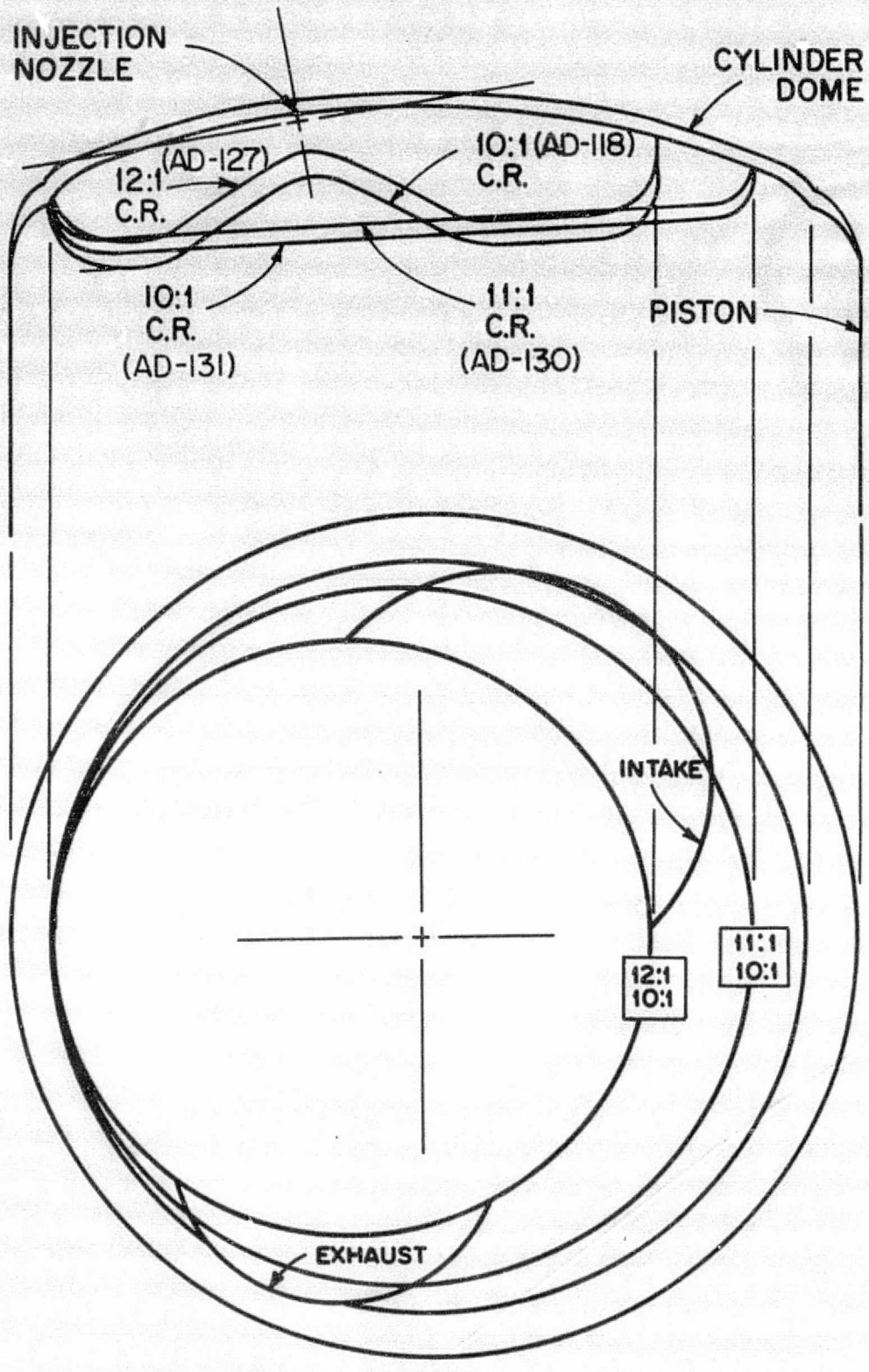

Figure 16. Four Fabricated Piston Configurations

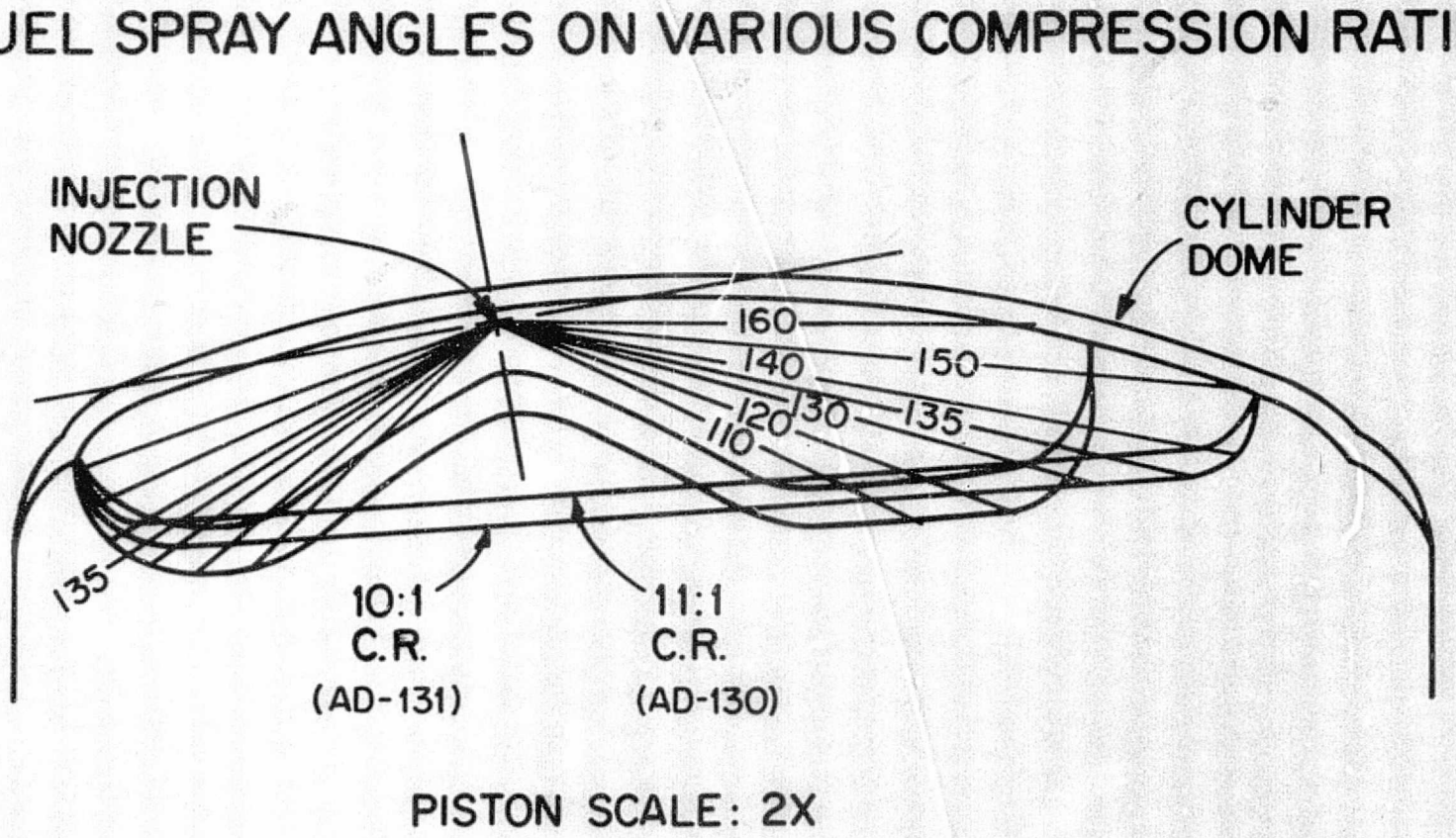

Figure 17. Projected Path of Unperturbed Fuel Spray

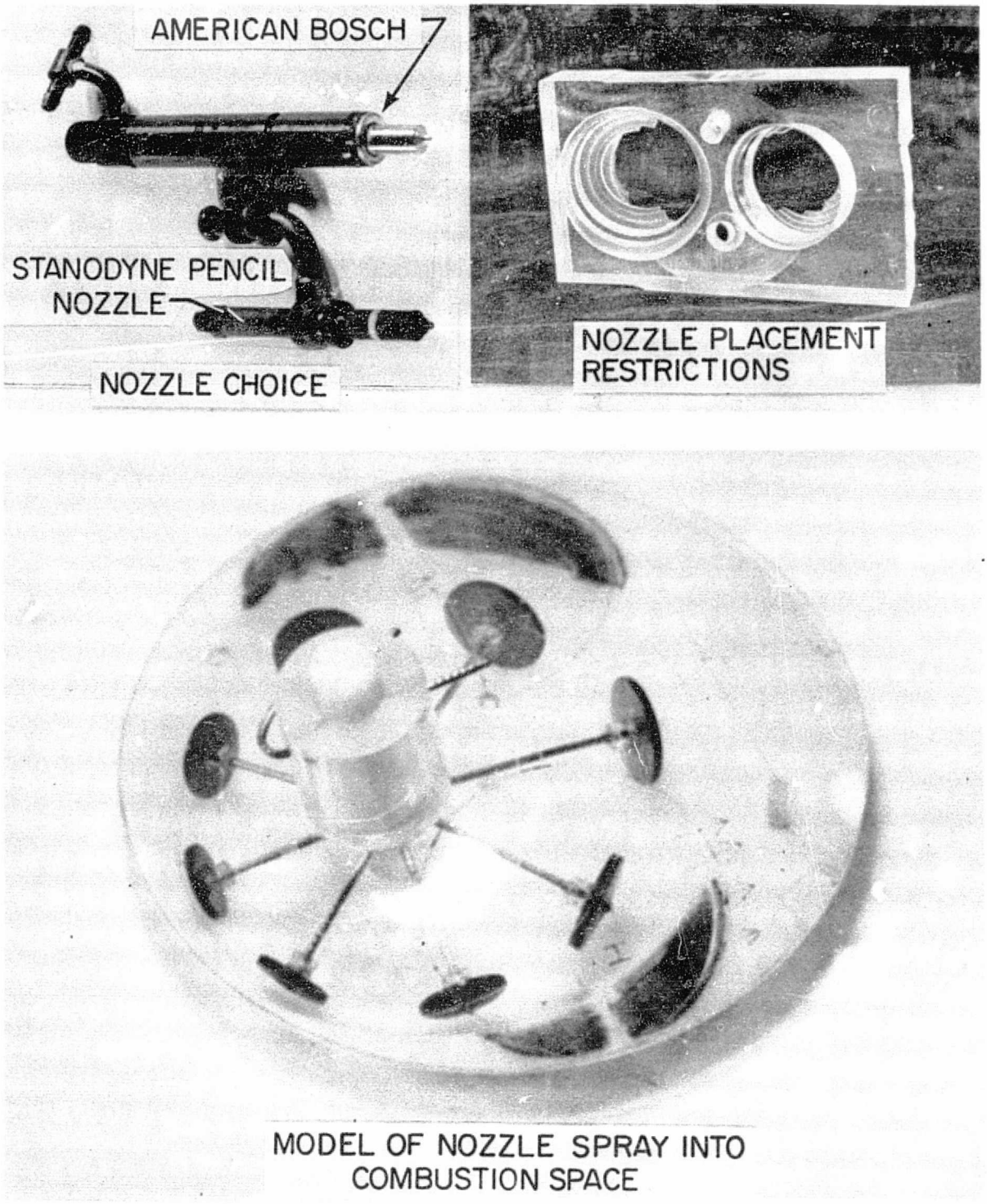

Figure 18. a) Two injection nozzles which can be used in Modified GTSOP-520 Cylinder
b) Nozzle Placement restriction model
c) Three dimensional View of Possible Fuel spray into Combustion space

EFFECT OF FUEL INJECTION NOZZLE SPRAY ANGLES ON ENGINE PERFORMANCE

Fuel Cetane, 47.5
Piston, 10:1 CR (AD-118)
IHP, 45.5 ± 1.3 Hp
Fuel Injection Nozzles, AD-120 to AD-125
RPM, 2500

Induction Air Pressure: 1397 ± 42 mm Hg Abs
Induction Air Temp: 110-121.1°C (230-250°F)

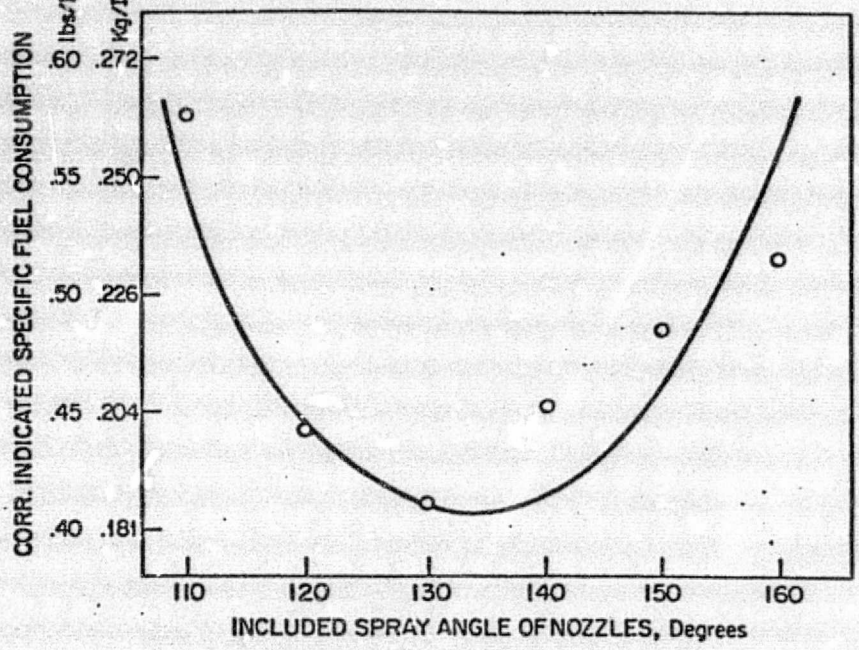

(a)

EFFECT OF INDUCTION AIR PRESSURE AND TEMP. AND RPM ON MOTORING FRICTION

Piston, 10:1 CR (AD-118)
Intake Air Temp: 121.1-126.6°C (250-260°F)

Oil Temp: 46.1-73.3°C (115-164°F)

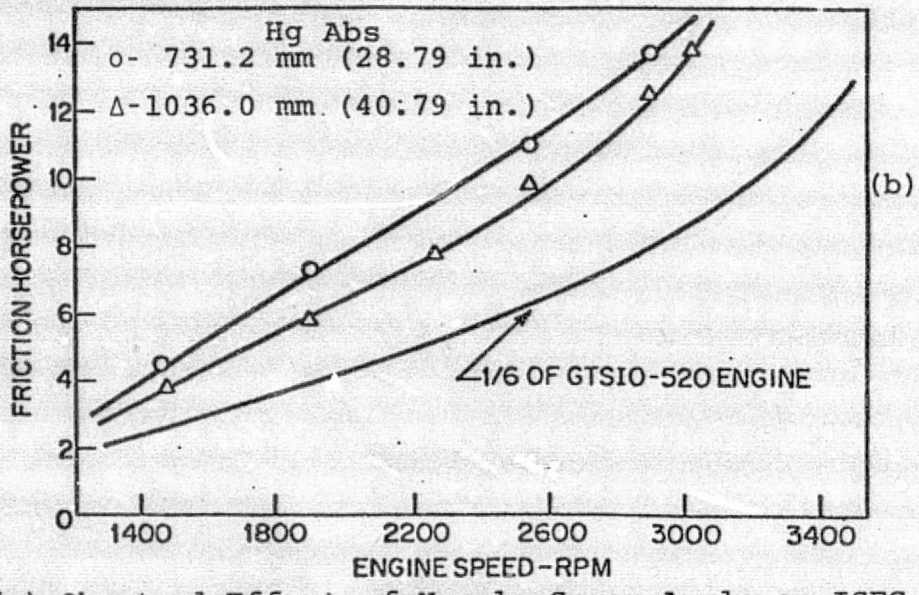

(b)

Figure 19. (a) Observed Effect of Nozzle Spray Angle on ISFC
(b) Observed Effect of Intake Air Pressure Temperature, and RPM on Friction

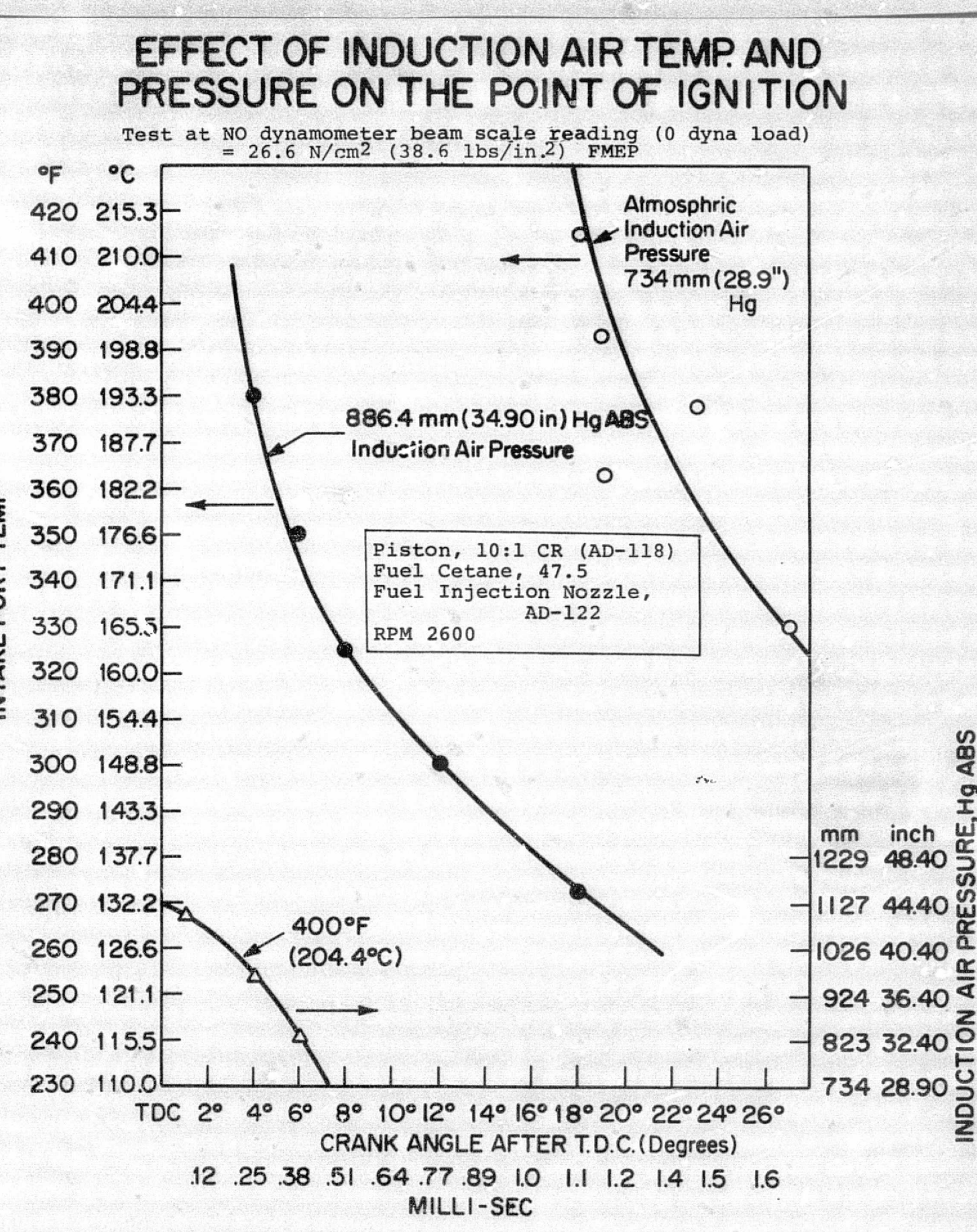

Figure 20. Observed Effect of Intake Air Temperature and Pressure on Point of Ignition

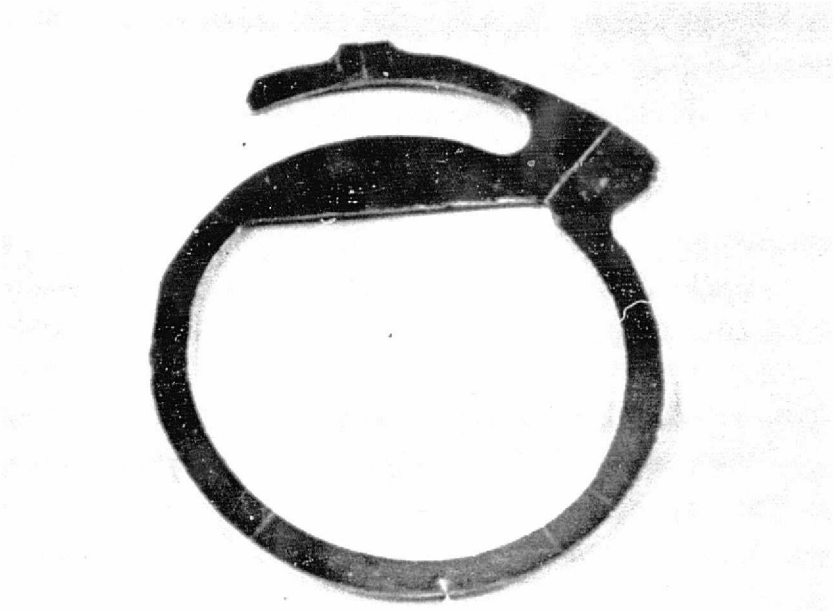

SWIRL PLATE WITH 45° ROTATABLE LIMITATION

(a)

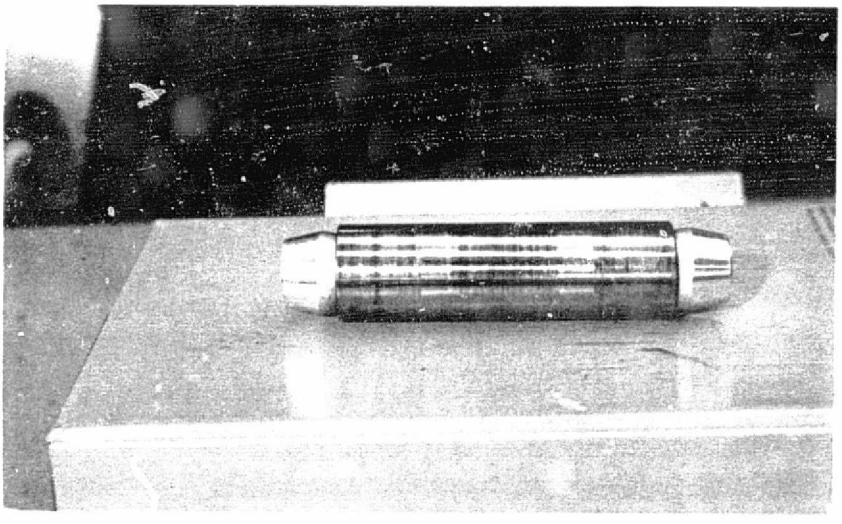

PISTON PIN AFTER 40.7 HRS. FIRING TIME

(b)

Figure 21. a) Swirl Plate Used for Early Swirl Testing
b) Standard GTSIO-520 Piston Pin Showing Normal Wear (P/N 530658)

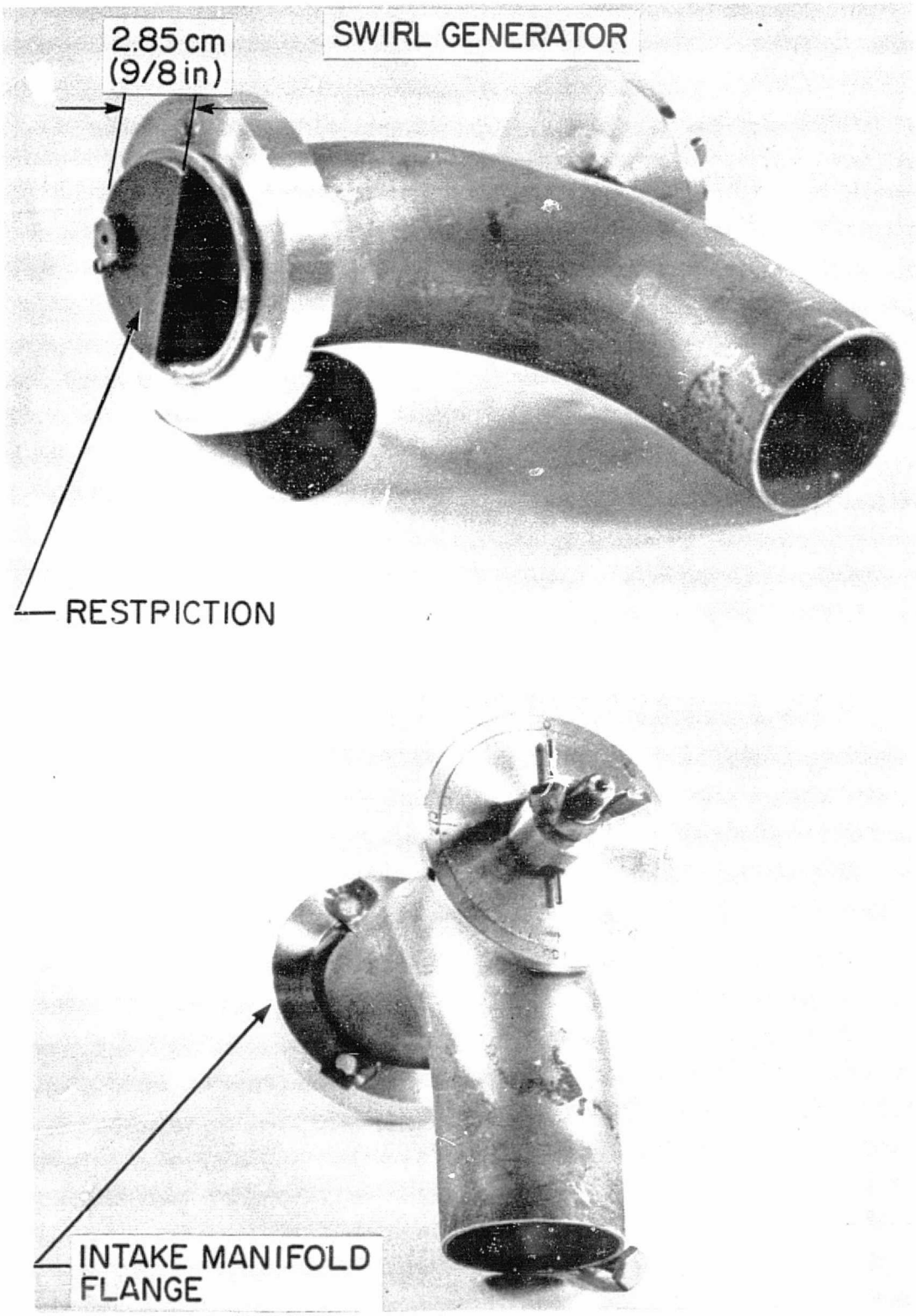

Figure 22. Air Intake to Cylinder with Adjustable Swirl Baffle

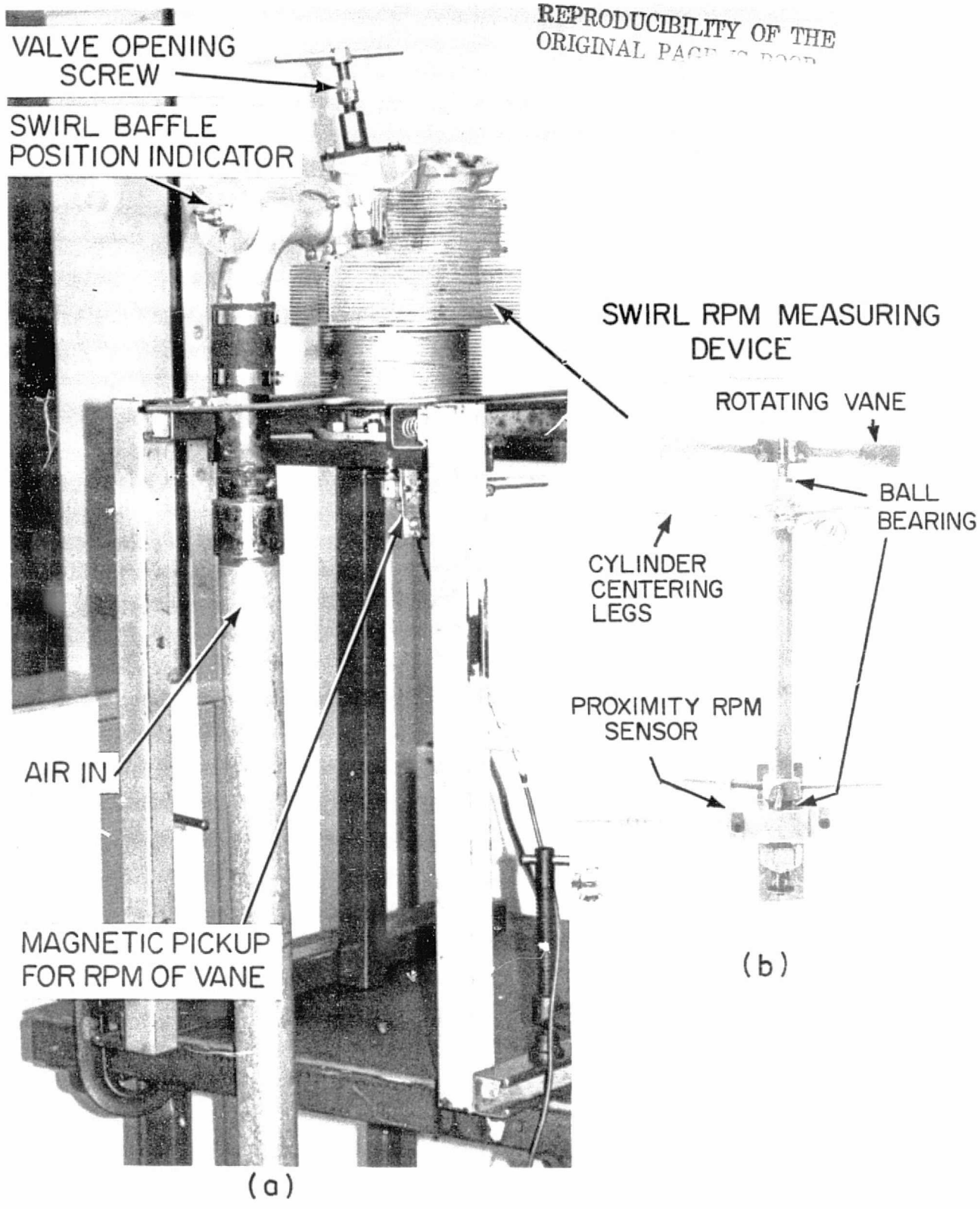

Figure 23. (a) Bench Arrangement to Determine Air Swirl
ΔP = 50.8 mm (2 in. Hg)
(b) Vane used to Determine Swirl

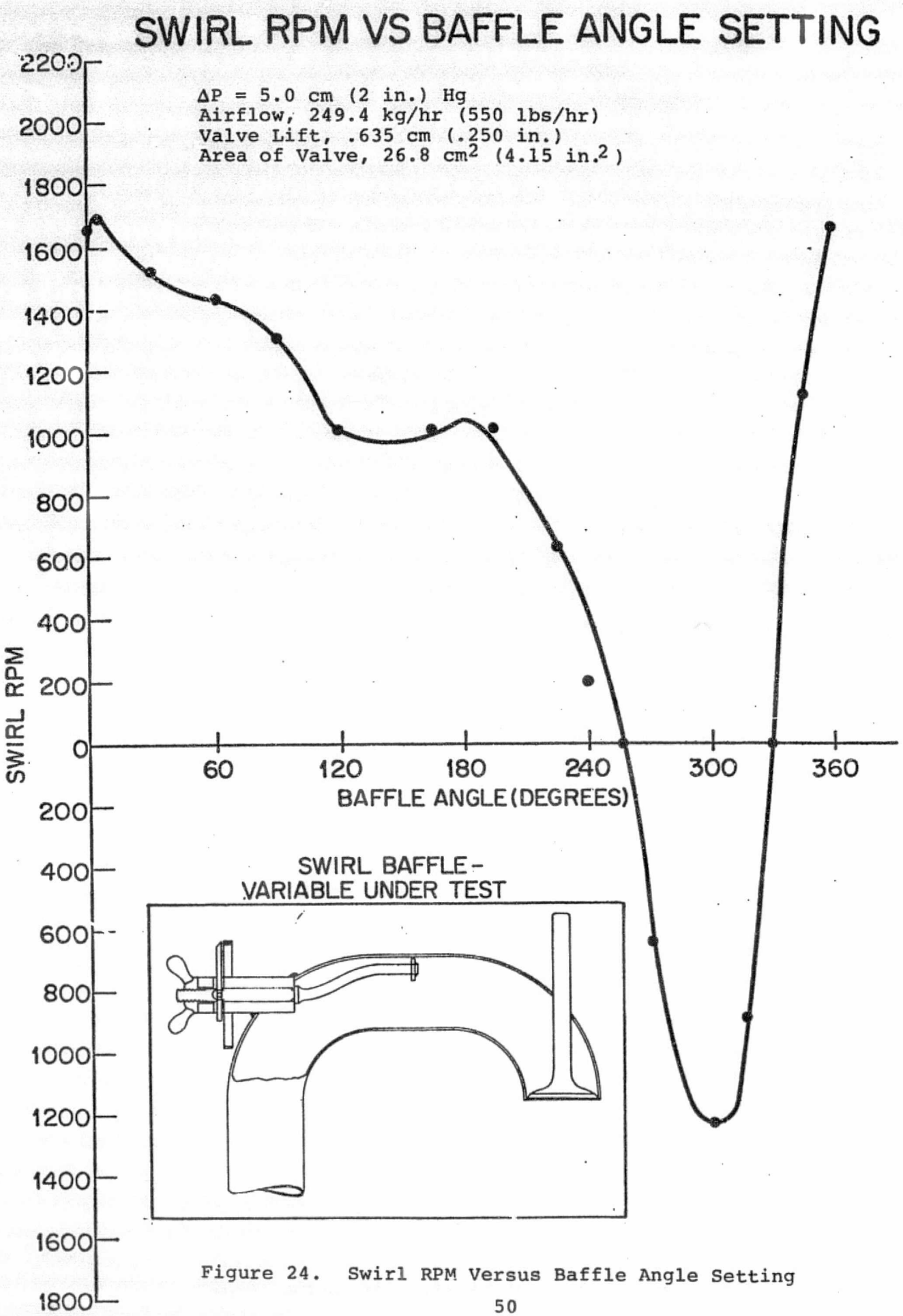

Figure 24. Swirl RPM Versus Baffle Angle Setting

EFFECT OF 11:1 C.R. (AD-130) PISTON ON ENGINE PERFORMANCE

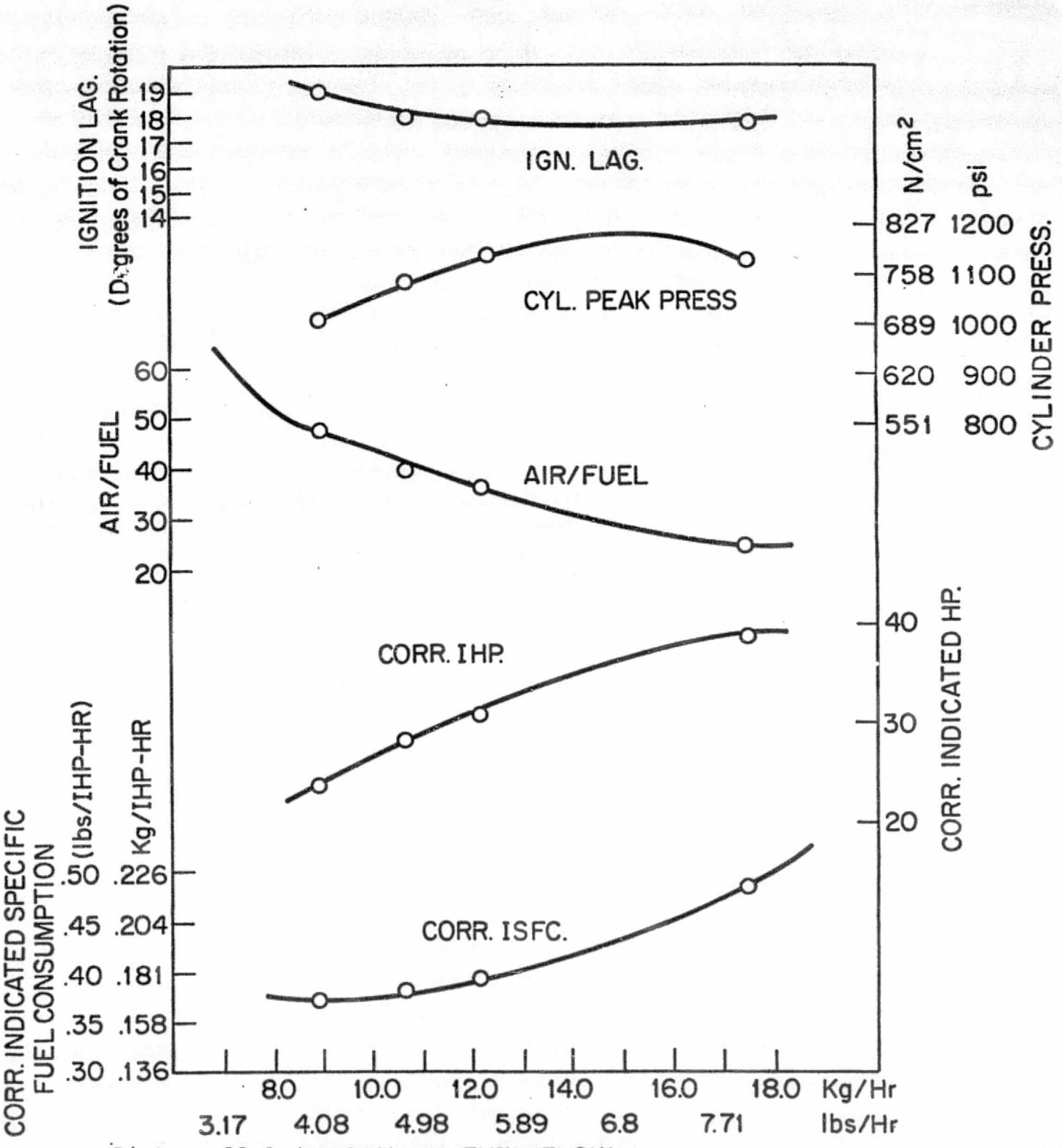

Piston, 11:1 (AD-130)
Cetane 47.5
Induction Air Temp:
107-121°C (225-250°F)
RPM 2600
Fuel Injection Nozzle, AD-129
Induction Air Pressure:
1490 mm (58.66 in.) Hg Abs

Figure 25. Performance of 11:1 CR Piston (AD-130)

EFFECT OF 10:1 CR (AD-131) PISTON ON ENGINE PERFORMANCE

Fuel Cetane, 47.5
Piston, 10:1 CR (AD-131)
Fuel Injection Nozzle, AD-129
RPM 2600

Induction Air Temp:
118.3°C (245°F)
Induction Air Pressure:
904-1844 mm
(35.6-72.6 in.) Hg Abs.

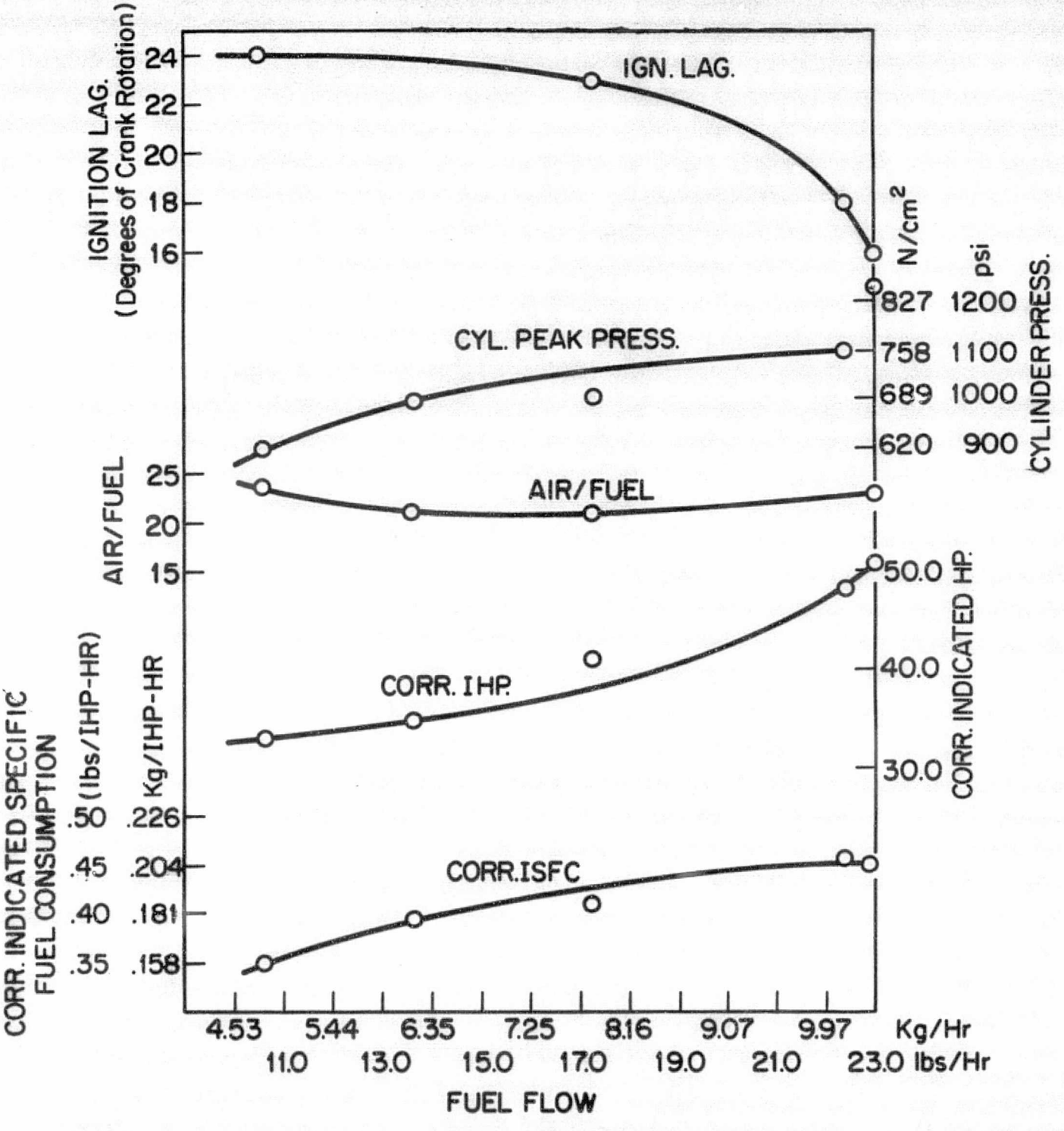

Figure 26. Performance of 10:1 CR Piston (AD-131)

EFFECT OF CETANE VALUE ON ENGINE PERFORMANCE

o - C-B Fuel - 47.5 CETANE
Δ - Reference Fuel - 71 CETANE
Piston, 11:1 CR (AD-130)
Fuel Injection Nozzle, AD-129
Induction Air Temp:
107.2-121.1°C (225-250°F)
RPM 2600
Induction Air Pressure:
1495 mm Hg Abs (58.86 in.)

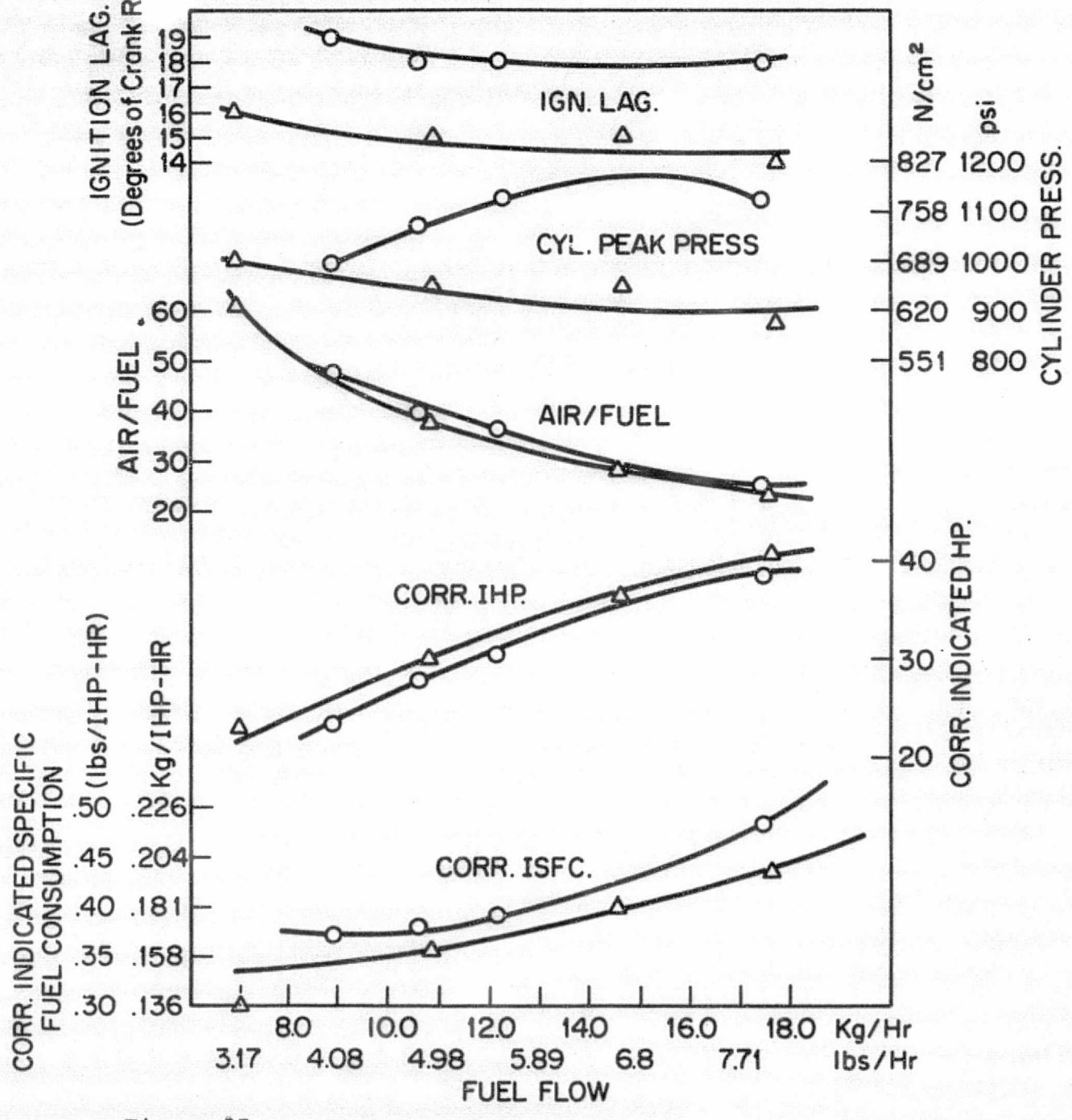

Figure 27. Comparison of Engine Performance with Variation in Fuel Cetane Rating

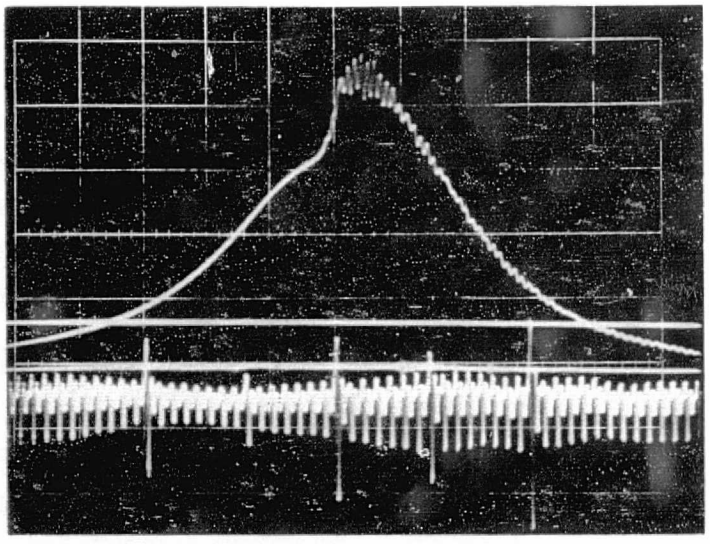

RPM	2611
IHP	35.8
IMEP	86.4 N/cm^2
ISFC	.220 kg/IHP-Hr
Cyl Pres	775 N/cm^2
Ignition	4° BTC
Air/Fuel	25.2

TYPE C-B DIESEL FUEL OIL
47 CETANE

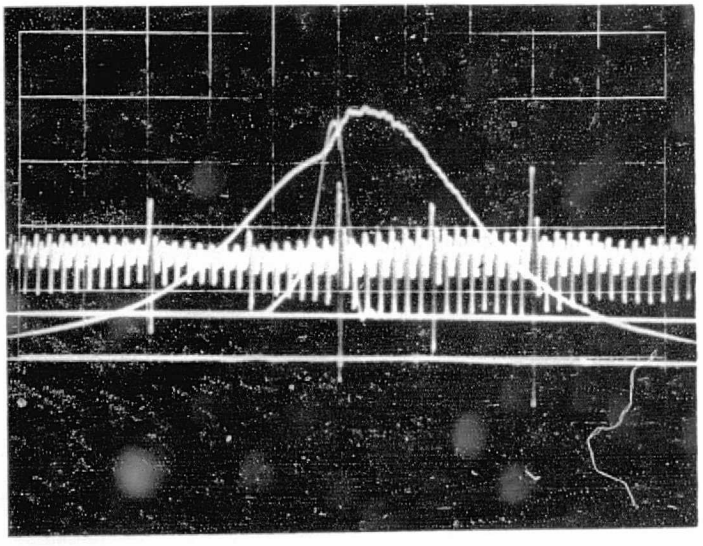

RPM	2610
IHP	36.3
IMEP	87.5 N/cm^2
ISFC	.181
Cyl Pres	654 N/cm^2
Ignition	4° BTC
Air/Fuel	29.0

REFERENCE FUEL - 71 CETANE

Vertical Scale is 172 N/cm^2
(250 psi/cm)

Horizontal Scale is 3° Crankshaft
Rotation/Increment

Figure 28. 47 Cetane Fuel Versus 71 Cetane Fuel

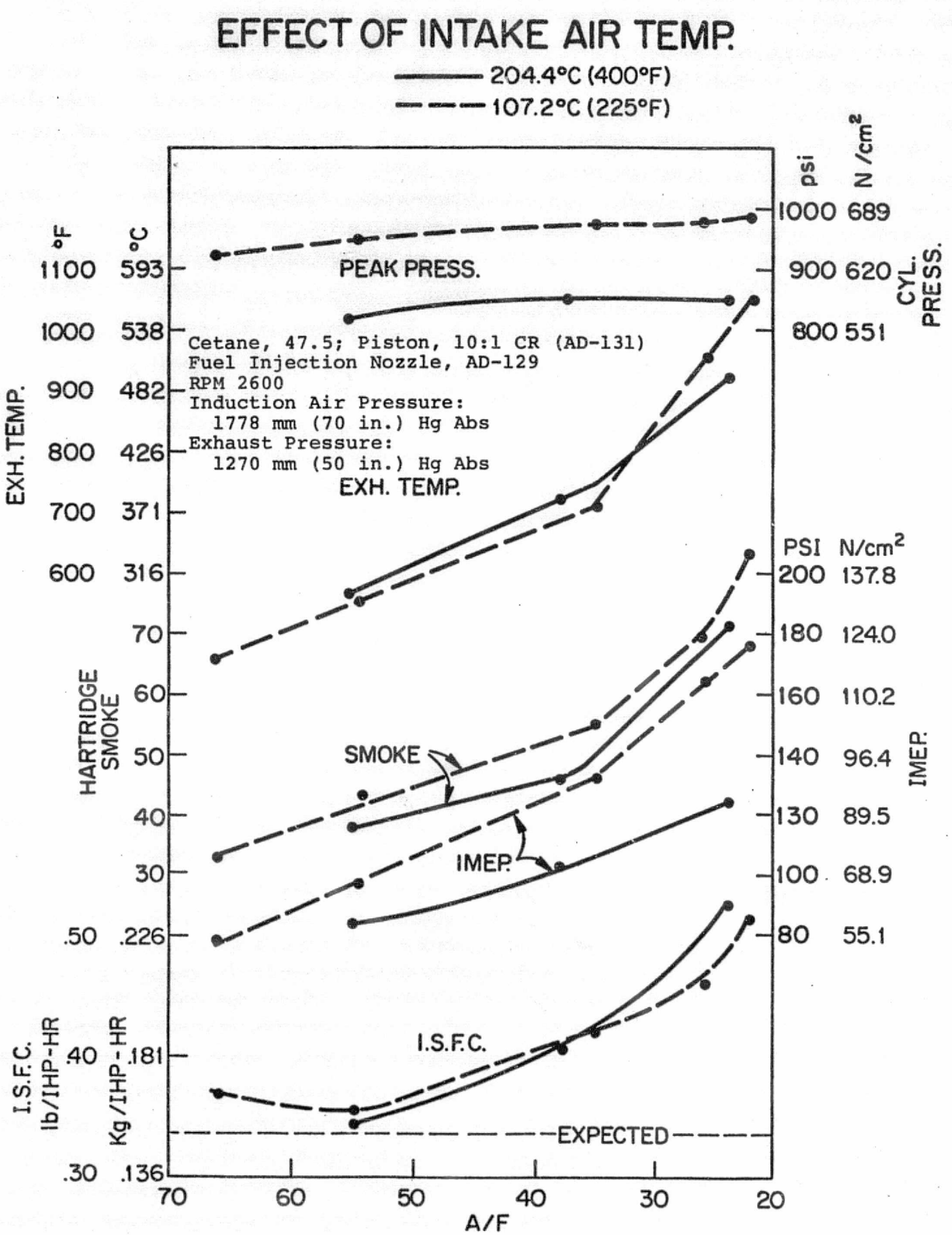

Figure 29. Effect of Intake Air Temperature on Engine Performance

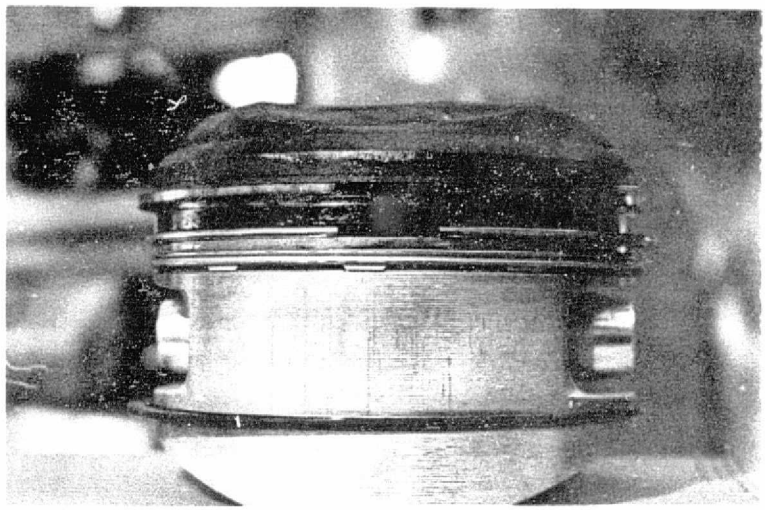

ANTI-THRUST SIDE

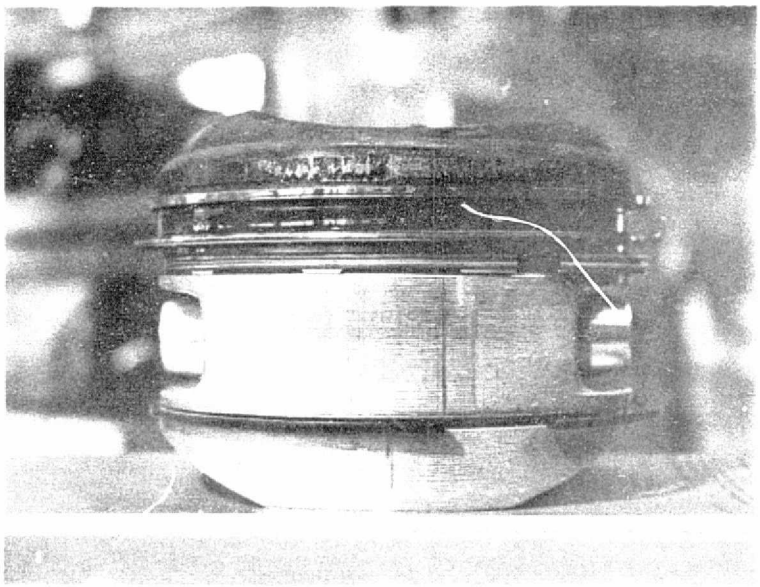

THRUST SIDE

AD-118 PISTON (10:1 C.R.) AFTER 40.7 HRS.

Figure 30. AD-118 Piston Showing Minor Skuffing of the Top Land on the Thrust Side

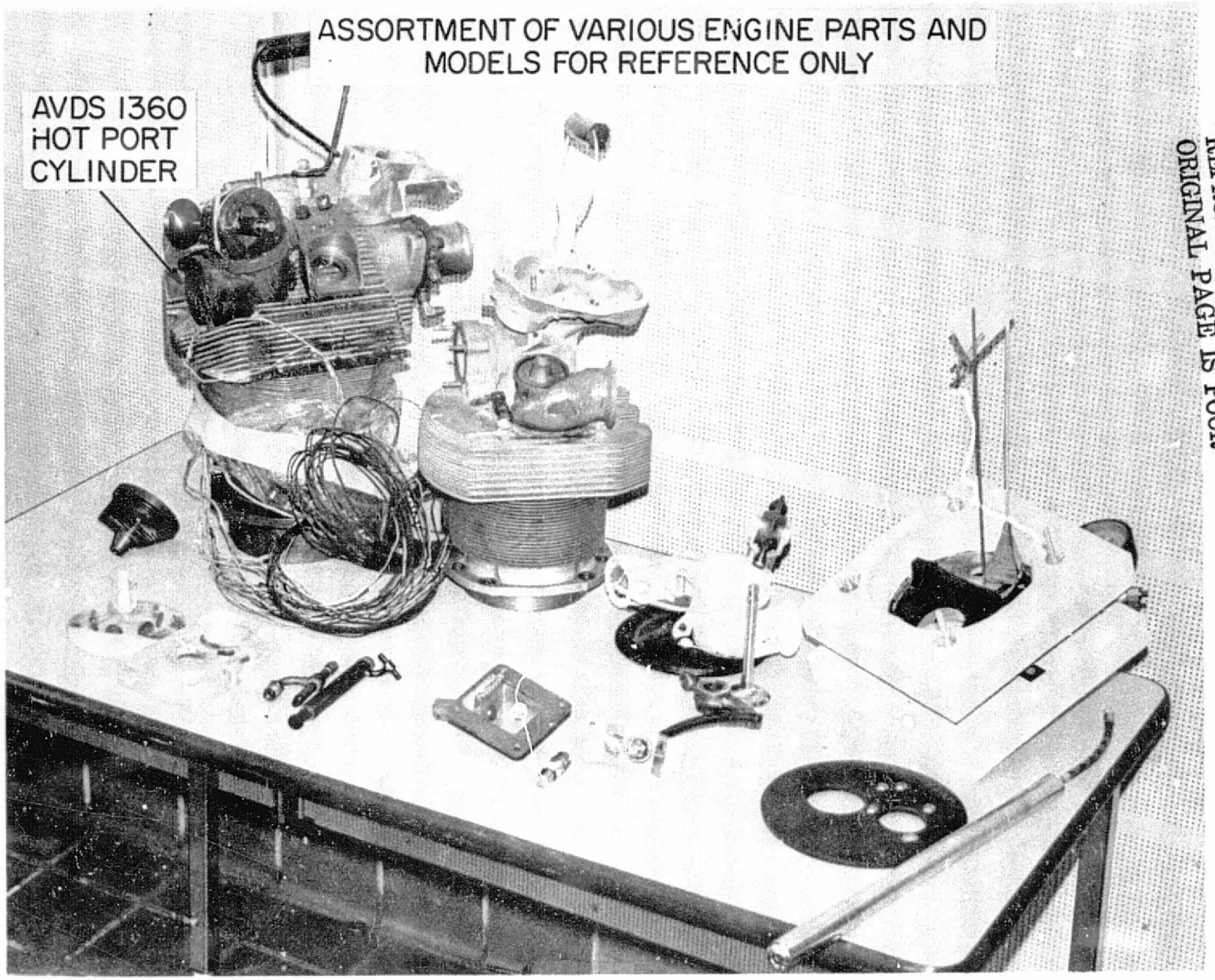

Figure 31. Various Hot Port Engine Parts and Models

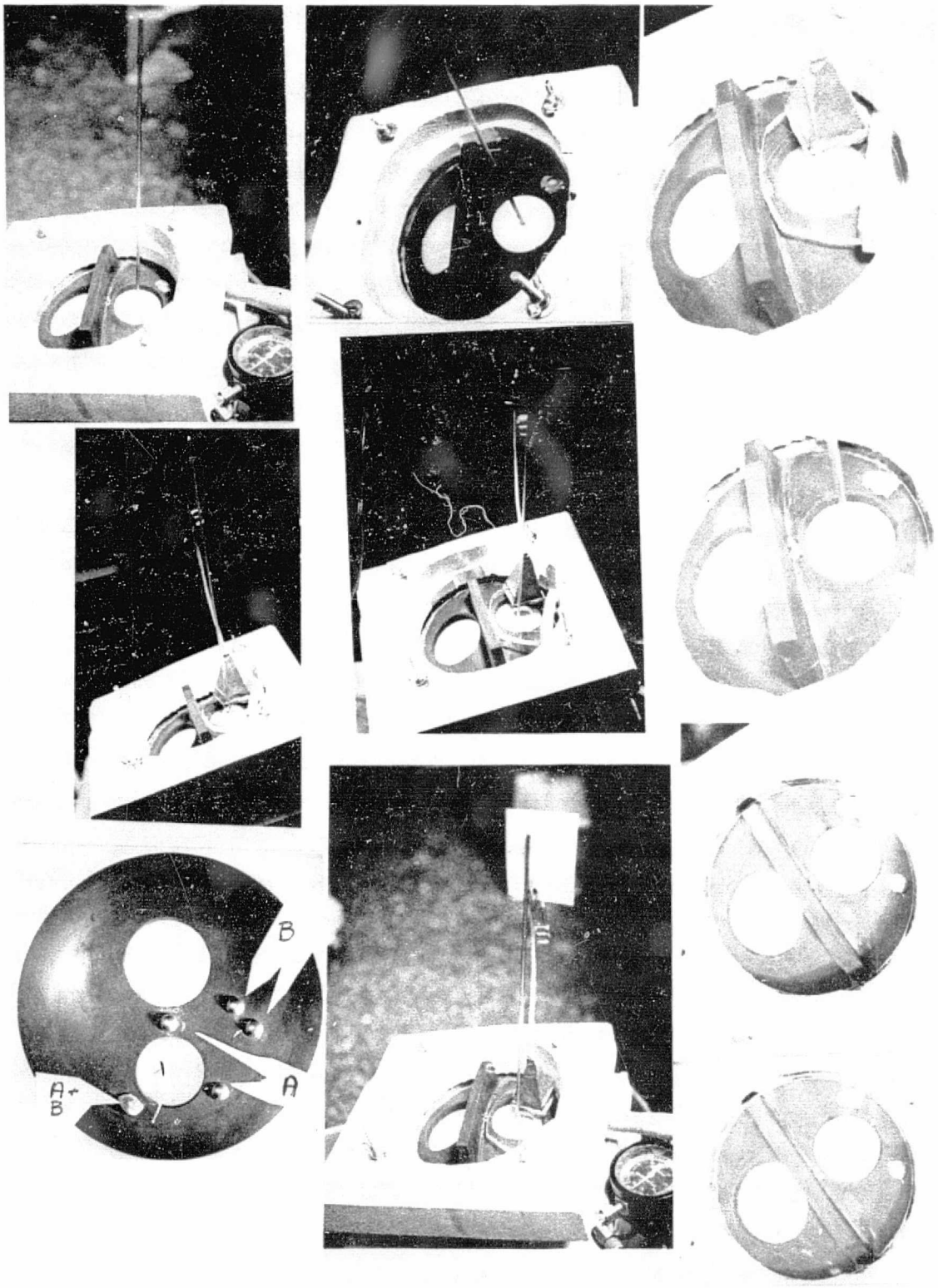

A rubber dome 6.25 mm (.25 in) thick was clamped between two surfaces and air pressure up to 4.13 Nt/cm^2 (6 psi) was applied. One 35.5 cm (14 in.) pointer was responsive to valve seat in the head movement, and the 2nd pointer moved with the dome distortion. Valve guide structure attachement at point "B" give 16 times more relative movement than did "A".

Figure 32. Rubber Dome Model Study

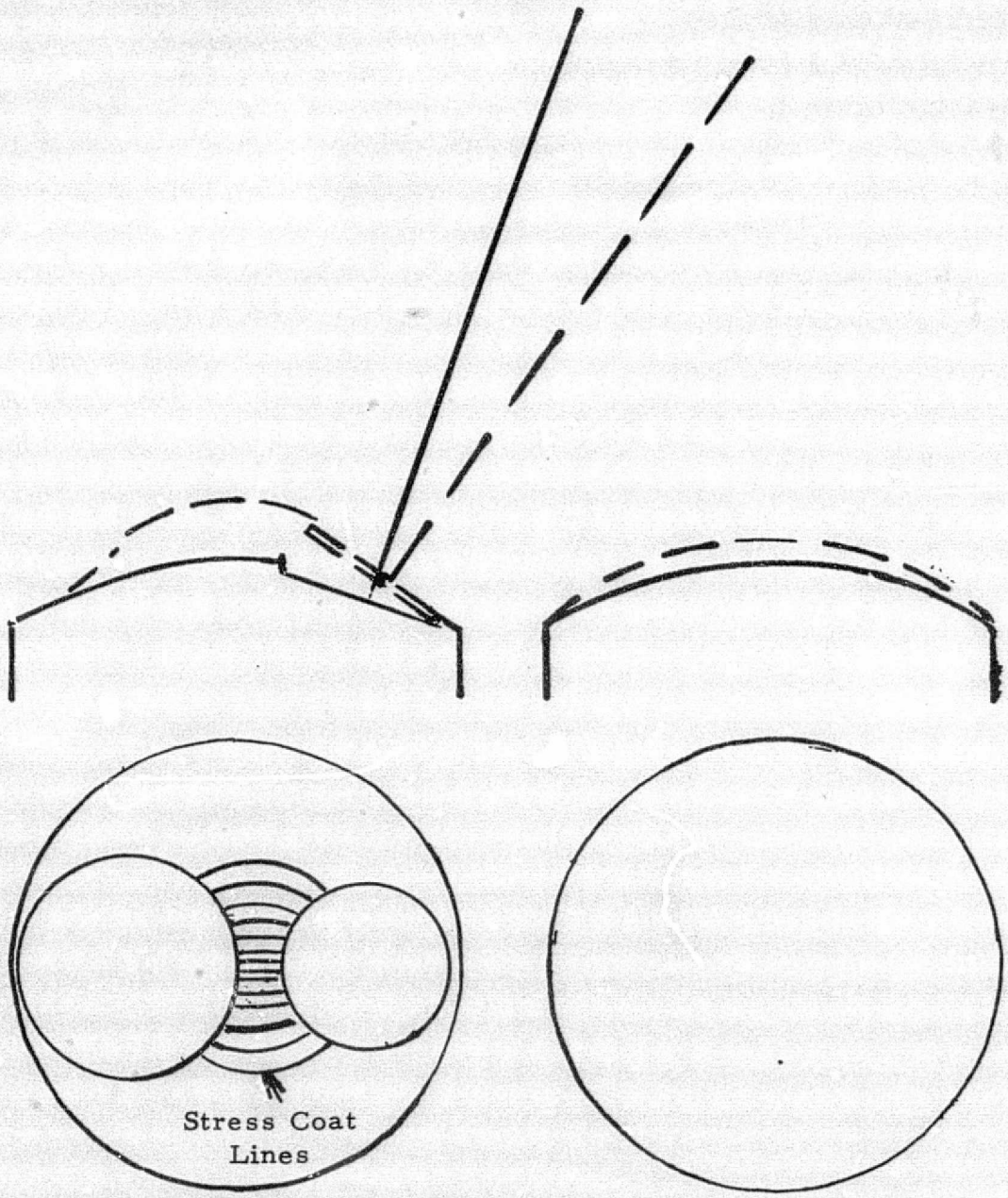

With Valve Cut Outs

High Distortion at Center
Between Valves

No Valve Cut Outs

Low Distortion at Center

Figure 33. Dome Distortion from Combustion Pressure

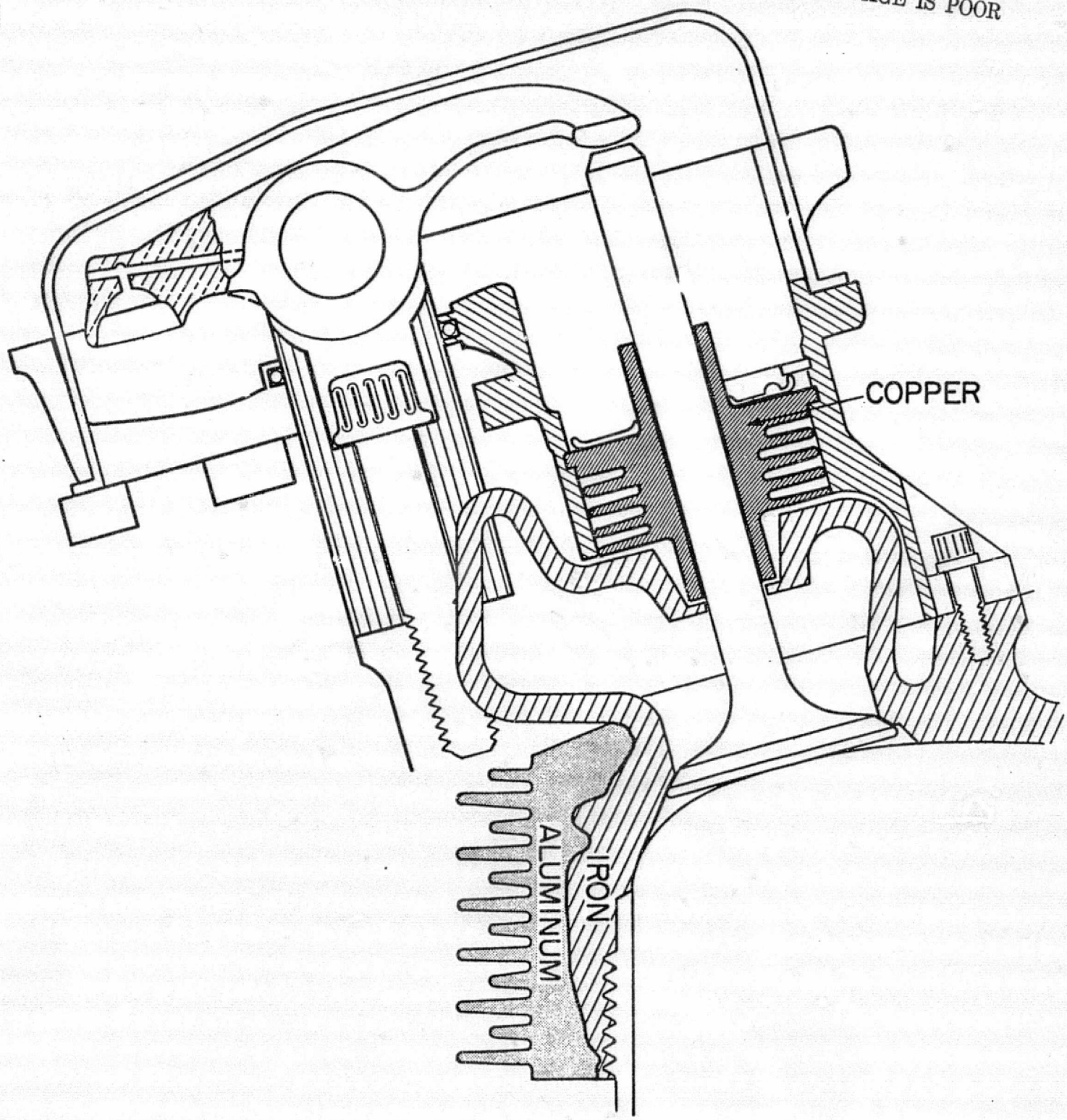

Figure 34. Sketch Representation of Hot Port Model

Figure 35. Wood and Plastic Model of the Hot Port Cylinder Used for Preliminary Design Studies

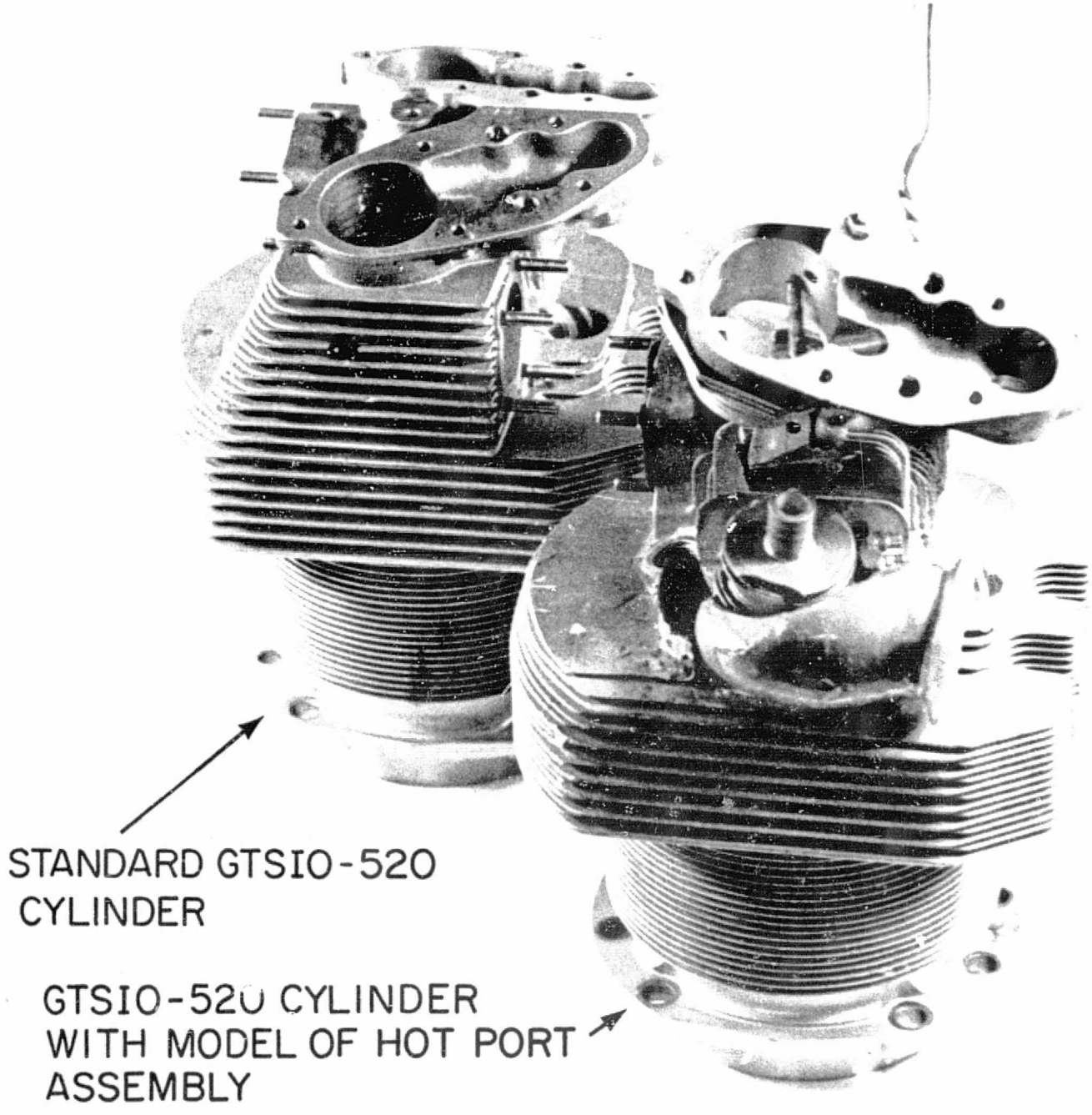

Figure 36. Hot Port Model Compared to standard GRSIO-520 Cylinder

GROSS WEIGHT = 3,380 kg (7450 lb) PASSENGERS = 6

FUSELAGE	LENGTH	10.23 m	33.57 ft
	WIDTH	1.52 m	5.00 ft
	WETTED AREA	39.2 m^2	422.0 ft^2
WING	ASPECT RATIO	7.37	7.37
	AREA	19.7 m^2	211.6 ft^2
	QUARTER CHORD SWEEP	0.0 deg	0.0 deg
	TAPER RATIO	0.653	0.653
	WING LOADING	171.8 kg/m^2	35.2 lb/ft^2
	MEAN GEOM. CHORD	1.66 m	5.44 ft
	WING FUEL VOLUME	1.4 m^3	48.1 ft^3
HORIZ. TAIL	ASPECT RATIO	4.76	4.76
	AREA	5.6 m^2	60.7 ft^2
	MEAN GEOM. CHORD	1.11 m	3.63 ft
	VOLUME COEFF.	1.058	1.058
VERT. TAIL	ASPECT RATIO	1.17	1.17
	AREA	4.5 m^2	48.0 ft^2
	MEAN GEOM. CHORD	2.04 m	6.68 ft
	VOLUME COEFF.	0.122	0.122

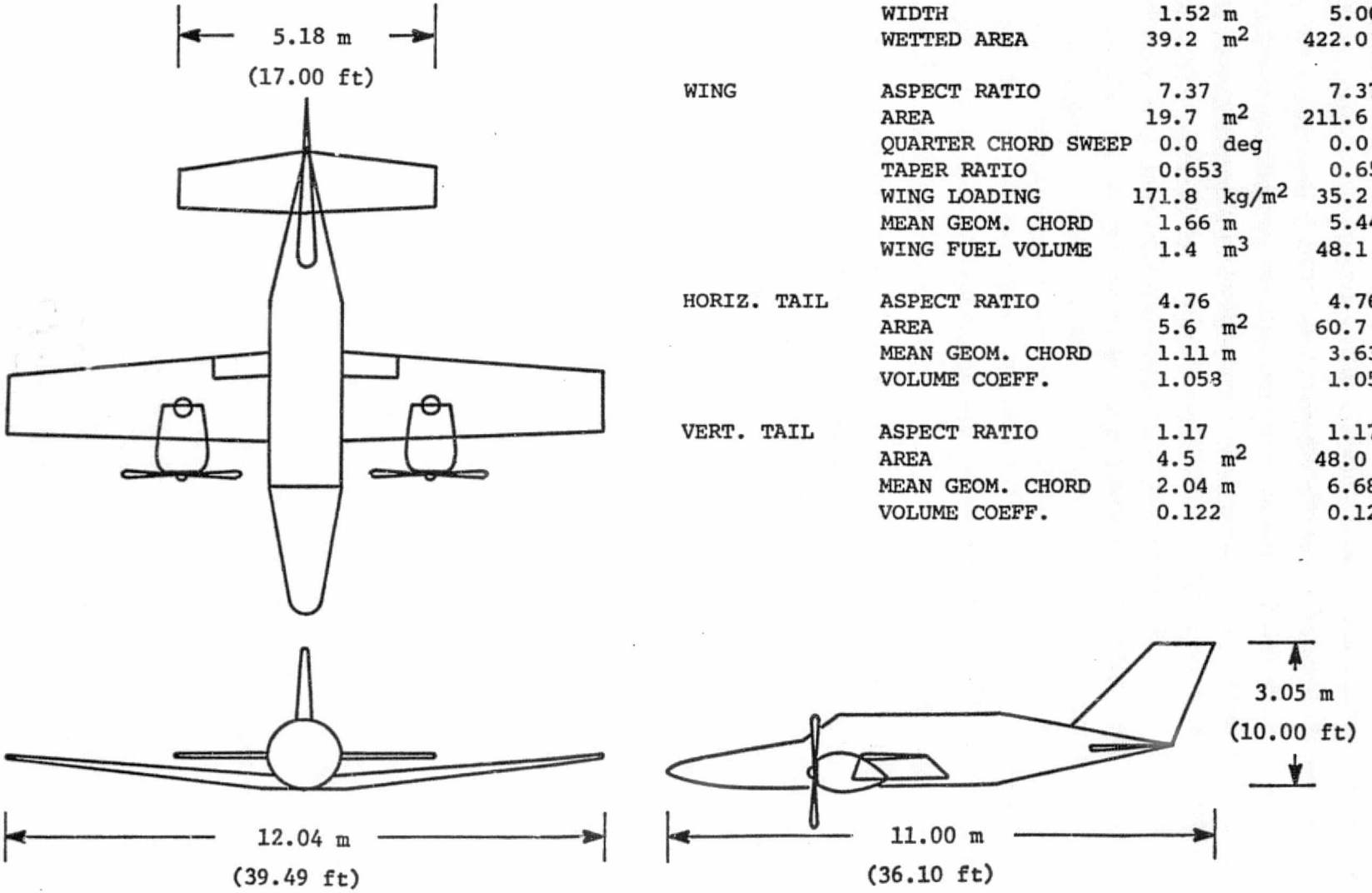

Figure 37. Baseline Aircraft Geometry from Gasp Survey

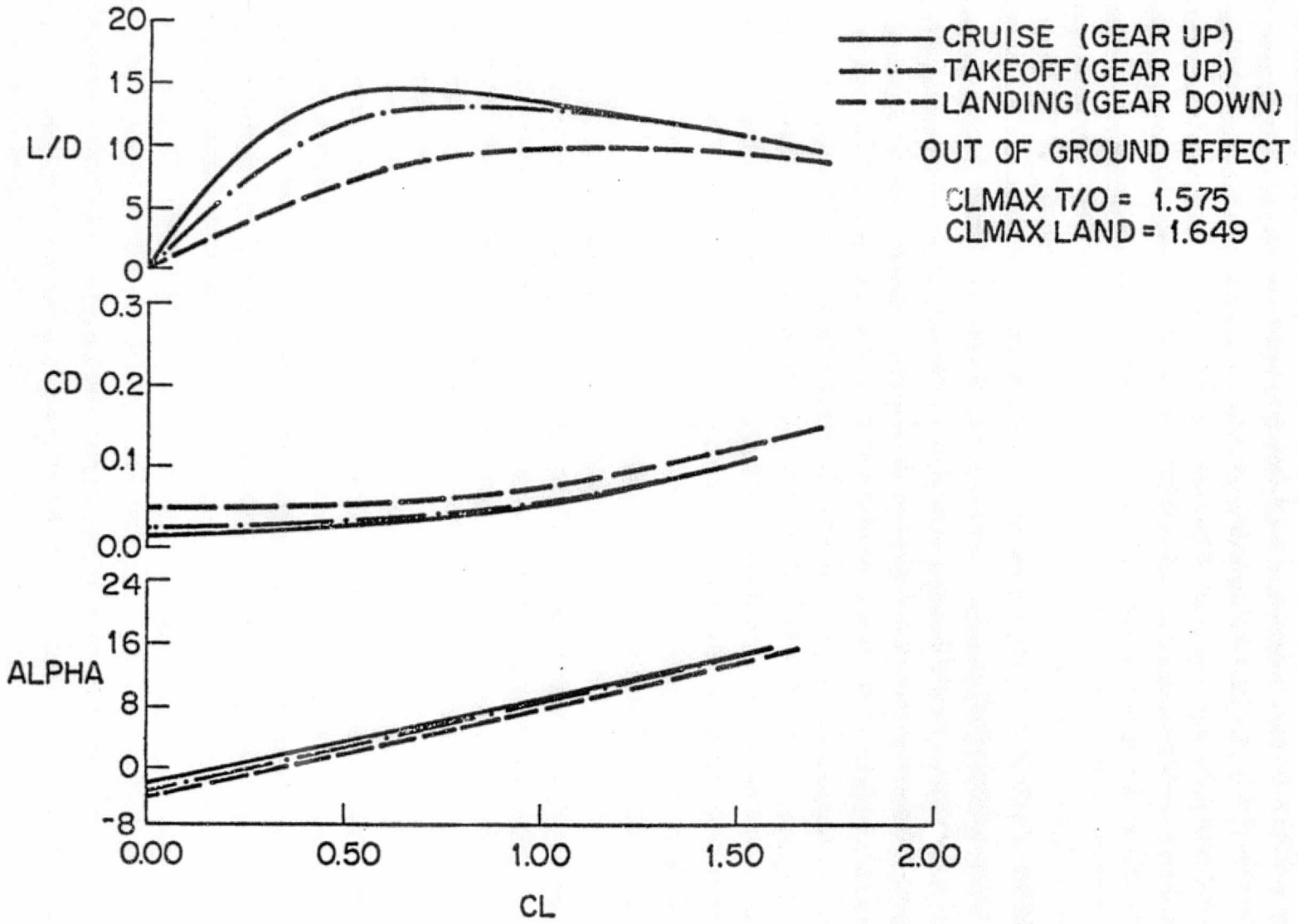

Fig. 38. Baseline Aircraft Aerodynamic Performance

BASELINE CRUISE PERFORMANCE

CRUISE AT 25000 FT., MACH NO. 0.389
TAS = 234.0 EAS = 156.0

TIME hrs.	0.472	7.232
RANGE KM (NM)	55.59 (30)	2992 (1615)
FUEL USED kg (lb)	61.23 (135)	611.0 (1347)
WEIGHT kg (lb)	3317.6 (7314)	2767.4 (6101)
CL	0.4149	0.3461
L/D	11.227	10.117
FUEL FLOW, kg/hr (lb/hr)	84.82 (187)	78.0 (172)

RESERVE FUEL = 63.5 kg (140 lb)
RANGE WITH MAXIMUM PAYLOAD = -0.
RANGE WITH MAXIMUM FUEL (MINIMUM PAYLOAD) = 5364 km (2895 NM)

Figure 39. Baseline Cruise Performance from Gasp Survey

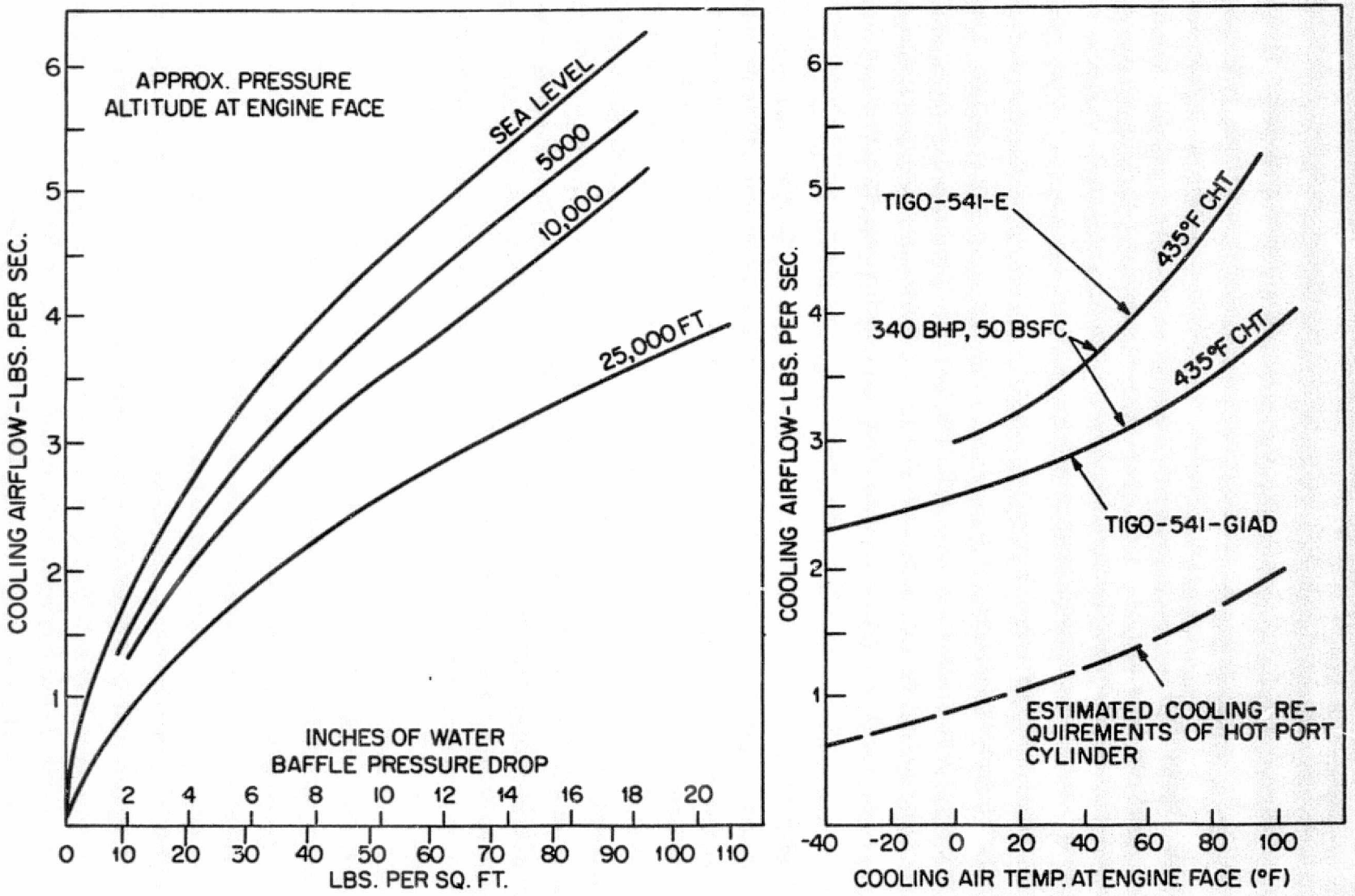

Figure 40. Cooling Airflow Requirements of a Representative Spark-Ignition Engine with Respect to the Hot Port Diesel.

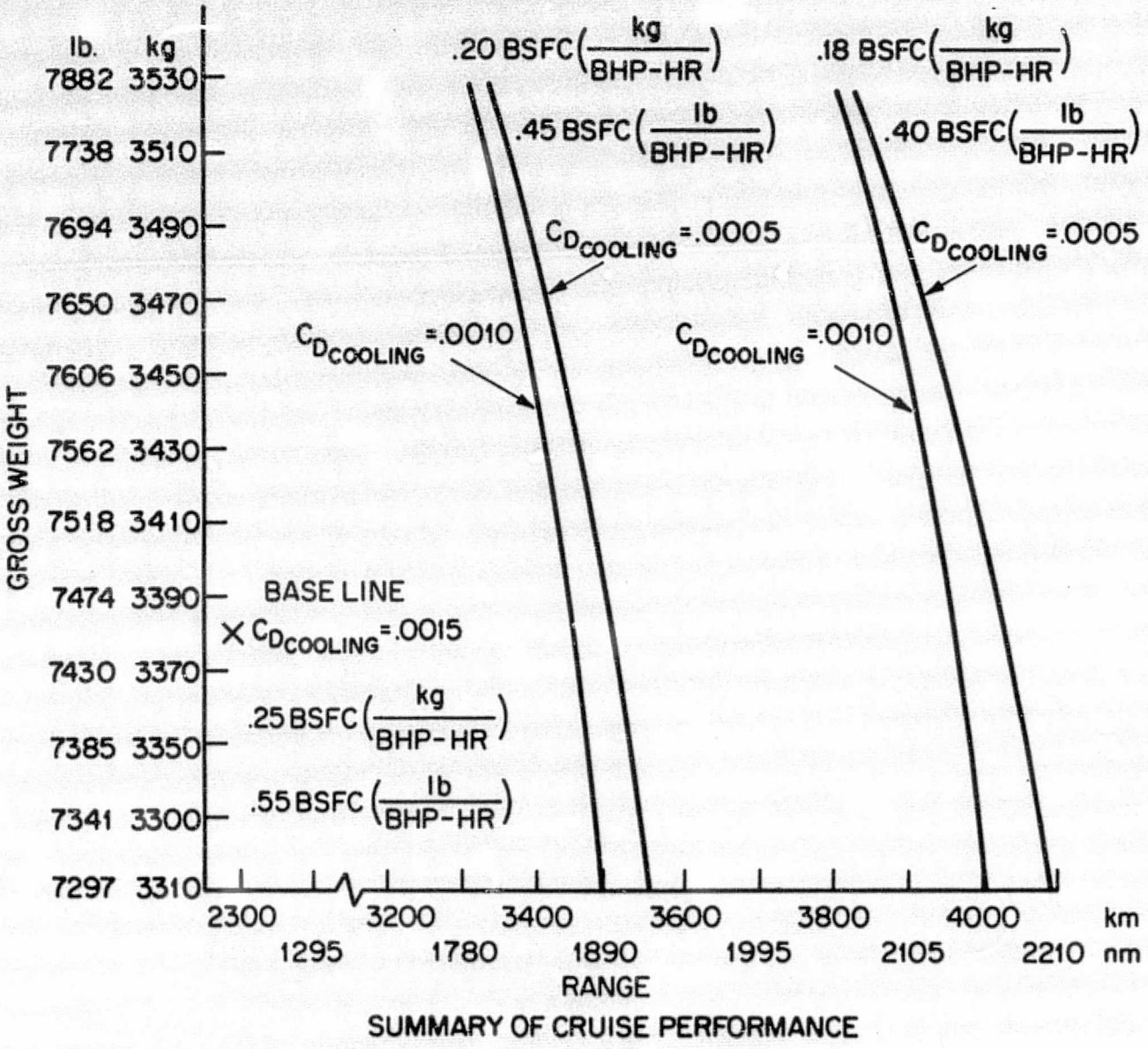

Figure 41. Low Compression Aircraft Diesel Performance with Respect to Baseline.

Table I. Inventory of Fuel Injection Nozzles

INJECTION NOZZLES

P/N	NO. OF HOLES	INCLUDED ANGLE	HOLE DISTRIBUTION, DIA INCHES	ORIFICE AREA IN^2	ORIFICE AREA mm^2	ADAPT TO NEEDLE LIFT
AD-120	8	160°	2@ .0085 2@ .01 2@.011 2@.012	0.000686	0.443	NO
AD-121	8	150°	" " " " " " " "	"	"	NO
AD-122	8	140°	" " " " " " " "	"	"	NO
AD-123	8	130°	" " " " " " " "	"	"	NO
AD-124	8	120°	" " " " " " " "	"	"	NO
AD-125	8	110°	" " " " " " " "	"	"	NO
AD-126	8	135°	2@ .009 2@ .01 4@ .012	0.000736	0.475	YES
AD-128	8	135°	4@ .01 4 @ .012	0.000766	0.494	YES
AD-129	7	135°	2@ .01 2 @ .012 3@ .015	0.000913	0.589	YES

Table II.

PISTON COMBUSTION CHAMBER CHARACTERISTICS

Part No.	CR (Nominal)	CR (Measured)	Clearance Vol. (Nominal)		Clearance Vol. (Measured)*		Squish
			$in.^3$	cm^3	$in.^3$	cm^3	
631475	7.5:1	---	13.32	218.5	----	-----	0.7
--	8.5:1	---	11.55	189.5	----	-----	0.7
--	9.0:1	---	10.82	177.5	----	-----	0.7
AD-118	10.0:1	9.92:1	9.63	157.9	9.71	159.1	0.7
AD-131	10.0:1	10.07:1	9.63	157.9	9.55	156.6	0.8
AD-130	11.0:1	11.14:1	8.66	142.0	8.54	140.0	0.8
AD-127	12.0:1	---	7.87	129.0	----	-----	0.7

$$\text{CR (measured)} = \frac{\text{Swept Volume}}{\text{Clearance Volume}} + 1$$

Swept Volume = 1420 cm^3 (86.66 $in.^3$)

*Clearance volume determined by filling combustion chamber at TDC with known quantity of type C-B Diesel fuel oil.

TABLE III

GTSIO-520 DIESEL GOALS

	CRUISE		TAKE-OFF	
	SPARK	DIESEL	SPARK	DIESEL
H.P.	325	325	435	435
H.P./cm^3 (H.P./in^3)	.037 (.62)	.037 (.62)	.050 (.83)	.050 (.83)
RPM	2900	2900	3400	3400
BMEP N/cm^2 (lb/in^2)	118.5 (172)	118.5 (172)	134.3 (195)	134.3 (195)
Piston Speed meters/min (ft/min)	588.2 (1930)	588.2 (1930)	688.8 (2260)	688.8 (2260)
Fuel Cons. kg/BHP-HR (lb/BHP-HR)	.250 (.55)	.185 (.41)	.304 (.672)	.204 (.45)
Air Fuel Ratio	15:1	20:1	12:1	25:1
Intake Press mm (in) Hg	914.4 (36)	1143 (45)	1155.7 (45.5)	1422.4 (56)
Intake Temp °C (°F)	57.7 (136)	57.7 (136)	87.7 (190)	87.7 (190)
Exh. Press mm (in) Hg	914.4 (36)	914.4 (36)	1143 (45)	1270 (50)
Exh. into Turbo °C (°F)	860 (1580)	860 (1580)	860 (1580)	860 (1580)

-Equal weight, bulk, cost and power with minimum change in tooling

-30% increase in range

-Emission; meet EPA goals

Table IV . Operating Conditions Used in Engine Testing

The following is a synopsis of test operating conditions listed according to test objectives. Data presented includes:

1. Reading Number
2. Indicated Horsepower
3. Revolutions per Minute
4. Intake Pressure
5. Intake Temperature
6. Piston Designation
7. Point of Ignition
8. Peak Cylinder Pressure
9. Nozzle Designation

The following conditions should be noted:

1. All engine testing was conducted with a 2.13 mm ID x 6.3 mm OD x 838 mm (.084 x .250 x 33.0 in.) fuel line except for test No. 2. Here, the line size was increased to 2.36 mm ID x 6.3 mm OD x 838 mm (.093 x .250 x 33.0 in.).

2. All testing used type C-B diesel fuel oil as a fuel with a cetane value of 47.5 except for test No. 12 which used a reference fuel with a cetane value of 71.

3. All cylinder pressure measurements up to test No. 9 were 172 - 206 N/cm^2 (250-300 psi) too high due to poor calibration of the pressure transducer.

NOTE - Items marked with asterisks in Table IV have not been mentioned in the text, see page 12.

Table IV (cont.)

Experiment 1: Test effect of various spray angles on performance (Page 12)

Reading No.	31-36
IHP	45.5
RPM	2600
Intake Pressure Hg Abs	1354-1438 mm (53.33-56.63 in.)
Intake Temperature	121-110°C (250-230°F)
Piston (AD-118)	10:1
Point of Ignition, deg.	TDC
Peak Cylinder Pressure	827-861.7 N/cm^2 (1200-1250 psi)
Nozzle	--

Experiment 2: Determine presence of after injection (Page 13)

Reading No.		38-40
IHP		46.0
RPM		2600
Intake Press. Hg Abs		1302-1429 mm (51.26-56.26 in.)
Intake Temperature		117.2°C (243°F)
Piston (AD-118)		10:1
Point of Ignition, deg.		TDC
Peak Cylinder Pressure		896.2 N/cm^2 (1300 psi)
Nozzle	AD-123	130°
	AD-122	140°
	AD-121	150°

Experiment 3: Effect of induction air temperature and pressure on point of ignition (Page 13)

Reading No.			no number	
IHP			no load	
RPM			2600	
Intake Pressure Hg Abs	mm		886.4	835.6	734
	in.		(34.9)	(32.9)	(28.9)
Intake Temperature		°C	123.8-193.3	204.4	165.5-212.7
		°F	(255-380)	(400)	(330-415)
Piston (AD-118)			10:1	10:1	10:1
Point of Ignition, deg			20-4 ATC	6-1 ATC	27-19 ATC
Peak Cylinder Pressure			-	-	-
Nozzle (AD-122)			140°	140°	140°

Table IV (cont.)

Experiment 4: Effect of induced swirl on engine performance (Page 14)
(a) Testing with instrument imperfection
(b) Engine testing

		(a)	(b)
Reading No.		46-86	no number
IHP		24-39	no load
RPM		2600	2600
Intake Pressure mm Hg Abs	in.	739-1041 (29.13-41.0)	1778 (70)
Intake Temperature	°C	121 ± 27	121
	°F	(250 ± 15)	(250)
Piston		10:1 (AD-118)	10:1 (AD-131)
Point of Ignition, deg		20 ATC-1 BTC	--
Peak Cylinder Pressure		344-896 N/cm^2 (500-1300) psi	--
Nozzle		140° (AD-122)	135° (7-hole) (AD-129)

Experiment 5: Comparison of 130° nozzle to 140° and 150° nozzle with swirl at position 8*

Reading No.		72-76 & 87-90		
IHP		26.4-36.8	27.3-37.0	25.8-33.9
RPM		2600	2600	2600
Intake Pressure mm Hg Abs		760.7-1007.1	746-1005	734-899.1
	in.	(29.95-39.65)	(29.4-39.6)	(28.9-35.4)
Intake Temperature	°C	113 ± 10.8	107 ± 16.3	111.6
	°F	(236 ± 6)	(226 ± 9)	(233)
Piston (AD-118)		10:1	10:1	10:1
Point of Ignition, deg		14 ATC @ 26.4 IHP to TDC @ 36.8 IHP	10 ATC @ 27.3 IHP to TDC @ 37.0 IHP	11 ATC @ 25.8 IHP to 4 ATC @ 33.9 IHP
Peak Cylinder Pressure		448-827 (650-1200)	517-827.2 (750-1200)	517-758 N/cm^2 (750-1100) psi
Nozzle		140° (AD-122)	130° (AD-123)	150° (AD-121)

Table IV (cont.)

Experiment 6: Friction check oil temp = 93.3°C (200°F)
two values of RPM tested; 2600 and 2900*

Reading No.		104-105	104-105
IHP		--	--
RPM		2600	2900
Intake Pressure	mm	754.3	812.8
Hg Abs	in.	(29.7)	(32.0)
Intake Temperature	°C	114.4	117.2
	°F	(238)	(243)
Piston (AD-118)		10:1	10:1
Point of Ignition, deg		--	--
Peak Cylinder Pressure		396	413 N/cm^2
		(575)	(600) psi
Nozzle		--	--

Experiment 7: Effect of varying engine speed on ISFC*

Reading No.		96-100	101-103
IHP		27.2-42.3	27.7-36.5
RPM		2600	2900
Intake Pressure	mm	721.3-1107	746.7-1028.7
Hg Abs	in.	(28.4-43.6)	(29.4-40.5)
Intake Temperature	°C	112.7	120.5
	°F	(235)	(249)
Piston (AD-118)		10:1	10:1
Point of Ignition, deg		12 ATC @ 27.2 IHP to 1 BTC @ 27.7 IHP	15 ATC @ 27.7 to 3 ATC @ 36.5
Peak Cylinder Pressure		517-861	517-758.3 N/cm^2
		(750-1250)	(750-1100) psi
Nozzle (AD-122)		140°	140°

Experiment 8: Motoring friction determination (Page 15)

(a) Testing with instrument imperfection effect of RPM and intake pressure on friction Hp
(b) Engine testing effect of oil temperature on friction - two oil temperatures were used; 76.6°C and 62.7°C (170°F and 145°F)

		(a)	(b)
Reading No.		108-118	234-245
IHP		--	--
RPM		1467-3027	2600
Intake Pressure	mm	731.2 or 1036	1778
Hg Abs	in.	(28.79 or 40.79)	(70)
Intake Temperature	°C	121-126	104.4
	°F	(250-260)	(270)
Piston (AD-118)		10:1	10:1 (AD-131)
Point of Ignition, deg		--	--
Peak Cylinder Pressure		331-482	-- N/cm^2
		(480-700)	psi
Nozzle (AD-122)		140°	135° (7 hole) (AD-129)

Table IV (cont.)

Experiment 9: Effect of manifold pressure on ignition lag (Page 16)

Reading No.		127-132
IHP		27.7-29.1
RPM		2600
Intake Pressure	mm	820-1384.3
Hg Abs	in.	(32.3-54.5)
Intake Temperature	°C	118-124
	°F	(245-256)
Piston (AD-118)		10:1
Point of Ignition, deg		1 ATC for 32.3 to 3 BTC for 54.5
Peak Cylinder Pressure		448-534 N/cm^2 (650-775) psi
Nozzle (AD-126)		135° (8 hole)

Experiment 10: Obtain performance Hook of 11:1 piston (AD-130) (Page 16)

Reading No.		141-148
IHP		28.6-35.8
RPM		2600
Intake Pressure	mm	896-1498
Hg Abs	in.	(35.3-59.0)
Intake Temperature	°C	95-108
	°F	(203-227)
Piston (AD-118)		11:1
Point of Ignition, deg		6 ATC for 32.3 to 4 BTC for 54.5
Peak Cylinder Pressure		551-775.3 N/cm^2 (800-1125) psi
Nozzle (AD-129)		135° (7 hole)

Experiment 11: Obtain performance Hook of 10:1 piston (AD-131) (Page 17)

Reading No.		136-137, 157, 162
IHP		30.2-50.7
RPM		2600
Intake Pressure	mm	904.2-1844
Hg Abs	in.	(35.6-72.6)
Intake Temperature	°C	112.2 @ 30.2 IHP (234) to
	(°F)	121 @ 50.7 IHP (250)
Piston (AD-131)		10:1
Point of Ignition, deg		3 ATC-5 BTC
Peak Cylinder Pressure		620-844 N/cm^2 (900-1125) psi
Nozzle (AD-129)		135° (7 hole)

Table IV (concl.)

Experiment 12: Effect of Cetane value on engine performance (Page 17)

Reading No.		143,145-147,149-152
IHP		23.4-40.7
RPM		2600
Intake Pressure	mm	1559-1508
Hg Abs	in.	(61.4-59.4)
Intake Temperature	°C	115.5 ± 12.6
	°F	240 ± 7
Piston (AD-130)		11:1
Point of Ignition, deg		4 BTC
Peak Cylinder Pressure		654-723 N/cm^2
		950-1050 psi
Nozzle (AD-129)		135° (7 hole)

Experiment 13: Effect of 1.27 mm (.05 in.) less nozzle protrusion on engine performance*

Reading No.		158-162,163-165
IHP		33.6-53.6
RPM		2600
Intake Pressure	mm	1059-1968
Hg Abs	in.	(41.7-77.5)
Intake Temperature	°C	62.7 ± 12.6
	°F	(145 ± 7)
Piston (AD-131)		10:1
Point of Ignition, deg		TDC @ 33.6 IHP to 6 BTC @ 53.6 IHP
Peak Cylinder Pressure		620-827.2 N/cm^2
		(900-1200) psi
Nozzle (AD-129)		135° (7 hole)

Experiment 14: Effect of increasing induction air temperature from 107°C-204°C (225-400°F) (Page 18)

Reading No.		257-265
IHP		23.0-50
RPM		2600
Intake Pressure	mm	1778
Hg Abs	in.	(70)
Intake Temperature	°C	107.2-204.4
	°F	(225-400)
Piston (AD-131)		10:1
Point of Ignition, deg		4 BTC-TDC
Peak Cylinder Pressure		568-675 N/cm^2
		(825-980) psi
Nozzle (AD-129)		135° (7 hole)

TABLE V

BASELINE AIRCRAFT WEIGHT BREAKDOWN

	kg	lb
Propulsion Group		
Primary Engines	586	1292
Primary Engines Instl.	79	174
Fuel System	13	29
Propulsor Weight	141	311
Total Prop. Group Wt.	820	1808
Structures Group		
Wing	259	572
Hor. Tail	65	144
Vert. Tail	25	56
Fuselage	301	663
Landing Gear	98	216
Primary Engine Section	6	14
Total Struct. Group Wt.	756	1666
Flight Controls Group		
Cockpit Controls	11	25
Fixed Wing Controls	44	96
Total Control Wt.	55	121
Wt. of Fixed Equipment	376	829
Weight Empty	2007	4425
Fixed Useful Load	152	336
Operating Weight Empty	2160	4761
Payload	544	1200
Fuel	675	1488
Gross Weight	3379	7450
Wing Fuel Capacity	675	1488

TABLE VI

WEIGHT BREAKDOWN FOR STANDARD TCM-520
ENGINE AND DIESEL MODIFICATIONS

Item	Weight kg	Weight lb	Subtract kg	Subtract lb	Add kg	Add lb
Spark Plugs	1.22	2.70	1.22	2.70		
Magnetos	5.10	11.25	5.10	11.25		
Ignition Harness (Shielded)	1.25	2.75	1.25	2.75		
Starter	7.43	16.38				
Fuel Injection System	3.86	8.50	3.86	8.50		
Exhaust System	8.05	17.75				
External Oil and Fuel Lines	4.31	9.50				
Alternator	10.26	22.62				
Oil Cooler	4.20	9.25				
Tachometer Drive	0.63	1.38				
Turbosupercharger	22.00	48.50				
Intercooler	3.06	6.75				
Variable Controller	0.91	2.00	0.91	2.00		
Fuel Pressure Regulator	1.36	3.00	1.36	3.00		
Overboost Valve and Adapter	0.45	1.00	0.45	1.00		
Sonic Venturi	0.11	0.25	0.11	0.25		
Hot Prime System	0.34	0.75	0.34	0.75		
Nozzles					1.13	2.5
Injector Lines					1.81	4.0
Injector Pump					5.44	12.0
Intake Air Heater					1.81	4.0
			14.60	32.20	10.19	22.50
Weight Engine, No Accessories			278.83	614.70	278.83	614.70
Weight Engine, With Accessories			293.43	646.90	289.02	637.20

TABLE VII

SUMMARY OF CRUISE PERFORMANCE

The data presented below is for a 435 HP, 3400 maximum RPM turbocharged engine with a 2:3 gear ratio. The cruise configuration is at 75% power, 85% RPM and all missions begin with 675 kg (1488 lb) of fuel.

Case No.	Gross Weight kg(lb)	Drag Coef.	BSFC $\frac{kg}{BHP-HR}$	BSFC $\frac{lb}{BHP-HR}$	Range km	Range nm
Base-line	3380 (7450)	.0015	0.25	0.55	2290	1615
1	3310 (7300)	.0005	0.18	0.40	4095	2210
2		.0005	0.20	0.45	3555	1920
3		.0010	0.18	0.40	4020	2170
4		.0010	0.20	0.45	3500	1890
5	3380 (7450)	.0005	0.18	0.40	4020	2170
6		.0005	0.20	0.45	3500	1890
7		.0010	0.18	0.40	3955	2135
8		.0010	0.20	0.45	3445	1860
9	3450 (7600)	.0005	0.18	0.40	3955	2135
10		.0005	0.20	0.45	3445	1860
11		.0010	0.18	0.40	3890	2100
12		.0010	0.20	0.45	3390	1830
13	3515 (7750)	.0005	0.18	0.40	3845	2075
14		.0005	0.20	0.45	3355	1810
15		.0010	0.18	0.40	3835	2070
16		.0010	0.20	0.45	3335	1800

Appendix A

EQUIPMENT IDENTIFICATION

Dynamometer	General Electric, Type TLC50, S/N 1503625, Horsepower -150, Class 6-150-4000
Beam Scale	Kron, Capacity 300 lbs., S/N 22296, Calibrated Sept. 1976, HP = (Beam x RPM)/3000
Revolutions (RPM)	Electronic Counter, Hewlett Packard Models 521A and 5301A
Temperature	Brown Electronik by Honeywell, Model Y156X63-PSZY-II-III-IV-A4(L), S/N 951059, Calibration Check Sept. 1976.
Cooling Air Fan	American Fan Co., Model AF-15, with 10 Hp Motor and 8 in. (20.3 cm) fan outlet valve
Manometers	100 in.-U-Tube by Trimount, Type 40-100-U, S/N 42721
Airflow	Bank of Sharp Edge Orifices, Sizes 1/8 in., 7/32 in., 3/32 in., and 3/16 in. diameter, capacity 722 lbs/hr, manufacturer, unknown.
Fuel Flow	Time-weight system by Wakasha. Variable area flowmeter by Cox Instrument Div., Lynch Corp.
Induction Air Heater	20 KW Cromalox with Bartlow, Model M-2 Controller (1000°F capacity)
Oscilloscope	Tectronix Dual Beam, Type 502, S/N 005336
Charge Amplifier	(1) Kistler Model 566, S/N 1338 (2) Kistler Model 503M4, S/N 917
Pressure Transducer	Kistler Models 6005, S/N 78793 and 607 FX, S/N 25
Transducer Holder	Kistler Model 628C108
Oil Heater-Intercooler System	Assembled by Automotive Laboratory of The University of Michigan
Pressure Regulator	Rockwell International Boston Gear Division, Model E42460A
Smokemeter	Bosch smokemeter Model EFAW 68A Hartridge Smokemeter Leslie Hartridge LTD Model HR 142

EQUIPMENT SUPPLIED AT TELEDYNE CONTINENTAL MOTORS EXPENSE

ITEM	TCM PART #	QUANTITY
7.5:1 CR Piston	631475	1
Cooling Air Baffle	641339	4
Complete Cylinder Assembly (except piston)	639053	2
Piston Ring	640625	12
" "	640626	12
" "	640627	12
" "	640628	12
" "	629401	12
Expander	636146	12
Intake Elbow Assembly	633728	3
Gasket	630824	18
Flange	633730	2
Connecting Rod Pin and Bushing	530658	2
Camshaft	635033	2
Cylinder Head Thermocouple	Bayonet	3
Hydraulic Valve Lifter Assembly	628488	4
Crankshaft, 10.1cm (4.0 in.) Stroke Adapt to Labeco Crankcase	—	1
GTSIO-520 Partial Engine (page 82)	—	1

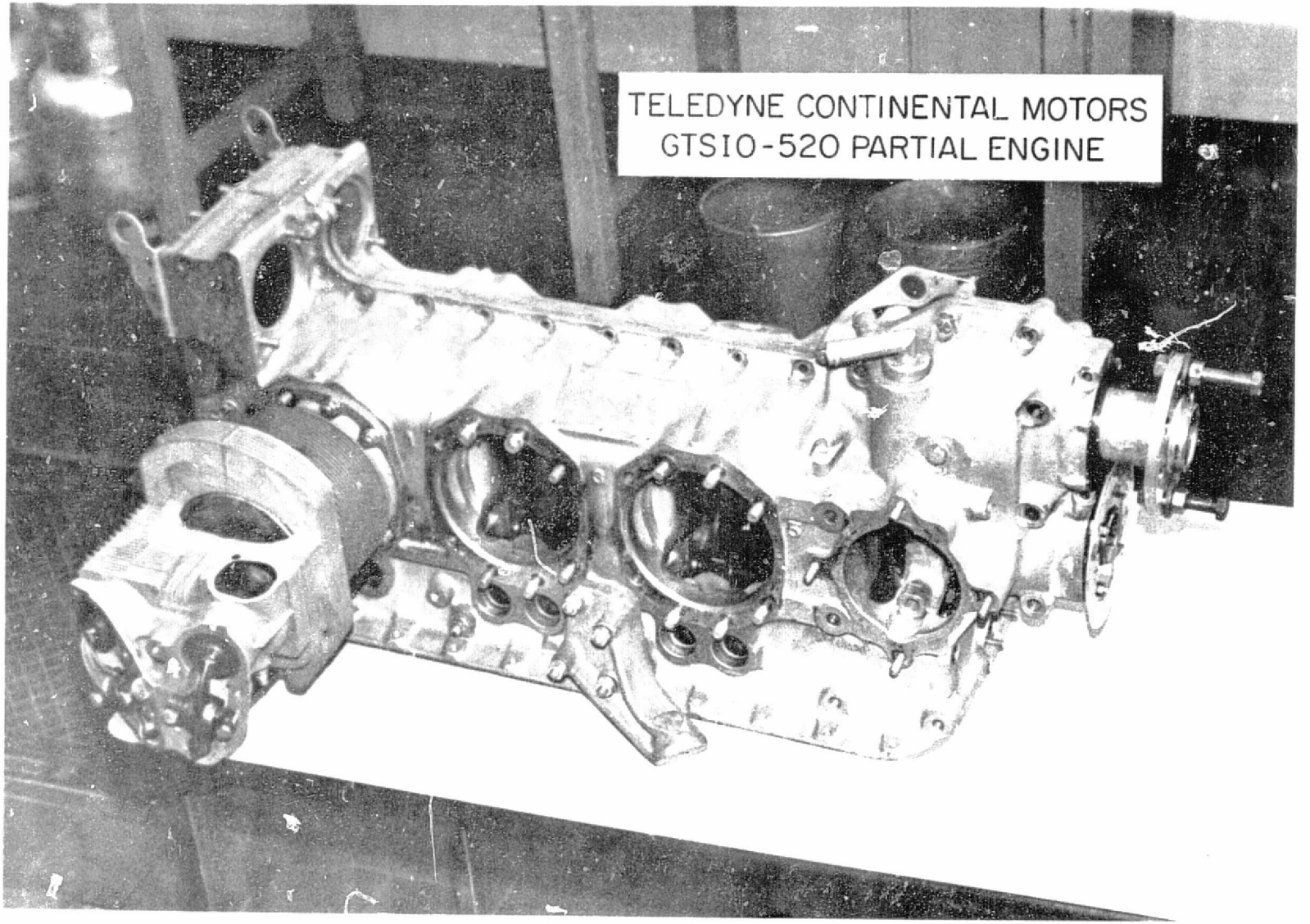

Figure 42. Partial GTSIO-520 Engine Supplied by TCM for Determination of Valve to Piston Clearance

APPENDIX C

TYPICAL GASP OUTPUT

CASE 3

Gross Weight = 3312kg (7301 lb) = 98% of base case
Wing Loading = 1651 N/cm^2 (34.5 lb/ft^2)
Delta C_D = .001
Required T/O Distribution = 654.1 m (2146 ft)
BSFC = .18 kg/BHP-HR (.40 lb/BHP-HR)

DRAG BREAKDOWN

	FLATPLATE AREA(SQFT)	CDO	WETTED AREA(SQFT)
WING	1.721	0.00813	391.07
FUSELAGE	1.837	0.00868	422.68
VERT. TAIL	0.349	0.00165	96.00
HOR. TAIL	0.506	0.00239	121.40
ENGINE NACELLES	1.161	0.00548	6.74
TIP TANKS	0.000	0.00000	0.00
INCREMENTAL	0.212	0.00100	0.00
TOTAL FE	4.624	0.02185	1031.15

O.K.? y

TAXI SEGMENT

TAXI AT IDLE THRUST

TIME	FUEL USED	WEIGHT	FUEL FLOW
0.000	0.	7301.	138.
0.250	34.	7266.	138.

HIT RETURN TO CONTINUE-

ALL ENGINES OPERATIVE

ROTATION SPEED= 87.2

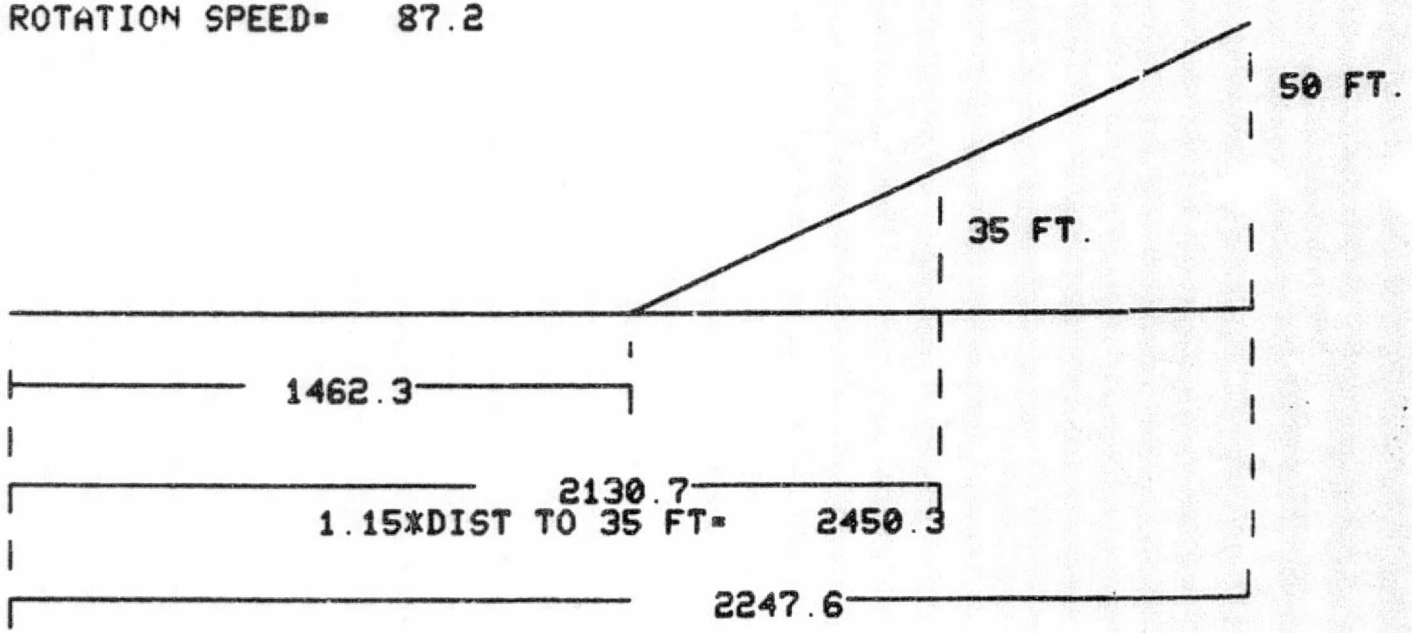

HIT RETURN TO CONTINUE-

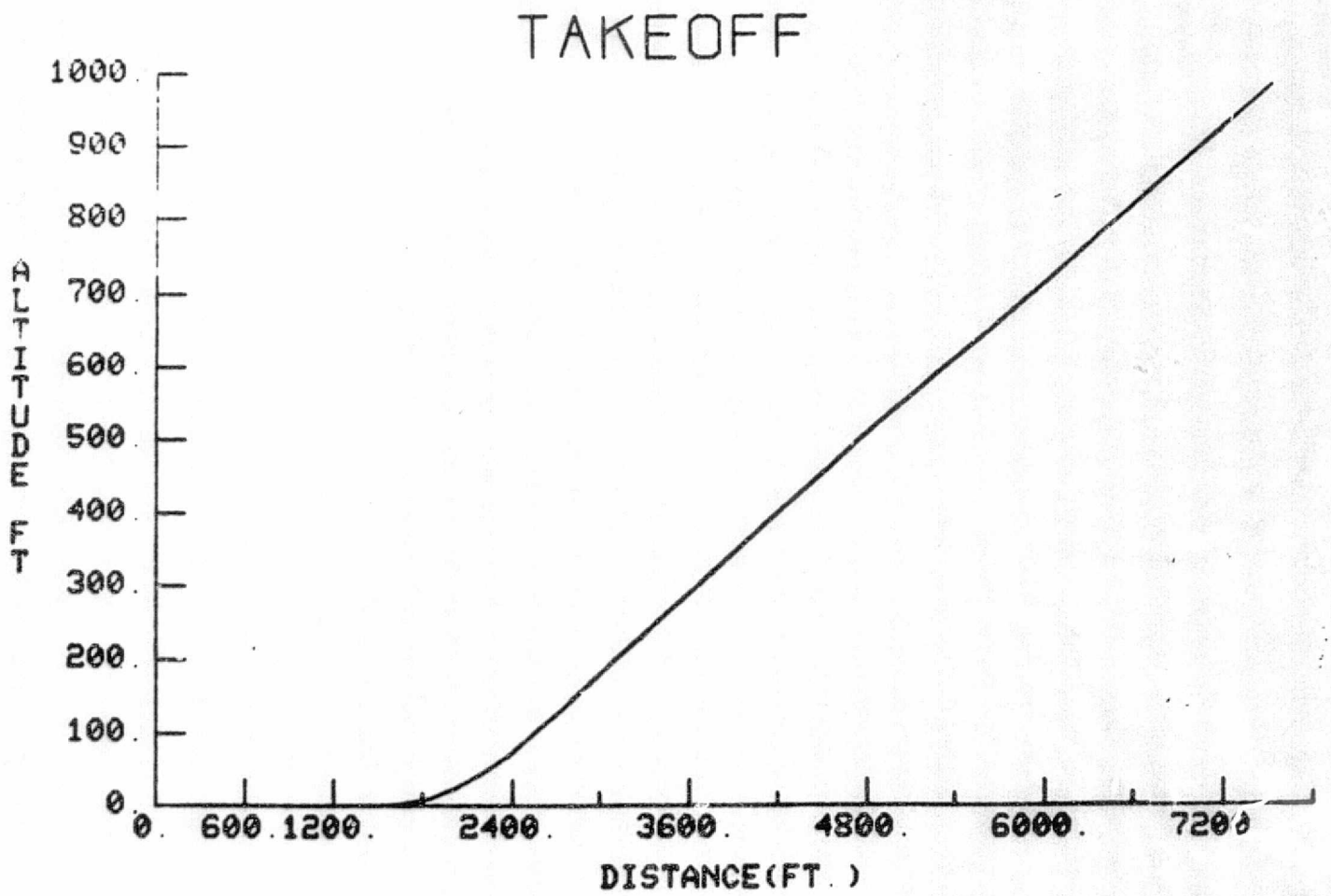

DISTANCE VS ALTITUDE

HIT RETURN TO CONTINUE-

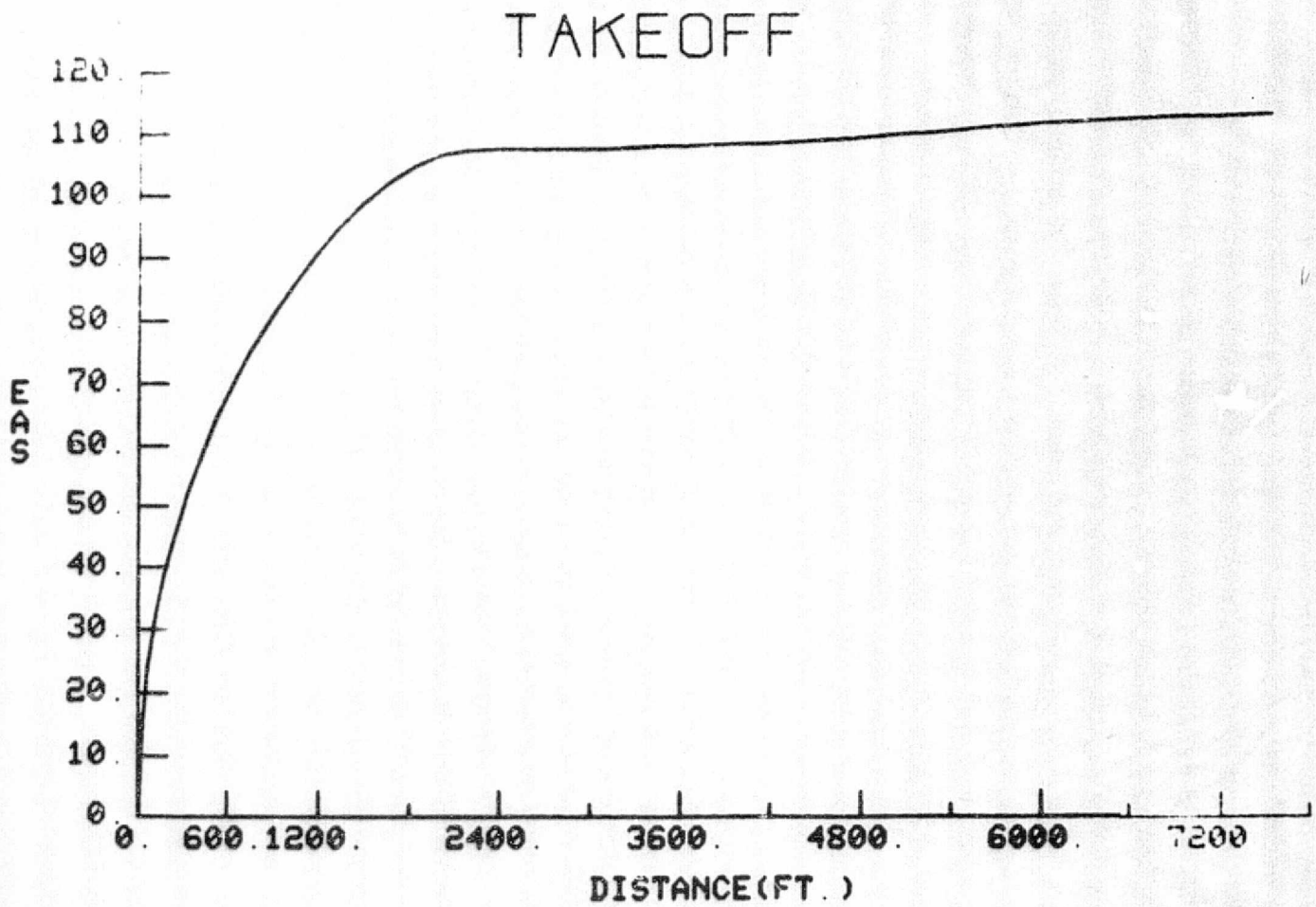

DISTANCE VS.EAS

HIT RETURN TO CONTINUE-

C-2

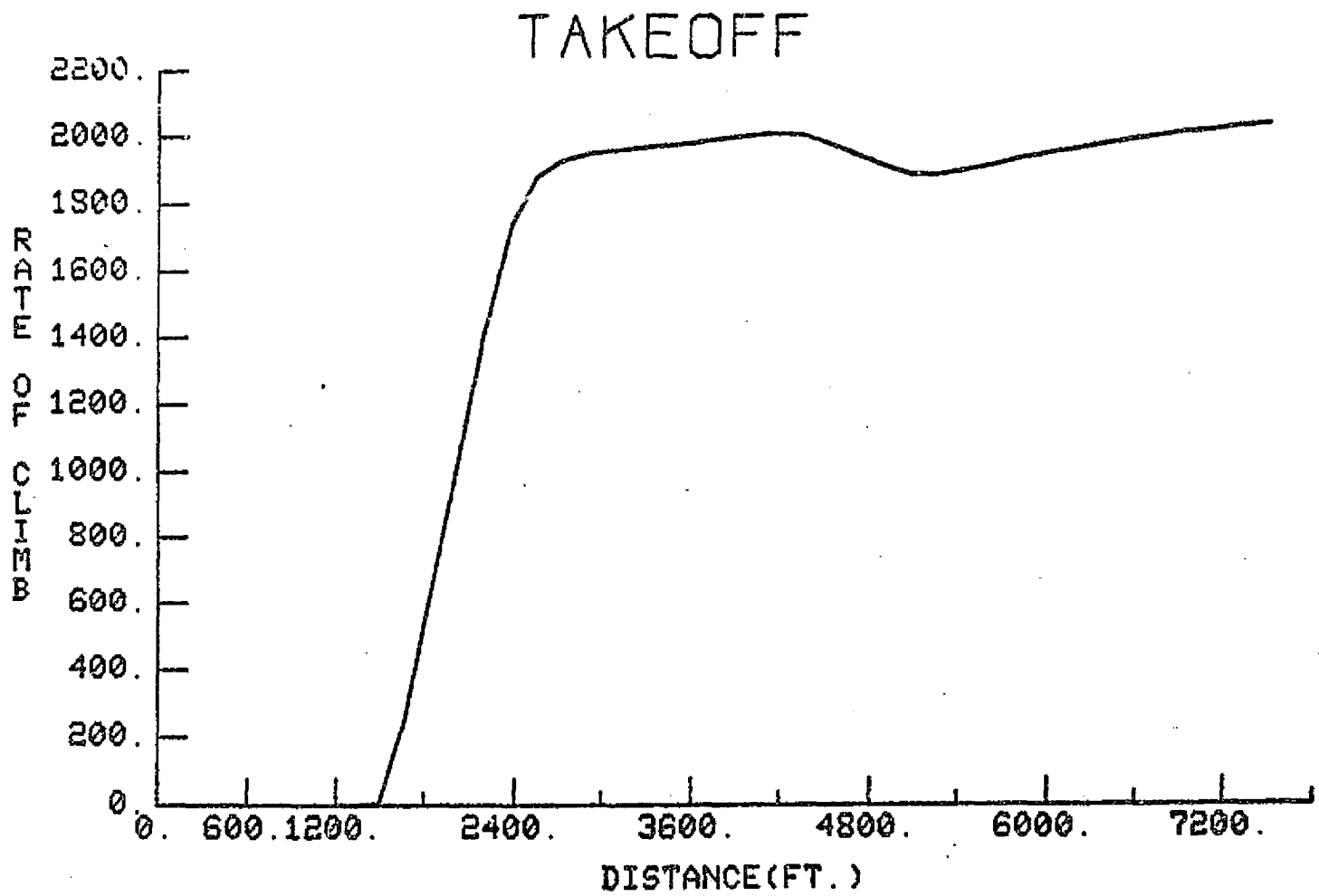

DISTANCE VS. RATE OF CLIMB

HIT RETURN TO CONT

```
CLIMB TO 25000. FEET
TIME   12.    MIN
FUEL USED=     105.  LB
RANGE=     29.  NM
MACH NO. @  25000.  FT= 0.298



INDICATE WHICH GRAPH YOU WISH TO SEE
ALTITUDE VS.
   TIME
   EAS
   MACH NO.
   R/C
   DONE
```

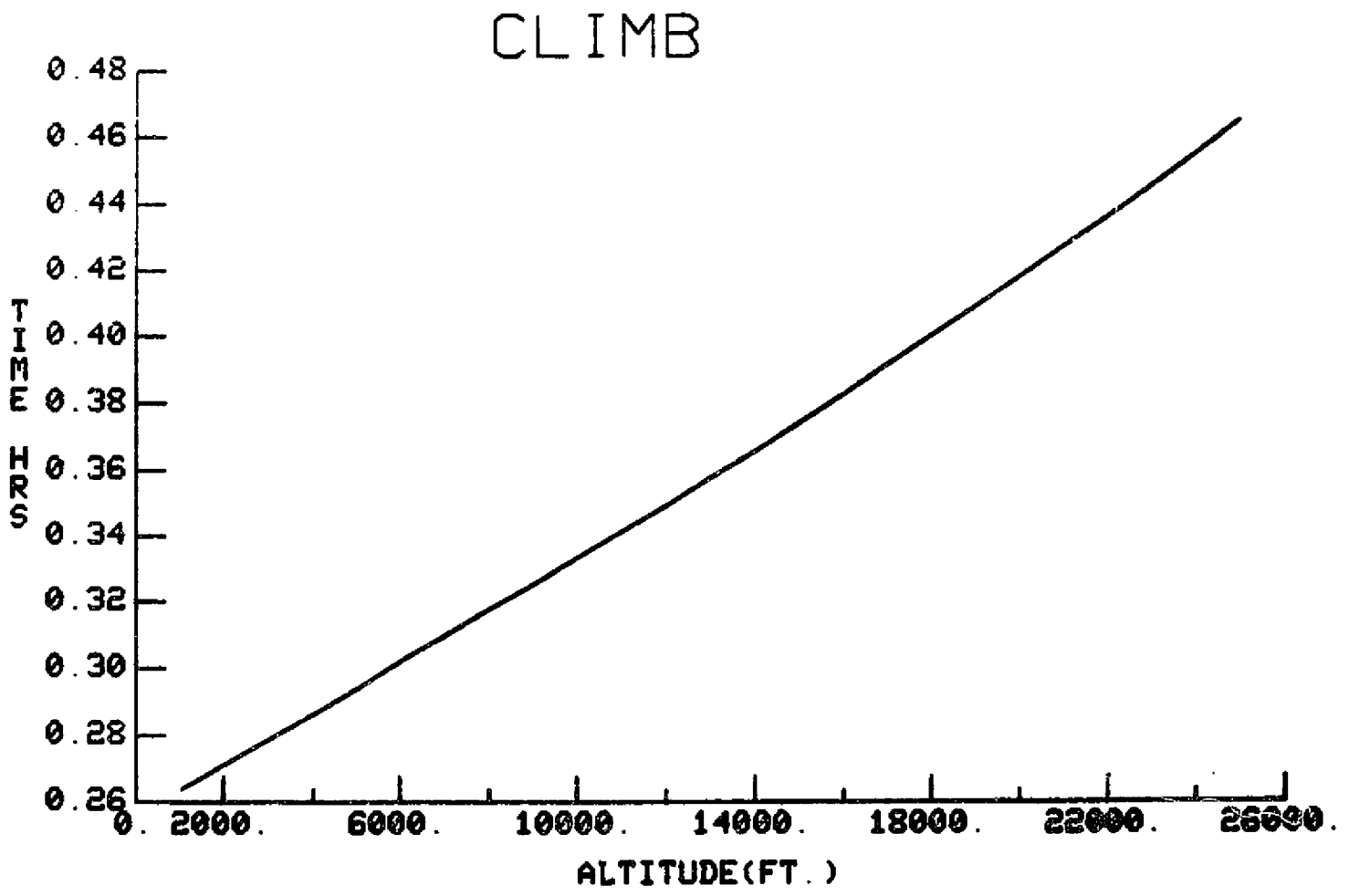

ALTITUDE VS. TIME

HIT RETURN TO CONTINUE-

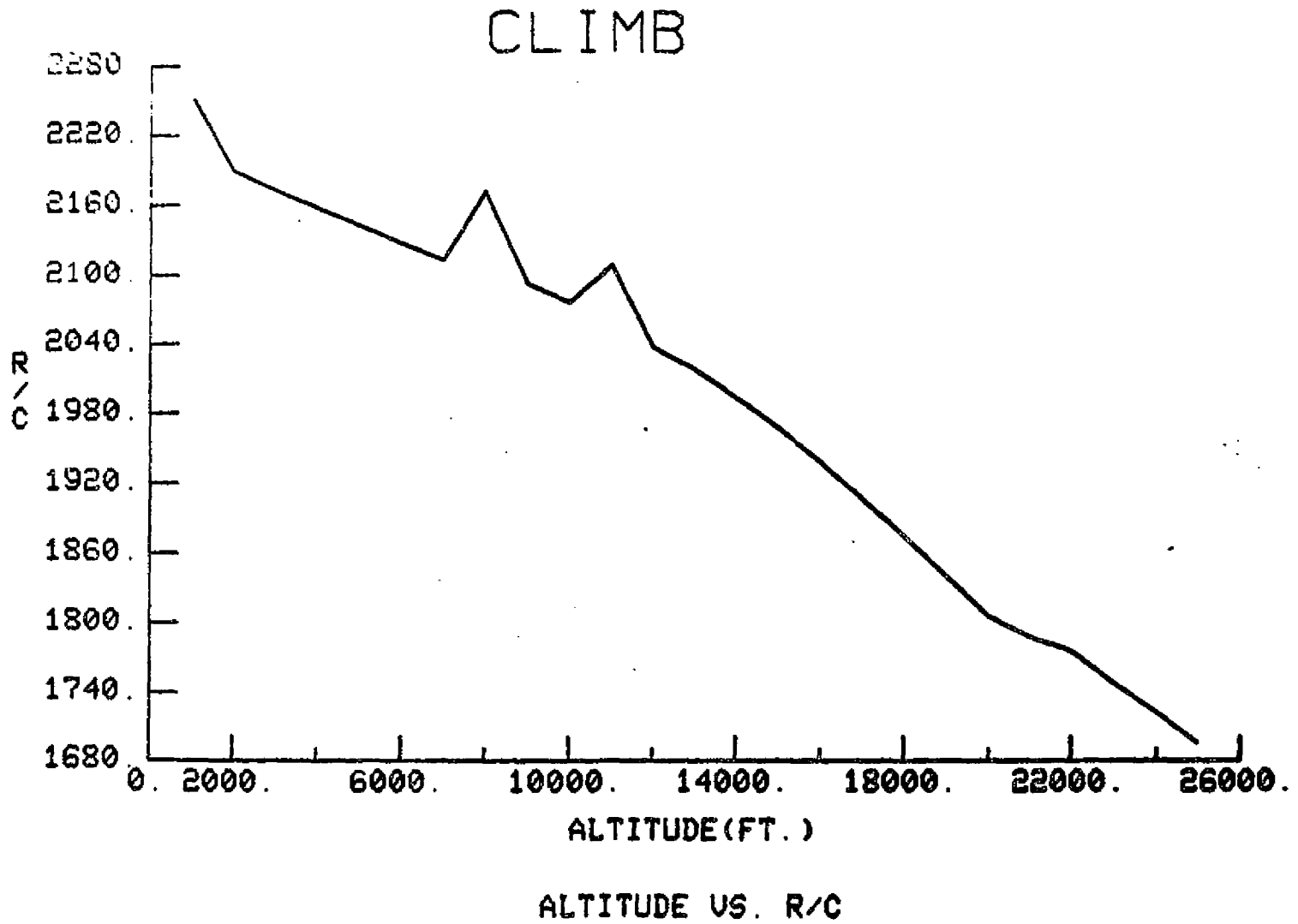

ALTITUDE VS. R/C

HIT RETURN TO CONTINUE-

CRUISE AT 25000 FT ,MACH NO. 0.389
TAS= 234 EAS= 156.

	START	END
TIME(HRS.)	0.465	9.595
RANGE(NM)	29.	2169.
FUEL USED(LBS)	105.	1378.
WEIGHT(LBS)	7194.	5921.
CL	0.4082	0.3360
L/D	11.318	10.104
FUEL FLOW(LB/HR)	145.	133.

RESERVE FUEL= 109.
RANGE WITH MAXIMUM PAYLOAD= -0.
RANGE WITH MAXIMUM FUEL(MINIMUM PAYLOAD)= 3818.

RANGE REQUIREMENTS MET?(Y/N)? y

LANDING SEGMENT

APPROACH SPEED(KTS)= 91.82
APPROACH ANGLE(DEG)= 5.5
TOUCHDOWN SPEED(KTS)= 70.63

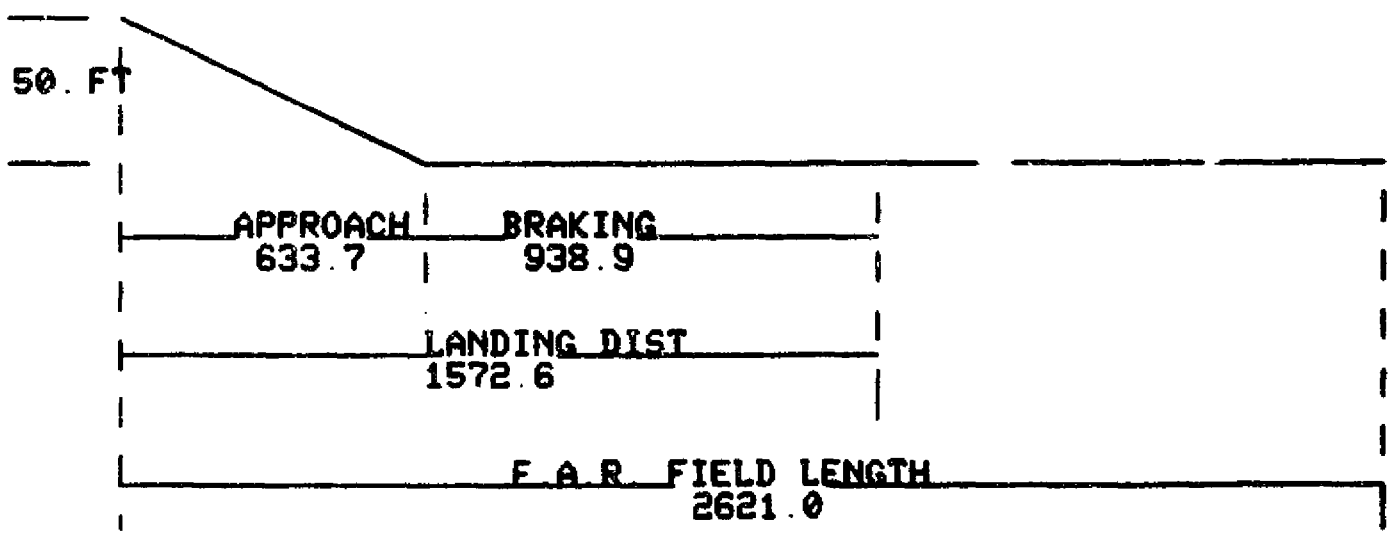

HIT RETURN TO CONTINUE-

References

1. Galloway, T.L. and Smith, M.R., "General Aviation Design Synthesis Utilizing Interactive Computer Graphics," SAE Paper 760476, April 1976.

2. Monts, F., "The Development of Reciprocating Engine Installation Data for General Aviation Aircraft," SAE Paper 730325, April 1973.